



Bibliothèque nationale
du Canada

THÈSES CANADIENNES
SUR MICROFICHE

PERMANENT ADDRESS/RESIDENCE FIXED Umuduru Olokoro, P.O. Box 258 Imo State
Imo STATE NIGERIA



National Library of Canada

Cataloguing Branch
Canadian Theses Division

Ottawa, Canada
K1A 0N4

Bibliothèque nationale du Canada

Direction du catalogage
Division des thèses canadiennes

NOTICE

The quality of this microfiche is heavily dependent upon the quality of the original thesis submitted for microfilming. Every effort has been made to ensure the highest quality of reproduction possible.

If pages are missing, contact the university which granted the degree.

Some pages may have indistinct print especially if the original pages were typed with a poor typewriter ribbon or if the university sent us a poor photocopy.

Previously copyrighted materials (journal articles, published tests, etc.) are not filmed.

Reproduction in full or in part of this film is governed by the Canadian Copyright Act, R.S.C. 1970, c. C-30. Please read the authorization forms which accompany this thesis.

THIS DISSERTATION
HAS BEEN MICROFILMED
EXACTLY AS RECEIVED

AVIS

La qualité de cette microfiche dépend grandement de la qualité de la thèse soumise au microfilmage. Nous avons tout fait pour assurer une qualité supérieure de reproduction.

S'il manque des pages, veuillez communiquer avec l'université qui a conféré le diplôme.

La qualité d'impression de certaines pages peut laisser à désirer, surtout si les pages originales ont été dactylographiées à l'aide d'un ruban usé. Si l'université nous a fait parvenir une photocopie de mauvaise qualité.

Les documents qui font déjà l'objet d'un droit d'auteur (articles de revue, examens publiés, etc.) ne sont pas microfilmés.

La reproduction, même partielle, de ce microfilm est soumise à la Loi canadienne sur le droit d'auteur, SRC 1970, c. C-30. Veuillez prendre connaissance des formules d'autorisation qui accompagnent cette thèse.

LA THÈSE A ÉTÉ
MICROFILMÉE TELLE QUE
NOUS L'AVONS REÇUE

THE UNIVERSITY OF ALBERTA

A REGIONAL SUBSURFACE CORRELATION OF SOME BENTONITE REDS
IN THE LOWER CRETACEOUS VIKING FORMATION OF
SOUTH-CENTRAL ALBERTA, CANADA

by



LEVI CHUKWUEMEKA AMAJOR

A THESIS

SUBMITTED TO THE FACULTY OF GRADUATE STUDIES AND RESEARCH
IN PARTIAL FULFILMENT OF THE REQUIREMENTS FOR THE DEGREE
OF MASTER OF SCIENCE

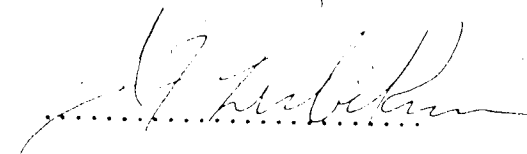
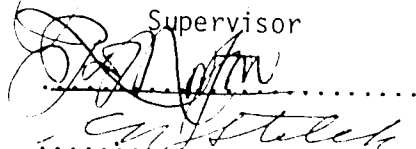
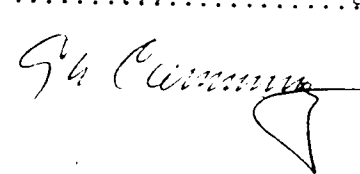
DEPARTMENT OF GEOLOGY

EDMONTON, ALBERTA

SPRING, 1978

THE UNIVERSITY OF ALBERTA
FACULTY OF GRADUATE STUDIES AND RESEARCH

The undersigned certify that they have read, and
recommend to the Faculty of Graduate Studies and Research, for
acceptance, a thesis entitled A Regional Subsurface
Correlation of Some Bentonite Beds in the Lower Cretaceous
Viking Formation of South-Central Alberta, Canada
submitted by Levi Chukwuemeka Amajor
in partial fulfilment of the requirements for the degree of
Master of Science.


Supervisor



Date Jan. 10th 1978

DEDICATION

This piece of work is only a bold step forward into the realms of Science.

It is dedicated to my wife 'Oge' and son 'Uzo', for their untiring and unwearied patience, encouragement, tolerance and realization that 'a friend in need is a friend indeed'.

ABSTRACT

A subsurface study of the five main bentonite beds (in ascending order designated 'E', 'D', 'C', 'B', 'A') in the Lower Cretaceous Viking Formation of southeastern and central Alberta, between Townships 21 and 60, and Ranges 3 and 28 west of the Fourth Meridian, shows their stratigraphic and geographic distributions through a combination of electric log and chemical correlations. More than 1000 electric well logs and 102 Viking cored wells were studied.

From one to a maximum of eight bentonite beds were observed in most of the cores, with thicknesses ranging from less than one inch to 24 inches. The bentonites are biotite-rich, although biotite grain size varies from very fine to coarse. Log correlations and core studies show that most of the bentonites are laterally restricted in occurrence, except for 'E', 'C' and 'A'.

X-ray fluorescence analysis of these bentonites for the elements Al, K, Ca, Ti, Mn, Fe, Sr, Rb, and Zr was carried out to determine the usefulness of each in characterizing the ashes, and to substantiate the log correlations. The element combination, K-Ca-Ti, and the ratios Ca/Sr and K/Rb were found to be the most useful in the characterization and discrimination of these ashes. The early bentonites are rich in calcium, while the later ones are potassium-rich.

The maximum biotite grain size distribution, and the positive linear relationship between the former and Fe/Mn ratio, tentatively indicate a southwesterly source location for the earlier bentonites. A rough positive linear relationship between maximum biotite grain size and Ca/Sr ratio for the uppermost bentonite, and Fe/Mn ratio for

the lowest bentonite support the hypothesis that a variation in bentonite chemistry with distance from source is in part a function of grain size.

Cross sections and a fence diagram utilizing the bentonites as time planes show that the Viking Formation is divisible into Basal, Lower, and Upper sand units. Deposition of the first thin northwest-trending Basal sand north of Township 30, followed the eruption of the earliest volcanic ash. However, deposition of the northwest-trending Lower sand in the extreme southeast of the study area began slightly earlier. Deposition of this Lower sand continued and extended to the southern and central parts of the study area during the eruption and subsequent deposition of the 'C' volcanic ash, while north of Township 39, deposition of another northwest-trending Lower sand succeeded it. This latter sand unit is separated from the former by an area of non-sand deposition, around Townships 34 and 37, Ranges 15 to 22W4. A probable marine incursion, or a temporary cessation of sand deposition possibly related to the depositing mechanism arrested sand development almost throughout the study area. Eruption and preservation of the 'A' volcanic ash occurred at this time. In the extreme southwest and southeast parts of the study area, this event coincided with the early deposition of the Upper sand which eventually terminated Viking deposition south of Township 34. Thus, the Viking Formation is generally younger to the south than in the north.

Relative to these time planes, there seems to be no dominant direction of sand progradation. Rather, sand progradation appears to change with time. An early westerly (landward) progradation is indicated by the lower sand in the southeast part of the study area,

where sand development is also thickest. Slightly north of this area, a late northwesterly or easterly progradation is also apparent. Between Townships 40 and 44, an early northeasterly shift in deposition and a later dominant westerly progradation are also indicated for the Lower sand of this area. The Upper sand unit also shows both easterly and westerly directions of progradation. These suggest opposing directions of sand transport. In general, the rate of sand deposition and progradation appears to have been rapid.

ACKNOWLEDGEMENTS

The author is highly indebted to Dr. J. F. Lerbekmo for suggesting the thesis topic, and intimately supervising the study.

Many thanks are due the Research Council of Alberta for providing electric well logs, and the Energy Resource Conservation Board of Alberta for making well cores available.

Special thanks to Dr. R. Smith and Mr. K. Macleod for discussions on XRF instrumentation techniques.

Grateful acknowledgement is made to Dr. C. R. Stelck and Dr. R. D. Morton for helpful discussions and criticisms.

I extend more thanks to Mr. F. Dimitrov for part of the drafting, and Miss V. Stephansson who typed the manuscript.

The financial assistance provided by the University of Alberta (Account number 55-46150), the National Research Council Operating Grant A2127 and by a Department of Geology Graduate Teaching Assistantship are especially appreciated.

Lastly, permission to undertake graduate studies through a junior fellow sponsorship by the University of Nigeria, Nsukka, is very gratefully acknowledged.

TABLE OF CONTENTS

ABSTRACT	Page v.
ACKNOWLEDGEMENTS	viii.
CHAPTER	
1 INTRODUCTION	1
Objectives and Scope of Study	1
Some Viking Oil and Gas Pools in Central and East Central Alberta	3
Previous Studies	7
2 METHOD OF STUDY	10
3 GENERAL STRATIGRAPHY AND SEDIMENTOLOGY OF THE VIKING FORMATION	14
4 VIKING BENTONITES	17
Bentonite 'E'	20
Bentonite 'D'	23
Bentonite 'C'	23
Bentonite 'B'	27
Bentonite 'A'	27
5 CHEMICAL CORRELATION OF THE VIKING BENTONITES	33
X-ray Fluorescence Analytical Procedure	36
Sample Preparation	36
Calibration Procedure	37
Standards	38
Operating Conditions	38
Calibration Curves	39
Analysis of Unknowns	40
Discussion and Application of Results	40
6 SOURCE AREA OF THE VIKING BENTONITES	49
Biotite Grain Size Distribution	49
Method	49
Discussion	50
7 DEPOSITION OF THE VIKING SANDBODIES	57
Cross Sections	57
Fence Diagram	72
8 SUMMARY AND CONCLUSIONS	76

TABLE OF CONTENTS (cont'd)

BIBLIOGRAPHY	Page 79
APPENDICES	
A	83
B	93
C	94
D	96

LIST OF TABLES

Table		Page
Ia	Geographic and Stratigraphic Distribution of Some Observed Occurrences of Bentonite 'E'	24
Ib	Geographic and Stratigraphic Distribution of Some Observed Occurrences of Bentonite 'D'	24
II	Geographic and Stratigraphic Distribution of Some Observed Occurrences of Bentonite 'C'	26
IIIa	Geographic and Stratigraphic Distribution of Some Observed Occurrences of Bentonite 'B'	29
IIIb	Geographic and Stratigraphic Distribution of Some Observed Occurrences of Bentonite 'A'	29
IV	Percentage Chemical Composition of Bentonites Obtained by X-ray Fluorescence Analysis	41
V	Biotite Grain Size (mm) Distribution and Mn/Fe Ratios for Bentonites 'A', 'C', and 'E'	51

LIST OF FIGURES

Figure		Page
1.	Location map of study area	2
2.	Stratigraphic position of the Viking Formation in study area	4
3.	Distributions of some Viking oil and gas fields and sample wells	
4.	Stratigraphic correlation of the Viking . . . Formation in Central Alberta and neighbouring areas	15
5.	Stratigraphic positions of the bentonites . . .	21
6.	Log correlations of the observed occurrences of bentonites 'D' and 'E'	22
7.	Log correlations of the observed occurrences of bentonite 'C'	25
8.	Log correlations of the observed occurrences of bentonites 'A' and 'B'	28
9.	Subdivisions of the Viking sandbodies into Basal, Lower, and Upper sandunits using bentonites 'A', 'C', and 'E'	32
10.	Plot of Ca/Sr against Rb/K ratios	45
11.	Triangular plot of Ca, Ti, and K relative percent concentrations showing the fields of the five bentonite beds: A, B, C, D, and E	48
12.	Areal distribution of maximum biotite grain size for Bentonite 'E'	52
13.	Mn/Fe ratio maps of Bentonites 'E', 'C' and 'A'	54
14.	Source area for the Bentonites	55
15.	Plot of Ca/Sr ratio against maximum biotite grain size for Bentonite 'A'	56
16.	Location map of cross sections	58
17.	Cross section D-D'	in pocket
18.	Cross section E-E'	in pocket

LIST OF FIGURES (cont'd)

Figure		Page
19.	Sketch of gross lithologic distribution for sections D-D' and E-E'	63
20.	Cross section F-F'	in pocket
21.	Cross section G-G'	in pocket
22.	Sketch of gross lithologic distribution for sections F-F' and G-G'	66
23.	Cross section H-H'	in pocket
24.	Cross section I-I'	in pocket
25.	Sketch of gross lithologic distribution for sections H-H' and I-I'	70
26.	Cross section J-J'	in pocket
27.	Cross section K-K'	in pocket
28.	Sketch of gross lithologic distribution for sections J-J' and K-K'	73
29.	Fence diagram of the Viking Formation (Large scale fence diagram)	74 in pocket

CHAPTER 1

INTRODUCTION

Objectives and Scope of Study

A previous study by Tizzard (1974) and Tizzard and Lerbekmo (1975) resulted in the correlation of a thick coarse biotite-rich bentonite bed in well cores from the Viking Formation in the Suffield area of southern Alberta (Townships 19 to 26, Ranges 1 to 16W4M). Tizzard ~~also~~ further observed that the characteristic electric log signature of the bentonite (positive spontaneous potential and a low resistivity) was present in electric logs of wells to the west and north of his study area. This observation stimulated the present project. The thickness and composition of this bentonite apparently made it unique and easily differentiable from other thin fine bentonites within the formation in the Suffield area. The primary objective of the present study was to trace this bentonite horizon to the north and west of the Suffield area and thus attempt to establish a time datum in the Viking Formation on a more regional scale. This datum could then be used to interpret the depositional history of the Viking sandbodies which act as reservoirs for petroleum hydrocarbons. It was envisaged that a chemical correlation based on elemental analyses would be necessary to strengthen visual log correlation on a regional scale of wider observation points.

Figure 1 shows the geographic setting of the area of study located in south-central Alberta as well as that of Tizzard's study (1974). It embraces Townships 27 to 60, Ranges 8 to 28 west of the 4th meridian, covering an area of approximately 24,480 square miles. The presence of oil and gas fields insured availability of well logs and cores.

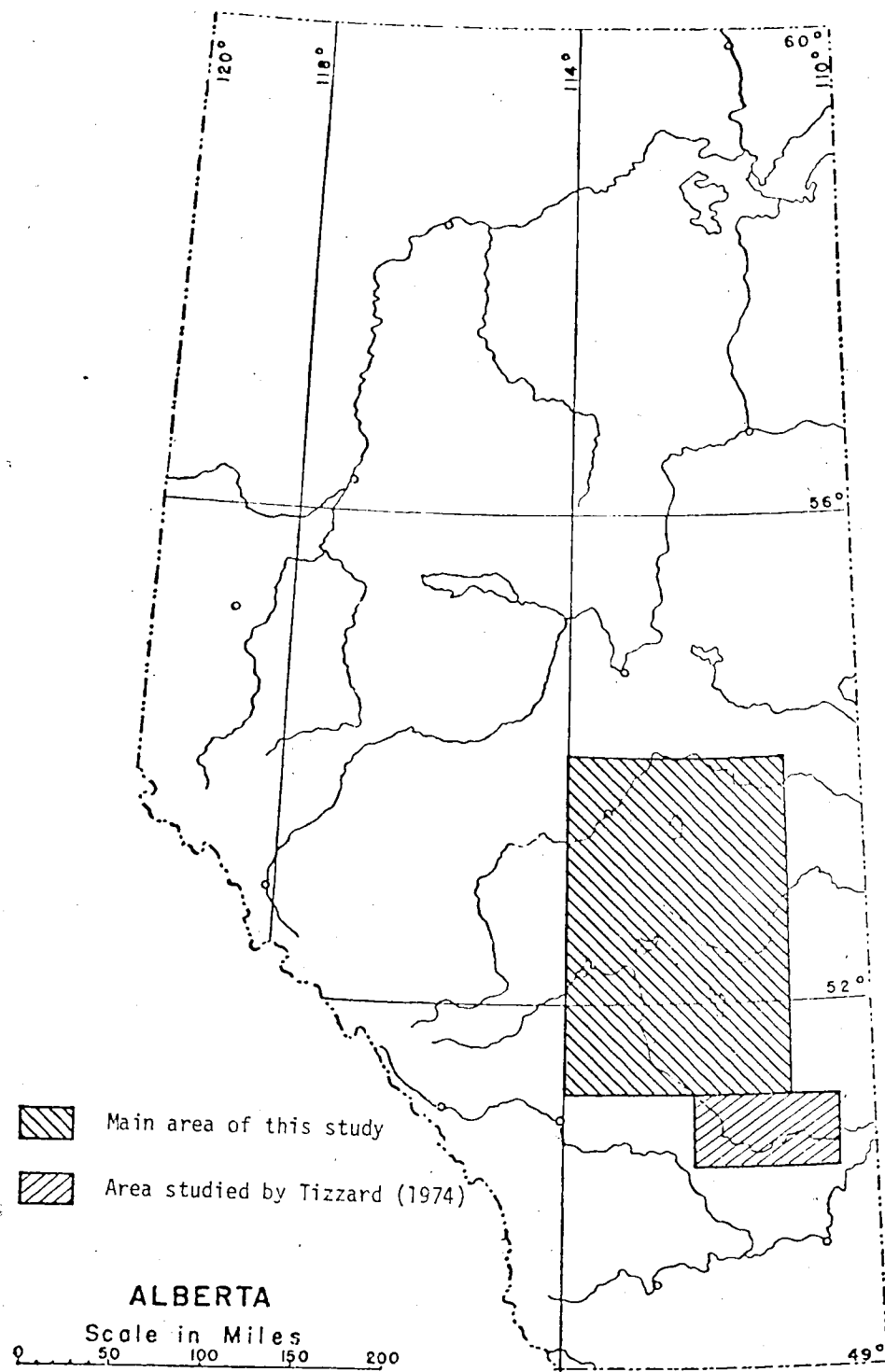


Figure 1. Location map of study area.

A preliminary study of the geographic distribution of bentonites as interpreted from well logs helped to delineate the study area.

Some Viking Oil and Gas Pools in Central and East Central Alberta

The stratigraphic position of the Viking Formation and the geographic distribution of some of its oil and gas fields are shown in Figures 2 and 3. The former is illustrated with electric logs from wells 10-32-28-16W4M and 11-33-59-27W4M, approximately 208 miles apart. They show a multiple sand development (2 or 3 sand bodies) characteristic of the formation in the study area. These sand bodies are intercalated with sandy shale, shale and silty shale units. However, exceptions occur, particularly in the east and west, where only one thin sand body developed. In other places, sand development is very poor to absent. Individual sand bodies vary in maximum thickness from 70 ft. to about 5 ft. The formation in the study area occupies a relatively constant stratigraphic position with respect to time. Regionally the formation is underlain by the Joli Fou shales, except in the south and west of Alberta. South of twp. 20 it loses its lithologic identity and is indistinguishable from the overlying Bow Island sands and shales - a stratigraphic equivalent of the Viking. To the west, the Joli Fou pinches out and the Viking Formation merges with the underlying Blairmore Group of the Foothills. The Lloydminster Shale overlies the Viking in the central Alberta Plains. Economically, the formation produces 11% of the gas reserves of Alberta and 2% of the oil reserves (Larson, 1969; White, 1960). The significant oil fields in terms of reserves include Joarcam, Joffre and Hamilton Lake.

The Joarcam field, discovered in 1949, is situated approximately

11-30-59-27MM

10-30-78-10MM

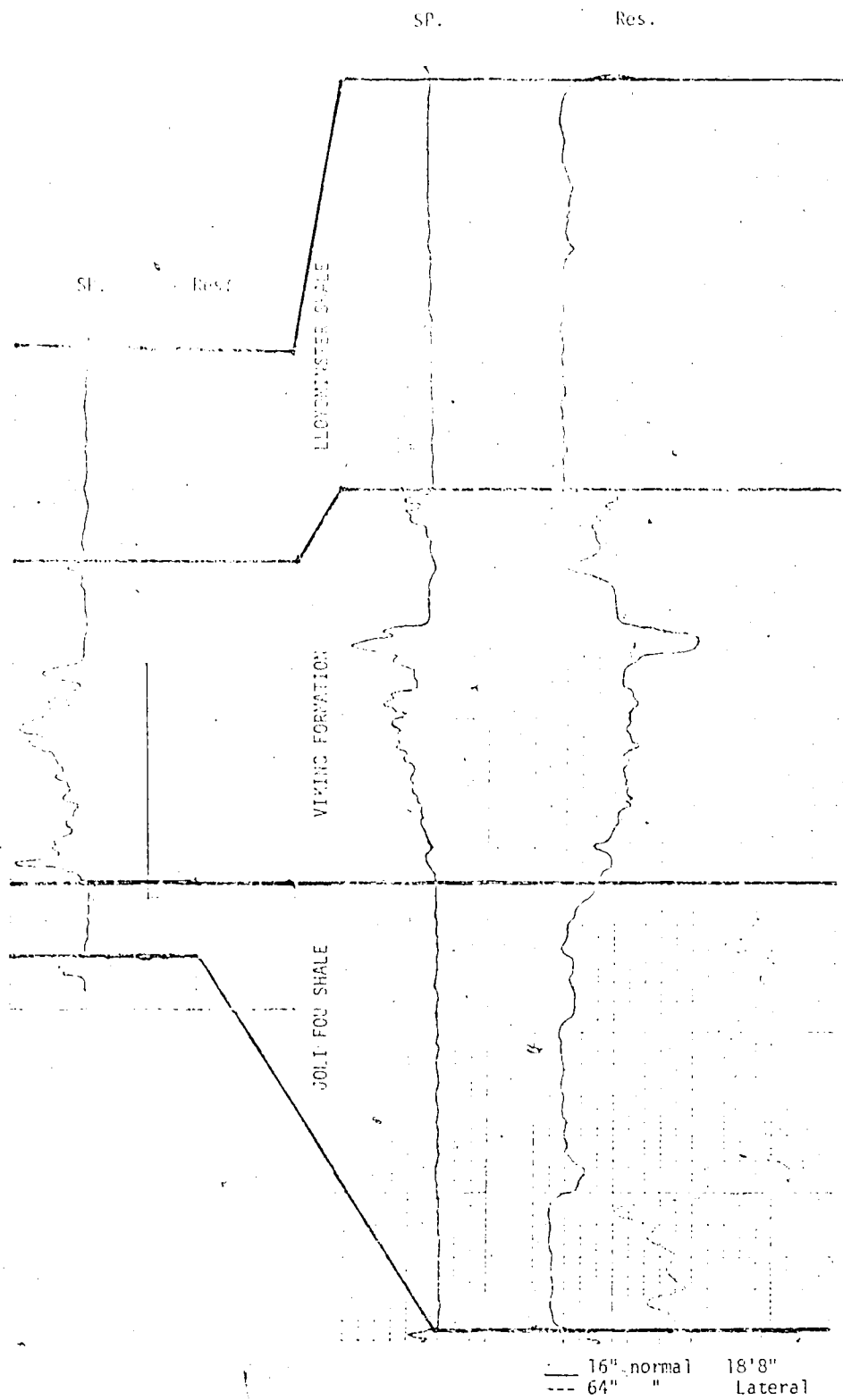


Figure 2. Stratigraphic position of the Viking Formation as observed in Electric logs.

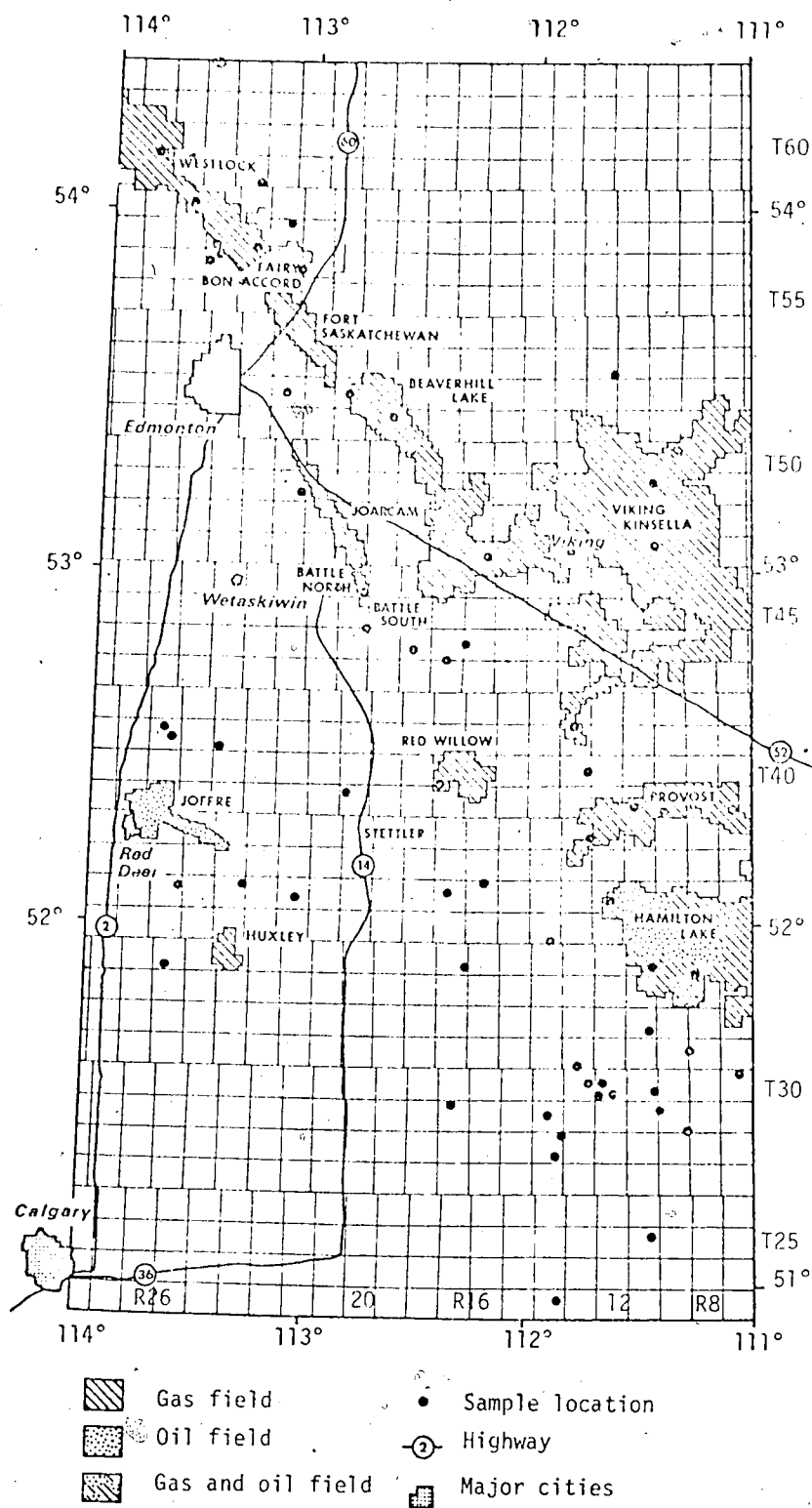


Figure 3. Distributions of some Viking Oil and Gas fields and sample wells.

20 miles southeast of Edmonton. It is roughly 30 miles long and 2 to 4 miles wide, occupying an area of approximately 20,000 acres. The stratigraphic trap-type reservoir sand, changes facies laterally to shale to the northeast on a homoclinal structure. The maximum reservoir thickness of the lower sandstone is about 30 ft. with an average of 21% intergranular porosity. Maximum oil zone thickness is 28 ft. with an average of 7 ft. The northern part of the reservoir is capped by a maximum gas zone 23 feet thick. Estimated oil in place is 150 million stb.

The Joffre field was discovered in 1953. It is located to the immediate east of Red Deer. The field is 23 miles long and about 1½ miles wide, an area of about 12,400 acres. The reservoir is a porous sand lens surrounded by impermeable sandy shale and shale beds. It is a lower Viking sandbody within a localized sand development along the Joffre - Gilby trend. Average porosity and permeability are 13.2% and 190 md. respectively. Estimated maximum reservoir thickness is 30 ft. with an average oil zone thickness of 10.2 ft. Estimated reserves (in-place) are 79 million stb.

The Hamilton Lake field discovered in 1952 is also a stratigraphic trap. The reservoir sand pinches out into shale. Two pools are present. The estimated in-place reserves of the lower Viking A and B pools adds up to 43 million stb.

Other oil fields in the study area include Battle North and South, and the Gilby - Bentley field to the immediate southwest of the study area.

The main gas fields in the area include Viking-Kinsella, Provost and Westlock. The Viking-Kinsella field is located about 85 miles

southeast of Edmonton and was discovered in 1914. The name Viking Formation hails from this locale. The reservoir sand pinches out up-dip due to a lateral facies change. It covers an approximate area of 342,000 acres. Maximum gas pay thickness of the lower sand is 15 ft. with an average of 5.3 ft. Porosity is 24%, and estimated in-place reserves are 947 bcf.

The Main Provost field, discovered in 1946, is situated 140 miles southeast of Edmonton near the Alberta-Saskatchewan border. The Provost lower Viking reservoir sand is a lens enclosed in impermeable shale. Average porosity is 22.1%, and the maximum gas pay thickness is about 20 ft. with an average of 5.8 ft. The field occupies an area of approximately 416,600 acres with estimated in-place gas reserves of 813 bcf.

The Westlock field is located 80 miles northwest of Edmonton and is the northwesternmost field within the northwest-southeast trend of the Viking gas fields. It was found in 1949. The reservoir trap is an up-dip porosity pinchout due to facies change from sandstone to shale. It covers an approximate area of 200,400 acres. The lower and upper Viking sands are both productive. In-place estimated reserves of the non-associated gas is of the order of 456.5 bcf. Other gas fields in the area include Beaverhill Lake, Calmette-Vimy pools of Westlock, Fairy Dell Bon-Accord, Fort Saskatchewan, Huxley, Provost (Kessler and Brownsfield areas) and Red Willow. The foregoing show the economic importance of the Viking Formation.

Previous Studies

The Viking Formation in central and southern Alberta and south-

western Saskatchewan has been fairly intensively studied. This is obviously related to its economic significance. However, the focus of most published works appears to have centered on the environment of deposition. Gammell (1955) used petrographic evidence to interpret the regional composition of the formation. He further used the stratigraphic position and relationships of the Viking Formation to conclude that the sandbodies were generally regressive. Roessingh (1959) attempted an east-west correlation of Viking bentonites in the southern plains of Alberta. He concluded that the bentonites occurred approximately within the same stratigraphic position relative to the top of Viking Formation. He used this and the presence of chert pebbles and microstructural features in the formation to argue against regression and diachronism of the sandbodies, and preferred deposition by turbidity currents in agreement with Beach (1955, 1956). De Wiel (1956) and Jones (1961) opposed this idea and proposed deposition in a shallow epicontinental sea. Tizzard and Lerbekmo (1975) used sedimentary structures and the shape of the spontaneous potential logs to interpret these sandbodies as barrier bars, an idea previously forwarded by Stelck (1958) and for the correlative Muddy Sandstone, Berg and Davis (1968) and Shelton (1973). A tidal current origin of the Viking Formation sands in the Dodsland-Hoosier area of southwest Saskatchewan was advanced by Evans (1970) using geographic orientation, imbricate arrangement and size of the sandbodies. Koldijk (1976) used the absence of sedimentary characteristics of a normal barrier island, matrix supported conglomerates, and the sizes of the phenoclasts and matrix, as evidence supporting deposition offshore by ephemeral currents generated by severe storms for the Gilby Viking 'B' sandstone.

This degree of variation in the environment of deposition for the Viking sands is likely too extreme to be correct, but suggests the possibility of a complex dynamic depositional system within the Viking sea. This is likely because it was a "transitional" sea arising from the merger of the northern Boreal and the southern Gulf of Mexico seas. However, a detailed diagnosis of the anatomy and morphology of these sandbodies relative to Viking time planes in different areas will aid and promote an integrated interpretation and understanding of the various depositional environments in the Viking sea.

Stelck (1958, 1975) established the age of the Viking as middle Upper Albian using both macro and micro faunal evidence from the shale beds underlying and overlying the Viking Formation.

CHAPTER 2

METHOD OF STUDY

More than 1,000 electric well logs (spontaneous potential and resistivity) were examined at the Alberta Research Council, Edmonton, to establish the characteristic resistivity signature in the study area of the datum bentonite used by Tizzard (1974). This was possible because of the high well density due to the presence of oil and gas fields in the area. This exercise enabled a tentative decision on the presence or absence of the bentonite in the wells to be made, and gave a general idea of its geographic distribution. Copies were made of logs which indicated the bentonite horizon.

During this phase of the study, it was observed that the bentonite signature was missing in some logs while more than one signature showed up in others. The former situation implies that the volcanic ash does not occur in the area, or is intercalated with clay shale, in which case it is not easily differentiated on the log. If deposited on a sand bottom, the ash would be easily eroded by the more severe currents or waves common in such a depositional environment. The presence of more than one signature suggests that several bentonite horizons are present in the formation, as reported by some earlier workers (Roessingh, 1959; Jones, 1961; Tizzard and Lerbekmo, 1975). In logs where the bentonite type signals showed up, their depths and stratigraphic relationships to the sandbodies were noted. This facilitated later correlation with the cored wells in the Viking Formation.

The second phase of the study involved the inspection of more than 1500 well data cards at the Research Council. This was under-

taken to note wells with cores from the Viking interval, the location of the cores, and to see if bentonite intervals indicated in the logs were actually cored. Unfortunately, some wells which show the distinct bentonite signals were not cored. In some of the wells with both bentonites and cores, the bentonite horizons were either purposely skipped during coring operations or coring did not reach them. These are evident on inspection of the cored intervals.

For well logs without bentonite signals, the cored intervals were also recorded, since bentonite presence cannot be completely ruled out on the basis of lack of log characteristics. A total of 102 cored wells emerged from this search. This by no means implies that only 102 Viking cored wells are present in the study area.

The third phase of this study was to check the physical presence of the bentonites at the corehouse of the Alberta Energy Resources Conservation Board in Calgary. This initially involved examining the cores at the log indicated depths for the bentonite(s) and collecting bentonite samples. A base map of Alberta containing well locations, obtained from Canadian Stratigraphic Services, facilitated simultaneous location of the wells on map as the cores were examined. This made it possible to follow the geographic distribution of the bentonite(s) in the field and, most importantly, controlled the sequence in which the cores were examined. Figure 3 shows the locations of cored wells examined. It was observed that some of the cores whose logs showed the distinct bentonite signal did not contain the bentonite at the expected log depth. When these cores were examined, some were highly reworked or bioturbated at this horizon. This suggests that the volcanic ash was completely mixed with the sediments by organisms. However, the

ash still differentiates the horizon chemically from the rest of the bed, as the characteristic signal still shows up. In other cores, this horizon is missing in the core boxes, suggesting that if originally present, the sample was either lost or had been completely sampled by earlier workers. In those wells with cores but no bentonite log signal, bentonite horizons were usually found. In most of these cases they were located in thin shale units intercalated in sand, or at the immediate base of a sand, suggesting that the spontaneous potential of the sands must have in part obliterated the effect of the bentonites; hence they were not distinct in the logs. In others the bentonites were very thin and as such could not influence the electric log curve.

In general, 65 of the 102 cored wells contained bentonite horizons. Ten of these contained the initial bentonite of interest (a thick coarse biotite-rich bentonite) (see Appendix A for location and field descriptions). The maximum number of horizons observed in a single well varied from one to eight. Variations in thickness ranged from less than 1 in. to 24 in.. Qualitatively, the texture varies from coarse to fine. The bentonites occur in various lithologies ranging from shale through silty shale and sandy shale to rarely sand, and in varying degrees of preservation and purity. Four of the bentonites are rich in biotite, but the biotite grain size varies from medium to coarse; the thicknesses range from 1 in. to 24 in.. This examination thus showed the presence of more than one thick coarse biotite-rich bentonite as opposed to the observations of Tizzard and Lerbekmo (1975). These four bentonites constituted the bentonites of interest in this study.

Poor core recovery, different coring techniques and the

restriction by the Energy Resources Conservation Board on sample size allowed to be collected (1 cubic inch) limited the quantity of samples taken, which later influenced some analyses of interest.

Where practicable the collected samples were split into three unequal parts. Two were used for X-ray fluorescence and biotite grain size analyses. Small samples only were used for the former; the third split was preserved for reference.

The various techniques used in characterizing volcanic ashes and pyroclasts were exhaustively reviewed by Smith and Westgate (1968). It was felt that analyses of some major, minor and trace elements in the Viking bentonites using the XRF technique would characterize them, and hence make correlation possible. This would not only confirm or contradict their log correlations, but would serve to correlate them uniquely in the study area. Time planes would be established for the Viking Formation, and these used to discuss the time stratigraphic correlation and depositional history of the formation. Lerbekmo and Campbell (1969) studied the White River Ash in the Yukon Territory. They hypothesized that the relationship of chemistry to distance from source is a function of particle size and density. This was supported by the low ^{87}Rb ratio related to decrease in particle size of the glass fraction.

A few grain size analyses were carried out in the present study to examine the biotite-size distribution. This was to test the above hypothesis and determine in relative terms the approximate location of the eruption centre, as grain size will in general decrease with distance from eruptive centre. The distribution might also be used to characterize the bentonites.

CHAPTER 3

GENERAL STRATIGRAPHY AND SEDIMENTOLOGY OF THE VIKING FORMATION

The name 'Viking' was first used by Slipper (1917) to denote the gas reservoir sands of the Viking-Kinsella field in east-central Alberta. The sand is stratigraphically located approximately 140 ft. above the base of the Colorado Group in this area; it is underlain by marine Joli Fou shales, and overlain by the marine Lloydminster Shale. Usage of the term has been extended to include similar sandbodies in about the same stratigraphic position in central Alberta and southwestern Saskatchewan. The Viking was initially classified as a member of the Colorado Group (Hunt, 1954; Reasoner and Hunt, 1954; Gammell, 1955). It was later upgraded to the rank of formation (Magditch, 1955; Stelck, 1958). Figure 4 shows the stratigraphic position of the Viking Formation and its correlatives in Alberta and neighbouring areas.

The Colorado sea covered the continental Upper Manville in mid-Cretaceous time and the Joli Fou Shale was the first marine deposit in this sea. It is well marked on electric logs throughout the area of study. The westward pinchout of this formation resulted in a merging of the overlying Viking with the underlying non-marine Manville Group to form the Blairmore Group of the Foothills. To the south also, the Joli Fou becomes indistinguishable from the Viking Formation and both grade into the Bow Island Formation. Regionally the Viking Formation thins progressively to the northeast and east and finally pinches out in the vicinity of St. Paul (Twp. 58, Rge. 9W4M) (Gammell, 1955). Farther to the northeast and in the northwest of Alberta, sands in similar stratigraphic position are

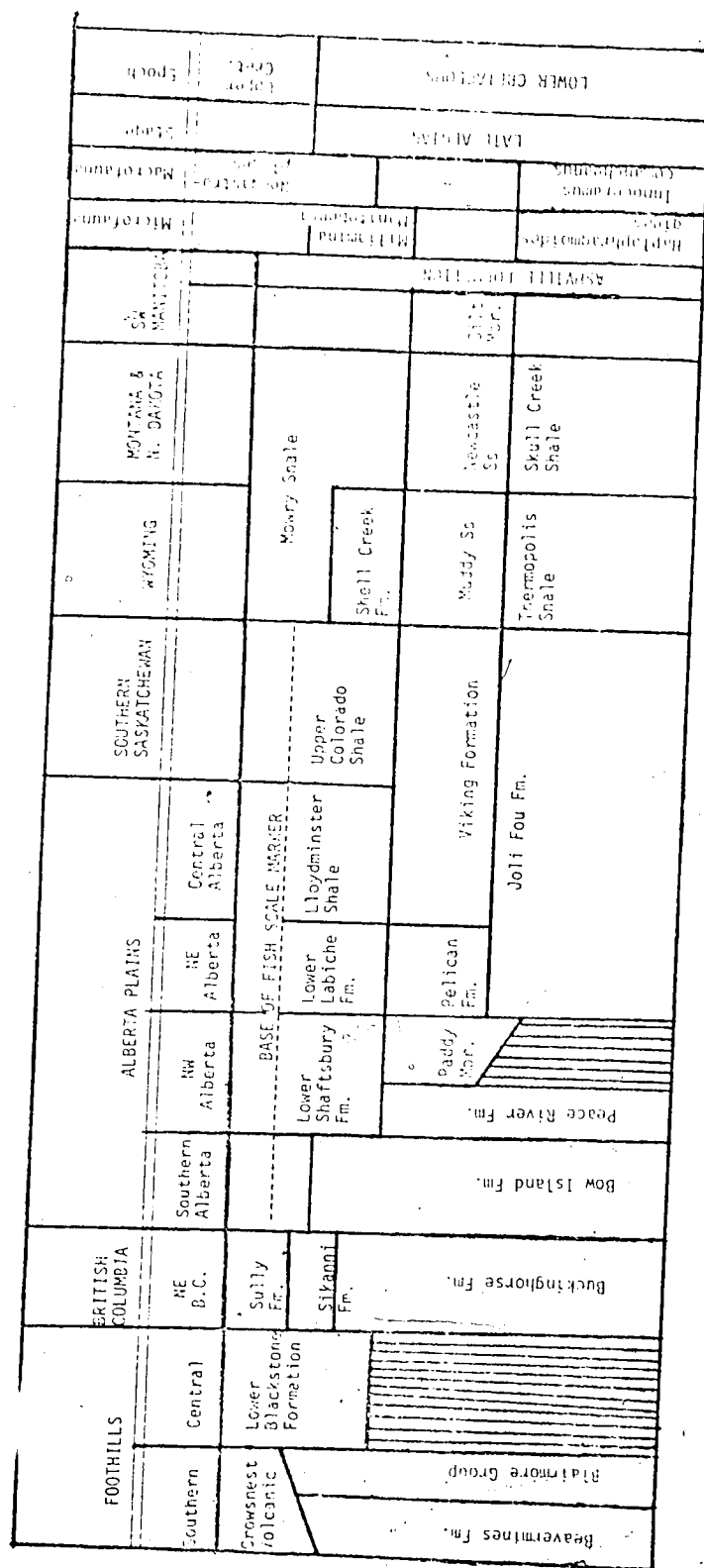


Figure 4. Stratigraphic Correlation of the Viking Formation in Central Alberta and Neighbouring Areas.

respectively known as the Pelican Formation and the Paddy Member of the Peace River Formation (in part). The Viking Formation is a time stratigraphic equivalent of the Silt Member of the Ashville Formation in southwestern Manitoba, the Muddy Sandstone of Wyoming, and the Newcastle Sandstone of Montana and northern Dakota (Stelck, 1958, 1975; Glaister, 1959; Rudkin, 1964; Berg and David, 1968).

Stelck (1958, 1975) used macro-and micro-faunal evidence in the formations above and below the Viking Formation to establish the age of the Viking Formation as of the mid-Upper Albian stage of the Lower Cretaceous. The underlying Joli Fou Shale carries the foraminifera Haplophragmoides gigas and the pelecypod Inoceramus comancheanus (a migrant form from the Gulf of Mexico). These species have been established to range from the uppermost Mid-Albian to the lowest part of the Upper Albian. The overlying shales yield the foraminifera Miliamina manitobensis and much higher the endemic Neogastrolites. The intercalated Viking Formation was therefore considered likely to be mid-Upper Albian. Potassium-argon absolute ages obtained from biotite and sanidine in some Viking Formation bentonites range from 94-118 ma. with an average of 100 ± 2 ma. (Tizzard, 1974).

Regionally the Viking consists of a sequence of proto-quartzites rich in chert pebbles, interbedded with dark grey to grey siltstones and bentonitic shales. Ironstone concretions occur in the sand units. Locally a chert pebble stringer or a chert-rich sandstone commonly tops the formation. The sandy unit varies greatly in coarseness and thickness. In general, it thins and becomes finer-grained and more shaly towards the northeast and east, suggesting a western or southwestern major source area for the clastics. The average thickness of the formation in the study area is about 75 ft.

CHAPTER 4

VIKING BENTONITES

Most published works on the Viking Formation mention the occurrence of bentonites or bentonitic shales. However, only a few workers have attempted detailed log correlations of these beds in spite of their time-stratigraphic significance. If their geographic distribution is regionally widespread and correlatable, time planes could be established facilitating interpretations of the depositional history of the formation.

Roessingh (1959) noted the presence of a bentonite horizon in approximately the same stratigraphic position, relative to the top of the Viking Formation, in well Parkland 4-12-15-27W4M and in a Grassy Island Lake well in twp. 32 rge. 7W4M in south-central Alberta. He used this relationship to contradict the concept of a transgressive or regressive Viking sand, as the sand did not transgress the time plane. The presence of more than one bentonite horizon in the formation, and the large distance between the wells (17 twps.) make his correlation doubtful and vague.

Jones (1961) observed and correlated in some detail two bentonitic shales within the Viking Formation and one bentonite horizon closely above it, in southwestern Saskatchewan. He labelled them beds 1, 2 and 3 in decreasing stratigraphic age. Bed 3 forms a useful stratigraphic marker when present. They vary in thickness from 1/10th in. to 18 in. He correlated bed 3, 1 in. thick, located at the top of the Viking in Husky Phillips Prelate well 11-28-23-25W3M, to a ½ in. thick bentonite located in shale two feet above the Viking in well Imperial Marengo 11-21-29-27W3M. He used the two-foot difference in shale thickness

between the two wells 38 miles (61 km) apart in a north-northwest direction to conclude that the Viking Formation is slightly diachronous nearly parallel to the paleo-strandline, and that one would expect greater diachronism at right angles to the shifting strandline. In Imperial Marengo 11-21-29-27W3M, bed 3 is 19 ft. above the Viking sand. He used this fact to suggest inclusion of an upper shale within the formation. The results of the present study support his findings.

Evans (1970) correlated two impure light-grey soapy shale units with a high bentonite content in wells located between twps. 32 and 30, rges. 20 to 28 W3M. His "MN" bentonitic shale, 3 ft. thick, merges with the bentonitic Joli Fou Formation, becoming unrecognizable north of the area. He interpreted this loss of identity to be related to subaqueous erosion prior to deposition of the overlying shale. Above this horizon, and located at the base of a sandstone unit, is his "K" bentonitic shale 1 to 3 ft. thick. Using these bentonitic shales, he, in part, established the imbricate linear arrangement of the Viking Formation sandbodies in the Dodsland-Hoosier area of southwestern Saskatchewan.

Tizzard (1974) noted the presence of several bentonite horizons in the Suffield area. He correlated one of them, a coarse biotite-rich bentonite 6-12 in. thick and established a time datum for the Viking Formation in this area. He further obtained potassium-argon radiometric ages from the biotite and sanidine in the bentonite from two wells 42 miles apart (11-23-23-14W4 and 1-13-23-7W4). Dates from the former ranged from 94-98 ma., and 95-118 ma. for the latter. This variation could in part be either related to the dating technique, or suggests a possible involvement of another stratigraphic bentonite horizon. He did

not recognize more than one coarse biotite-rich bentonite horizon in his area, whereas three such horizons occur north of his area. He used the coarse bentonite time datum to deduce a slightly diachronous nature for the Base of the Fish Scales marker and for the Viking Formation.

From 1 to a maximum of 8 bentonite horizons were seen in most Viking Formation cores examined in the present writer's area. They are stratigraphically distributed through a maximum thickness interval of 100 ft. Two wells (Great Basins et al. Bruce 10-13-47-16W4M and 10-13-30-11W4M) show 8 and 6 bentonite horizons respectively. This suggests a wide stratigraphic distribution of volcanic ash in Viking times, emphasizing the need for correlating them where and when possible. However, the apparent variations in composition, thickness, degree of preservation, grain size and geographic distribution of these bentonites initially restricted consideration of horizons of interest to five, and finally to three. In general, their color ranges from whitish-grey to darker grey and greenish-grey in places. Some of the darker grey and greenish-grey bentonites are either interlaminated with shale or sparingly mottled, and bioturbated. These colors in part reflect the varying degrees of diagenetic alternation to which they have been subjected for the past 100 ma. in relation to their initial composition. Megascopically they are biotite-rich although the biotite grain size varies from coarse to fine. This is related to the initial composition and distance from the eruptive centre, which in turn is related to the paleo-wind directions at the time of deposition. The lithology of enclosing sediment varies from shale to silty shale, sandy shale, siltstone and silty sand, and rarely clean sandstone. This complex

lithology association is due to the interaction between the nature and rate of sediment supply on one hand, and sediment dispersal in the environment at time of deposition.

Figure 5 shows the approximate stratigraphic positions of some of the bentonite beds. They have been labelled A to E in increasing stratigraphic age for convenience. Figures 6 to 8 show some log correlated bentonite horizons observed in the map area. Tables 1 to 3 show the well name, location, cored interval, depth and thickness of the bentonitic beds.

Bentonite 'E'

Figure 6 shows the subsurface correlation of this bentonite. It is the oldest of the bentonite set and lies at the base of the Viking Sandstone in well Ponderay et al. Youngstown 12-19-31-9W4M, and in silty shale approximately 26 ft. below the base of the Viking Sandstone in well 10-13-30-11W4M. It will hence be regarded as the basal Viking bentonite marking the end of Joli Fou and the beginning of Viking time. It occurs at a depth of 2907 ft. and 2903 ft., respectively, in cores and logs of these wells, which are approximately 12 miles apart. Thickness varies from 24 in. in the former well to 15 in. in the latter, decreasing westwards and northwards. Color varies from light grey to dark grey. Texture is generally coarse, but the biotite grain size varies from .27 mm to .42mm. In Ponderay et al. Youngstown 12-19-31-9W4M, the bentonite fines upward, suggesting gravity differentiation of the minerals in relation to their settling velocities. This bentonite was found in cores between twps. 29 and 53, rges. 8 to 27 W4M. South of this area it is well marked in most logs, while northwards it becomes

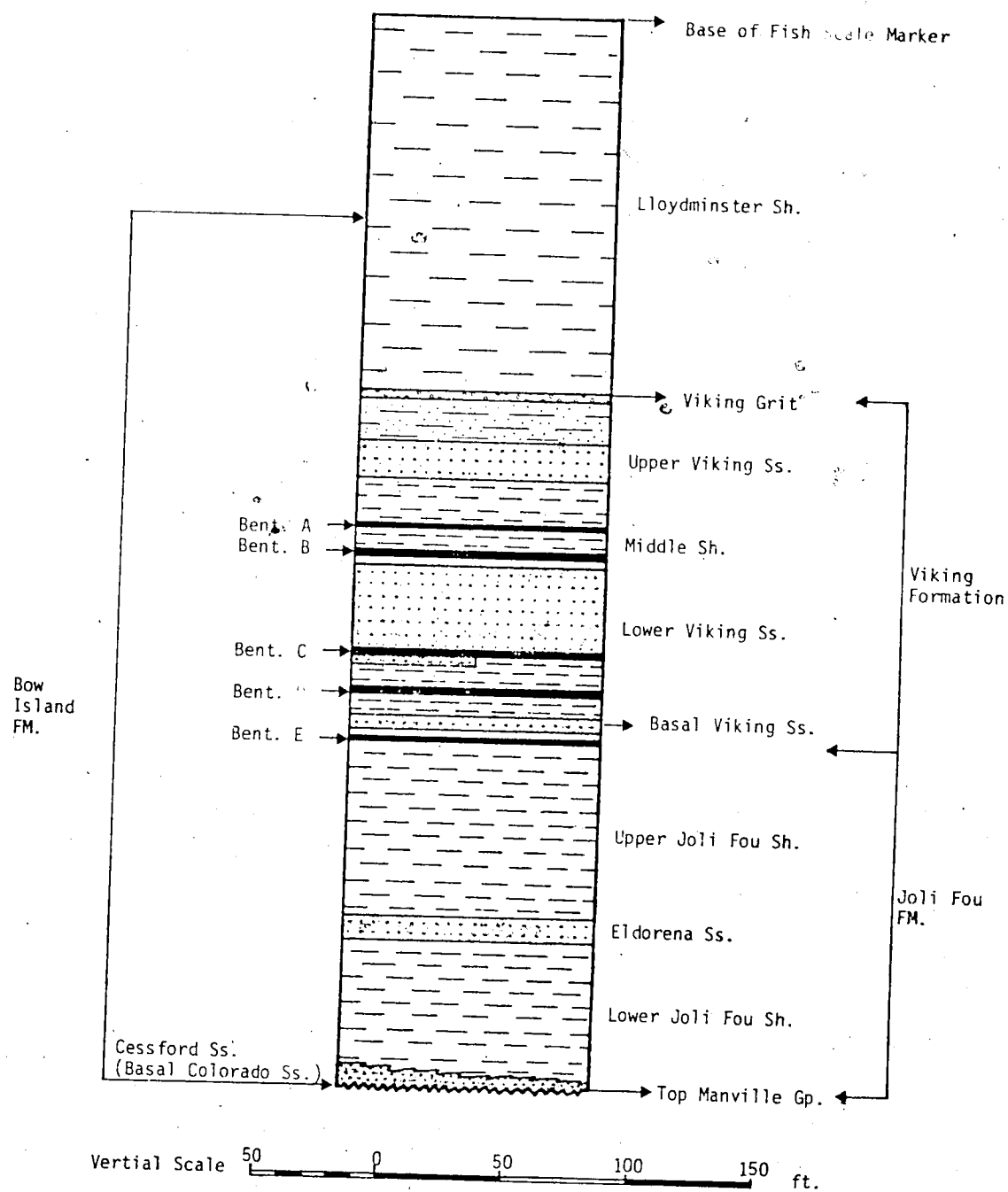


Figure 5. Schematic terminology diagram for the Viking Formation of East-Central Alberta (average stratigraphic position of units)

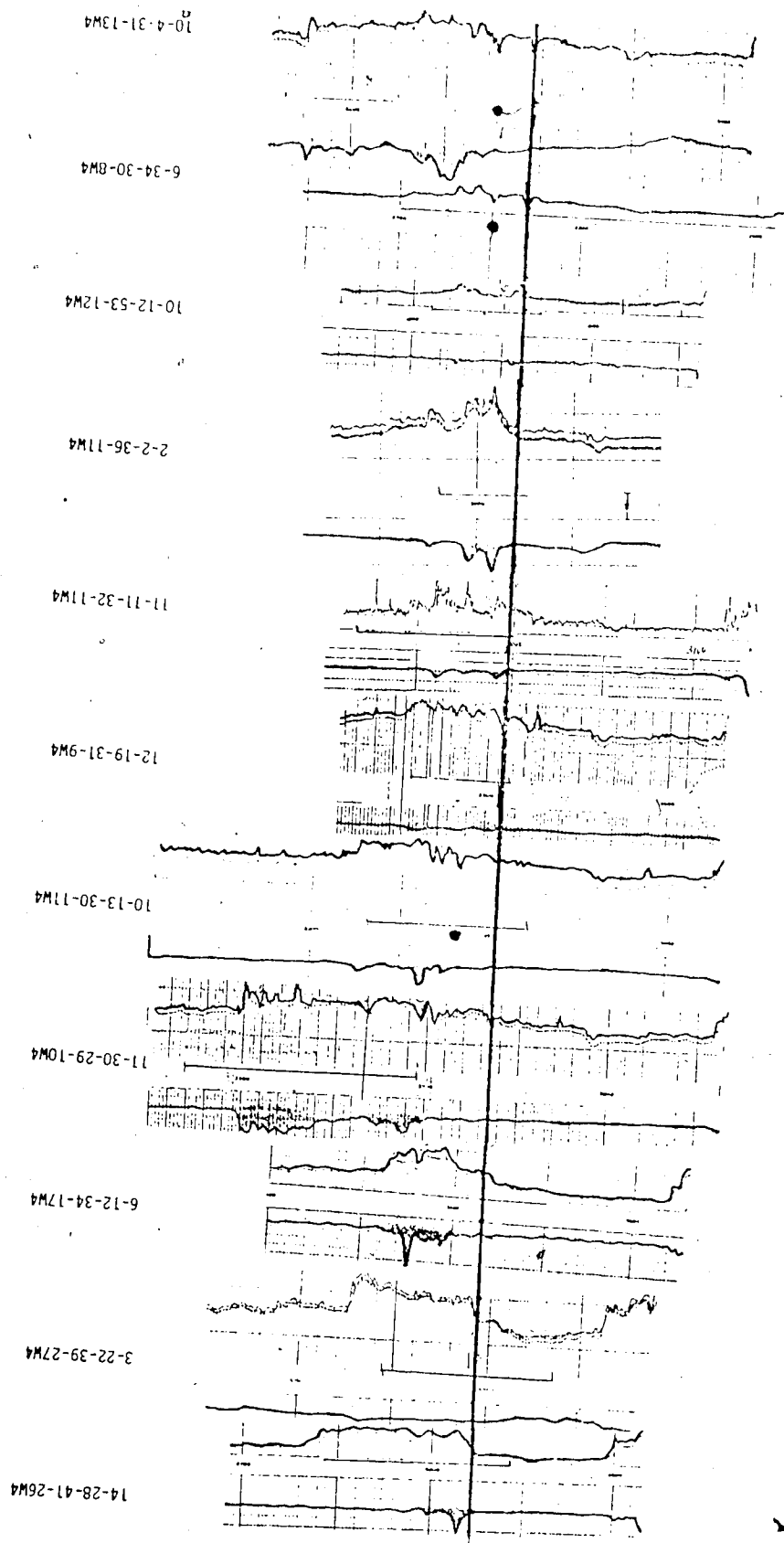


Figure 6. Log correlations of the observed occurrences of Bentonites 'D' and 'E'. Datum line = Bentonite 'E'; (o) = Bentonite 'D'.
Log Characteristics: left-SP; right-Resistivity.
I = cored interval.

indistinct. Chemical correlation suggests its presence in well Minerals Plains 10-12-53-12W4M. In general, its stratigraphic position is fairly constant in that it occurs consistently below the Viking sandbodies. Table Ia shows the distribution of the bentonite as observed in some wells in the area.

Bentonite 'D'

Figure 6 and Table Ib show the stratigraphic position and geographic distributions of this bentonite. It is located approximately 20 ft. above the basal bentonite in wells 10-13-30-11W4M and 6-34-30-8W4M. In cores, it occurs at depths of 2882 ft. and 2750 ft. in these wells, respectively. In the former, it is 6 ft. below the base of the Viking sand. It is light grey in color and the thickness varies from 3 in. in the former well to 6 in. in the latter. Biotite grain size is medium to fine sand. This bentonite appears to be geographically restricted, as it was not observed in other cores, and as such was not very useful in this study.

Bentonite 'C'

Figure 7 and Table II show the stratigraphic and geographic distribution of this horizon. In well C.S. Sulpetro et al. Farrel 6-12-34-17W4M it is encountered at a depth of 3479 ft., 35 ft. above the basal bentonite. In West Coast Sun Petro Smole 11-30-29-10W4M it occurs at a depth of 2895 ft., 36 ft. above the basal bentonite. In the above locations it is preserved approximately at the base of another Lower Viking sand unit. Its maximum thickness is about 15 in.

TABLE Ia. Geographic and Stratigraphic Distribution of some Observed Occurrences of Bentonite 'E'

	Well Name	Location	Cored Interval (ft.)	Depth Bentonite Observed (ft.)	Thickness (in.)	Remarks
1.	Amoco B-1 Youngstown	6-34-30-8W4M	2700-4800	2770	12	biotite-rich coarse bentonite
2.	-	10-13-30-11W4M	2831-2920	2903	15	"
3.	Ponderay <u>et al.</u> Youngstown	12-19-31-9W4M	2860-2913	2907	24	"
4.	C.S. Fenner	11-11-32-11W4M	2918-2996	2996	>12	"
5.	C.S. Sulpetro <u>et al.</u> Farrel	6-12-34-17W4M	3390-3550	3516	12	"
6.	Mosbacher <u>et al.</u> Provost	2-22-36-11W4M	2980-3027	3023	3	coarse to medium bentonite
7.	Great Plains Cdn. <u>Sup.</u> Lacombs	14-28-41-26W4M	4743-4843	4821	4	coarse bentonite
8.	Mineral Plains	10-12-53-12W4M	1810-1870	1861	1	"

TABLE Ib. Geographic and Stratigraphic Distribution of some Observed Occurrences of Bentonite 'D'

1.	Amoco B-1 Youngstown	6-34-30-8W4M	2700-4800	2750	6	medium to coarse bentonite
2.	-	10-13-30-11W4M	2831-2920	2882	3	medium bentonite

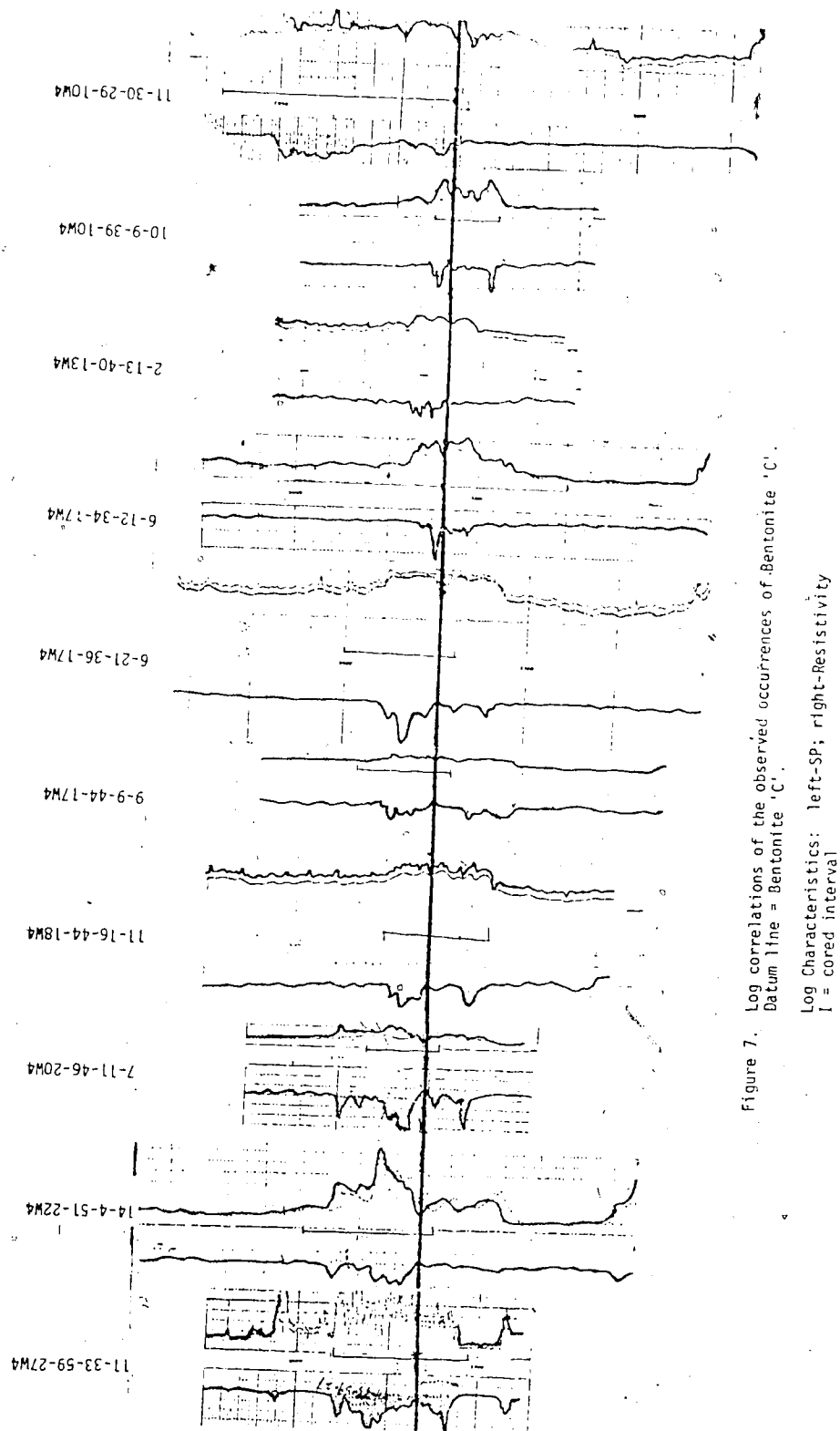


TABLE II. Geographic and Stratigraphic Distribution of some Observed Occurrences of Bentonite 'C'

	Well Name	Location	Cored Interval (ft.)	Depth Bentonite Observed (ft.)	Thickness (in.)	Remarks
1.	West Coast Sun Petro Smole	11-30-29-10W4M	2769-2895	2895	6	medium bentonite
2.	-	10-13-30-11W4M	2831-2920	2866	6	"
3.	Cesa PCP Leo	6-21-36-17W4M	3399-3459	3455	12	medium to fine
4.	C.S. Sulpetro et al. Farrel	6-12-34-17W4M	3390-3550	3479	3	medium to coarse
5.	Dome HBOG Provost	10-9-39-10W4M	2710-2747	2719	15	medium to fine
6.	Crown Tanner	7-11-46-20W4M	3215-3255	3246	14	fine to medium
7.	Texas Pacific Patterson #1	14-4-51-22W4M	3270-3340	3330	6	fine bentonite
8.	-	8-30-47-10W4M	2150-2199	2166	20	fine bentonite interlaminated with shale
9.	Provo Brown Field	7-16-39-11W4M	2642-2702	2684	2	medium bentonite

in well Dome HBPG Provost 10-9-39-10W4M at a depth of 2718 ft. The bentonite is medium to fine in texture, including the biotite grain size. Color varies from whitish grey to dark grey. It can be easily picked in some logs between twps. 29 and 59, rges. 10 to 27 W4M. To the south of this it possibly runs into an area of sand deposition where preservation was unusual because of erosion by currents, tides, or waves.

Bentonite 'B'

In wells Provo Halliday 13-11-28-14W4M and Calstan Handhills 10-36-28-14W4M, a coarse biotite-rich bentonite is located in silty shale approximately 6 ft. above the main Lower Viking sand. This horizon is about 80 ft. above the basal bentonite in the former well. It occurs at depths of 3131 ft. and 3107 ft., respectively, in these wells, and the thickness ranges from 3 in. to 4 in. In cores, it is restricted to these wells. However, it can be picked in logs in the immediate vicinity of these wells where it is possibly thicker. Deposition in sandy environments in other places possibly accounts for its restricted occurrence, making it not very useful in this study. Its stratigraphic position and geographic distribution are shown in Figure 8 and Table IIIa.

Bentonite 'A'

This is the youngest coarse biotite-rich bentonite in the Viking section encountered in the area. Figure 8 and Table IIIb show its stratigraphic and geographic distributions. In well Mobil Matzim 11-23-23-14W4M it lies in silty shale approximately 32 ft. above the

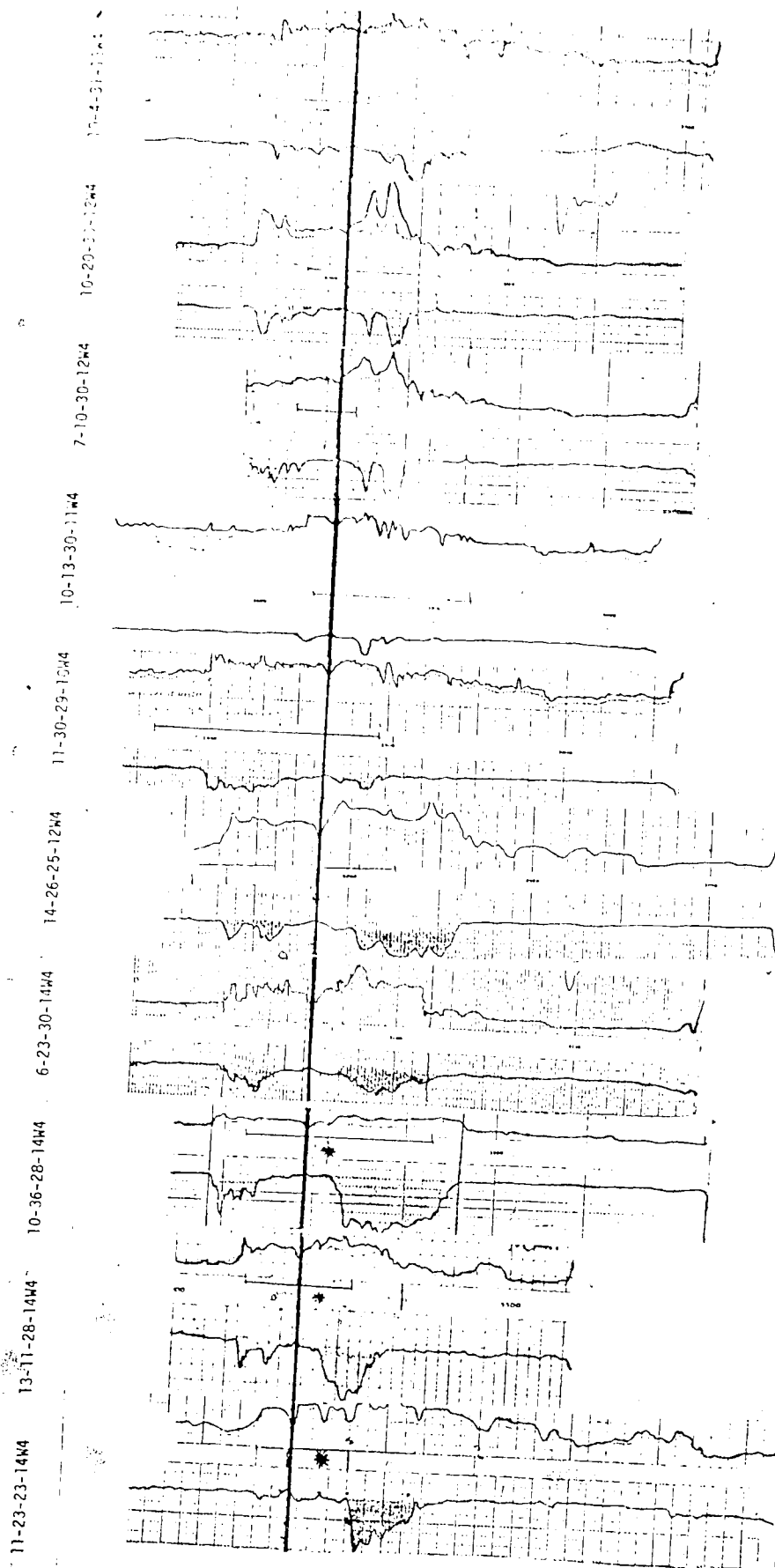


TABLE IIIa. Geographic and Stratigraphic Distribution of some Observed Occurrences of Bentonite 'B'

Well Name	Location	Cored Interval (ft.)	Depth Bentonite Observed (ft.)	Thickness (in.)	Remarks
1. Provo Halliday	13-11-28-14W4M	3065-3160	3131	3	coarse biotite-rich
2. Calstain Handhills	10-36-28-14W4M	3062-3164	3107	4	"

TABLE IIIb. Geographic and Stratigraphic Distribution of some Observed Occurrences of Bentonite 'A'

1. Mobil Matzim	11-23-23-14W4M	2630-2716	2647	12	biotite-rich bentonite
2. H.B. Cessford	14-26-25-12W4M	2710-2760 2784-2825	2785	12	"
3. Provo Halliday	13-11-28-14W4M	3065-3160	3116	9	"
4. Calstain Handhills	10-36-28-14W4M	3062-3164	3097	6	"
5. West Coast Sun Petro Smole	11-30-29-10W4M	2769-2895	2866	6	"
6. Fina Handhills	7-22-29-14W4M	3051-3113	3088	12	"
7. Westlock et al. Rothdale	11-7-30-12W4M	304-3150	3101	6	"
8. Oak Alta. Can. Pet. Richdale	7-10-30-12W4M	3025-3058	3042	2	"
9. Dome 10E Willdunn	6-23-30-14W4M	3088-3210	3153	6	"
10. -	10-20-30-12W4M	2987-3060	3007	3	"

main Lower Viking sand, and about 10 ft. above bentonite 'B' and approximately 90 ft. above the basal bentonite. Here it is 12 in. thick and at a depth of 2647 ft. This is in agreement with Tizzard (1974). Farther north from this well, at Provo Halliday 13-11-28-14W4M, it occurs at a depth of 3116 ft. and is 9 in. thick and in part inter-laminated with shale at the base. Here it is about 15 ft. above the 'B' bentonite and 95 ft. above the basal bentonite. In general bentonite 'A' lies stratigraphically in a silty shale unit between the Lower and Upper sandbodies. Shades of color vary from whitish grey to dark grey. Biotite grain size ranges from .38 to .53 mm., while thickness varies from 3 in. to 12 in.. It is equivalent to the thick bentonite in the Suffield area (Tizzard and Lerbekmo, 1975). Generally it is identifiable in logs between twps. 23 and 35, rges. 8 to 27 W4M. North of this area it is probably located in shale beds above the Viking sands on the assumption that its distribution extended to this area.

The three bentonites E, C, and A divide the Viking sand bodies into three stratigraphic entities. These have been designated the 'Basal', 'Lower' and 'Upper' sands for convenience and in agreement with the subdivisions of some earlier workers (Figure 9). The thin Basal sand lies between bentonites 'E' and 'C', and the Lower sand between 'C' and 'A' in some wells, while transgressing 'C' in other wells. The Upper sand, where present, overlies the 'A' bentonite.

From field evidence, it appears that bentonite 'A' is geographically restricted to the southern part of the study area, while 'C' is restricted to the north. However, 'E' extends across both areas, providing a link between the other two. Thus, a transitional area exists in which the three horizons overlap in space and can be reliably

picked in cores and well logs (e.g., 11-13-30-11W4M, 11-30-29-10W4M).

An attempt to correlate these bentonites with those used by Jones (1961), and Evans (1970), proved unsuccessful. This is due to distance and the poor sand development in their areas.

In spite of the seemingly unique stratigraphic positions of the bentonites, it is possible to misidentify them and hence produce wrong correlations. It was considered necessary to confirm and support the log correlations by chemical correlation, expecting that the bentonites could be distinguished from one another since they represent different events from either the same or different volcanic centres.

10-24-27-16W4

6-12-27-15W4

6-21-36-17W4

9-16-47-20W4



Figure 9. Subdivisions of the Viking sandbodies into Basal, Lower and Upper sand units using Bentonites A, C, and E. (Left - SP., Right - Resistivity)

CHAPTER 5

CHEMICAL CORRELATION OF THE VIKING BENTONITES

Bentonite is a smectite-rich clay formed from the decomposition of volcanic ash. Thus, it represents the products of a geologic event at a point in time. If this "time-point" can be identified and correlated over considerable distances, a time datum can be established. Such a datum can be useful in solving many geologic problems, including the depositional history of the adjacent beds.

However, if the bentonite horizons are numerous and occur in the subsurface at close stratigraphic levels with possible limited lateral extent, and with variations in thickness, texture and degree of preservation, correlation becomes difficult; more so if they are of similar aspect. An independent objective criterion is required to test any proposed correlation. The chemistry of volcanic products has been found to satisfy this objective on the assumption of slight, if any, regional variation in post-depositional alterations.

Criteria for characterizing and discriminating between volcanic products abound in the literature, and were critically reviewed by Smith and Westgate (1968). In brief, they include ranges and modal values of the refractive index of glass shards; mineralogy and relative abundance of the phenocryst assemblage; bulk chemical composition involving major, minor or trace elements; chemistry of the volcanic glass fraction; and the stratigraphic position, degree of weathering, thickness and grain size. These have been variously used by many workers with varying degrees of success.

Smith and Westgate (1968) analyzed the chemistry of volcanic glass

from the Mazama ash (6600 yrs.) in the U.S.A. and Canada, the Glacier Peak ash (ca. 12,000 yrs.), the St. Helens "Y" ash (ca. 3000 yrs.) and the Bridge River ash (ca. 2500 yrs.) using the electron microprobe. They found the following elements to be useful in identifying all of the ashes: namely Ca, K, Fe, Ca, K, Na.

Quaternary rhyolites and dacites (obsidian and pumice) from California were examined using X-ray fluorescence analyses by Jack and Carmichael (1969). Sr, Rb, Zr, Y, Nb, and Pb were found to generally characterize the acid extrusive rocks. However, acid volcanic rocks from two volcanic centres could not be characterized or distinguished chemically.

Borchardt et al. (1972) studied the glass fractions of the Bishop and Pearlette-like ashes of Pleistocene age in the U.S.A., using the neutron activation technique. They found Mn and Sm to be the discriminating elements.

Merriam and Bischoff (1975) studied the trace element composition of the ash and pumice from some occurrences in southern California using X-ray fluorescence. On the bases of the Sr, Zr and Rb concentrations present, they correlated this ash to the Pleistocene Bishop ash.

Lerbekmo et al. (1975) studied the composition of the ilmenites of the Recent White River ash, Yukon Territory, using the microprobe technique. They found that the Fe, Ti, and Mg concentrations were the most discriminatory.

Yen (1976) examined the compositions of the biotite phenocrysts in the tuffs from the Green River Formation (Eocene) of Utah using X-ray fluorescence. He found the following element and oxide ratios, $\frac{\text{Mn}}{\text{Fe}} + \text{Mg}$, $\frac{\text{Mn}}{\text{Ti}}$, and $\frac{\text{FeO}}{\text{MgO}}$ to be best for discriminating between individual tuff beds.

From the few studies mentioned above, one notices the absence of consistency in the choice of differentiating criteria, discriminating elements and analytical techniques. Yet each study produced satisfactory results. This suggests that there are no simple rules governing the characterization of volcanic products as they are unique events in time and space related to different geologic settings. One can only conclude that volcanic products can be treated within the above general framework. It is also important to note that most of the above volcanic products are surface exposures and relatively young (Eocene - Recent). They have not been long subjected to strong post-depositional changes, and we should therefore expect their primary chemistry to be only slightly modified, if at all. Their occurrence in outcrops also facilitates visual correlation.

On the other hand, since the subsurface Viking Formation bentonites are of Lower Cretaceous age, one would expect some diagenetic modifications of their chemistry. The occurrence of a maximum of 8 bentonite horizons within an approximate vertical interval of 100 ft. gives an average rate of eruption, or at least preservation, of one per, 12 ft. of sediment. Possible similarities in composition between some or all of the bentonites would further compound the problem of chemical correlation. In view of the above possible problems, and consideration of the stratigraphic and geographic distributions of the bentonites, attention was focused on A, C and E bentonites.

The composition and small sample size led to the choice of the X-ray fluorescence technique to study these bentonites. It seemed likely that the ratios of some major, minor or trace element combinations would possibly differentiate them irrespective of possible attendant

diagenetic changes.

X-ray Fluorescence Analytical Procedures

Basic X-ray fluorescence theory and instrumentation are treated by Kiley (1960), Norrish et al. (1967) and Jenkins (1967). A Phillips manual vacuum X-ray spectrometer PW 1410/00/10/60/70 was used for the analyses. A tungsten target X-ray tube, evacuated X-ray path (0.15 - 0.2 torr), flow proportional counter with methane argon (P10) gas, pentaerythritol (PET) analyzing crystal, pulse height analyzer (PHA), and a strip chart recorder were used for elements lighter than titanium. A scintillation counter was used for the titanium. For elements heavier than titanium, the X-ray path was not evacuated, a scintillation counter, lithium fluoride 220 (Lif 220) analyzing crystal, and a molybdenum target X-ray tube were used. Appendix B shows the operating conditions for the analyses.

Sample Preparation

Samples selected for analyses varied in texture and biotite grain size. This variation was taken into consideration during grinding. Samples were ground in an NV Tema swingmill, type T.100A. Grinding times varied from 60 seconds to 30 seconds at full speed for coarse and medium textured samples respectively. This was in an attempt to approach uniformity in grain size. The effect of grinding times was evaluated by comparative XRF runs on the same sample with different grinding times. No difference was observed in peak counts.

Approximately 1½ to 2 g. of sample was diluted with acetone to prevent disaggregation and sample splitting and to ensure coherence.

The preparation was then put in a 1½ in. diameter copper cylinder and pressed at about 50,000 psi into a cellulose-backed briquette for about 3 minutes. This presents a smooth surface to the incident X-ray beam. A preliminary study of a set of briquettes in which the volume of ground bentonite was varied from 1 to 4 volumes showed no difference in counting rates. This served as a control for the sample size and thickness used for the analyses.

Calibration Procedure

Comparisons of the peak height and element concentration in a known standard to the peak of the element in the unknown sample, provide a good approximation of the element concentration in the unknown sample as shown in equation 1 below.

$$C_{sp} = \frac{I_{sp}}{I_{st}} \times C_{st} \quad (1)$$

where C_{sp} = unknown concentration of an element in the sample

C_{st} = known concentration of an element in the standard

I_{sp} = peak intensity of X-ray line of the element in the sample

I_{st} = peak intensity of X-ray line of the element in the standard

This procedure was used for calibration.

The relatively large number of samples, related to the regional nature of the study, and availability of standards limited analysis to some of those elements previously found useful by previous workers who used XRF in characterizing volcanic rocks.

Standards

Appendix C shows the analyses and standards employed for calibration in this study. The problem of interference effects necessitates that standards used for calibration be similar in composition and texture to the unknowns. A series of bentonites previously analyzed in the Dept. of Geology, University of Alberta, certain U.S.G.S. standards, and analyzed samples of the Pierre Shale, were available in the Dept. of Geology, University of Alberta, and used for this study. Thus, relatively good standards in terms of similarity in composition were available for Al, K, Ca, Ti, Mn, and Fe, while less similar standards had to be used for Rb, Sr, and Zr.

Operating Conditions

An initial survey scan over the fluorescence spectrum of the samples was made to ascertain the presence of elements of interest. This was followed by three specific scans.

The first scan was at a speed of $1^{\circ}2\theta$ per minute, using LIF 220 analyzing crystal, molybdenum X-ray tube, scintillation counter at 1000 volts, 60 Kv and 50 ma, and a spinner; 2θ range covered was from 25° to 45° .

In the second scan, the X-ray path was evacuated (0.15 - 0.2 torr), and the sample scanned from $40^{\circ}2\theta$ to $147^{\circ}2\theta$ at a speed of $1^{\circ}2\theta$ per minute using a tungsten X-ray tube, gas flow proportional counter at 1600 volts, PET analyzing crystal and power of 50 Kv and 50 ma.

The third scan was at a speed of $1^{\circ}2\theta$ per minute with the X-ray path evacuated (0.15 - 0.2 torr) and sample scanned from $25^{\circ}2\theta$ to $45^{\circ}2\theta$, using a tungsten X-ray tube, scintillation counter at 1000 volts, PET

analyzing crystal and power of 55 Kv and 50 ma..

These scans confirmed peak heights and determined background positions for the following element groups respectively: Zr, Sr, Rb, Fe, Mn; Al, K, Ca; and Ti.

Samples were run two at a time for each element. The total counts on the K alpha peak and the background for each element were obtained over a fixed time which was 10 seconds for Fe and Ca, and 100 seconds for the others. For Fe and Ca this counting time was repeated 10 times, giving a uniform counting time of 100 seconds for all elements. The background count for each element was determined by finding the average count of two background positions one on each side of the peak. This, however, assumes symmetry in the location of these points with respect to the peak position. In practice this is not always the case, and as such constitutes a possible source of small error for which it is difficult to compensate. Background readings for the elements Sr, Rb, and Zr were obtained directly from the spectrum using the x-y recorder because of the high background intensity associated with low 2θ values. The net peak count was obtained by subtracting the average background count from the peak count.

The analysis for each element was conducted separately and in one day without changing the settings on the instrument so as to minimize instrument drift. Reproducibility of the intensity was achieved by making repeated counts and by using a long counting time.

Calibration Curves

The calibration 'curves' are shown in Appendix D. They were constructed by plotting net peak intensities against weight percent of

the elements and drawing a linear regression line through the points. The scatter is relatively small for Zr, Ca, Ti, Rb, Mn, and K, whereas a somewhat greater scatter of points exists for Al, Fe, and Sr, but is still considered reasonably good. Factors possibly responsible for scatter include heterogeneity of the samples, interfering radiations, and previous and present analytical errors. All prepared samples are subject to certain types of errors (weighing, mixing, contamination or incipient cracks). Since the standards were prepared and analyzed by someone else, these error sources are difficult to evaluate.

• Analysis of Unknowns

This involved the determination of peak heights and background readings, and obtaining the net peak height as for the standards. The net peak height was then used to determine the corresponding concentration of element from the calibration curve or regression equation. The results are given in terms of weight percent of elements so as to be consistent with the present accepted methods of presenting rock analysis. Table IV shows the element concentrations of bentonites A, B, C, D, and E.

Discussion and Application of Results

A primary object of this study was to find out whether or not some chemically significant differences exist between the bentonites. If such were present, it would serve to characterize them and could be utilized as a correlation tool.

Table IV shows that only slight variations exist in the element concentrations of the bentonites. In general, trace element (Zr, Sr, Rb)

TABLE IV. Percentage Chemical Composition of Bentonites Obtained by X-ray Fluorescence Analysis

Sample No.	K	Ca	Ti	Zr	Sr	Rb	Mn	Fe	Al
VB2647A	0.67	0.96	0.38	0.027	0.058	0.004	0.008	3.7	2.74
VB2785A	1.27	1.8	0.5	0.027	0.046	0.005	0.03	5.3	13.3
VB3116A	1.53	0.87	0.61	0.027	0.059	0.008	0.01	2.41	14.5
VB3097A	0.87	0.86	0.43	0.031	0.052	0.004	0.008	2.44	11.3
VB2866A	0.85	0.51	0.5	0.023	0.049	0.005	0.016	3.07	15.9
VB3088A	0.76	1.98	0.43	0.042	0.077	0.004	0.013	2.88	12.4
VB3101A	0.98	0.67	0.67	0.022	0.036	0.006	0.064	4.97	13.2
VB3042A	0.74	0.78	0.5	0.019	0.018	0.004	0.081	5.58	16.3
VB3153A	1.36	0.72	0.75	0.031	0.056	0.008	0.01	2.97	14.6
VB3007A	0.91	0.66	0.64	0.021	0.029	0.005	0.049	4.35	12.96
AVERAGE	0.99	0.98	0.54	0.03	0.048	0.005	0.029	3.77	12.72
VB3131B	1.32	0.23	0.32	0.023	0.059	0.005	0.001	1.91	16.4
VB3107B	0.65	0.25	0.25	0.021	0.061	0.004	0.001	2.44	14.5

TABLE IV (cont'd)

Sample No.	K	Ca	Ti	Zr	Sr	Rb	Mn	Fe	Al
VB2895C	0.33	0.78	0.72	0.043	0.038	0.003	0.086	4.18	14.9
VB2866C	0.4	0.72	0.90	0.042	0.041	0.003	0.056	3.76	11.6
VB3479C	0.28	0.88	1.08	0.041	0.066	0.002	0.021	3.69	12.9
VB3455C	0.37	0.81	0.44	0.03	0.054	0.002	0.014	2.38	11.1
VB2719C	0.18	0.87	0.98	0.061	0.058	0.002	0.004	2.75	12.5
VB3330C	0.5	0.5	0.71	0.056	0.054	0.003	0.011	2.33	15.0
VB3246C	0.73	0.75	0.76	0.058	0.054	0.003	0.027	3.04	11.1
VB2684C	0.73	0.83	1.60	0.051	0.034	0.004	0.011	2.55	12.0
VB2166C	0.25	0.92	0.70	0.04	0.06	0.003	0.006	3.02	11.1
AVERAGE	0.42	0.78	0.88	0.047	0.051	0.003	0.026	3.1	12.5
VB2882D	0.01	1.06	0.29	0.024	0.049	0.001	0.09	4.09	10.9
VB2750D	0.01	1.08	0.40	0.028	0.049	0.002	0.063	4.01	10.8

TABLE IV (cont'd)

Sample No.	K	Ca	Ti	Zr	Sr	Rb	Mn	Fe	Al
VB2903E	0.72	1.94	0.68	0.023	0.051	0.005	0.075	4.32	10.1
VB2770E	0.25	1.19	0.47	0.021	0.045	0.003	0.053	3.70	14.2
VB2907E	0.7	1.61	0.89	0.025	0.043	0.005	0.043	3.86	10.1
VB2998E	0.29	1.27	0.51	0.012	0.034	0.003	0.293	6.75	11.8
VB3023E	0.85	0.96	1.43	0.02	0.029	0.006	0.035	3.79	14.8
VB4821E	1.92	2.02	1.42	0.032	0.043	0.006	0.05	3.37	17.4
VB1861E	1.26	2.22	1.35	0.047	0.056	0.007	0.049	4.57	14.5
VB3516E	0.95	1.46	0.75	0.024	0.038	0.005	0.09	4.91	15.3
AVERAGE	0.87	1.6	0.94	0.026	0.042	0.005	0.086	4.41	13.5

variations within and between bentonites are small. However, the observed concentrations may reflect primary compositions. Variations in the Al concentration were also minimal. Lack of significant variations in the concentrations of these elements between bentonites limits their usefulness in characterizing and correlating the bentonites chemically.

Concentrations of the element groups Mn, Fe; and K, Ca, and Ti, show greater variations between bentonites. Variations within bentonites are also present but not significant. The within bentonite variation could be mainly due to post-depositional alterations, contamination and possibly to analytical errors. The between bentonite variations could be related to the primary compositions of the volcanic ashes.

Mn concentrations for the bentonites vary almost linearly with Fe, as reflected in the average concentrations (A; Mn = 0.029, Fe = 3.77); (C; Mn = 0.026, Fe = 3.1); (E; Mn = 0.086, Fe = 4.41). This relationship reflects their geochemical affinity.

On the average, bentonite A is relatively high in potassium (.99%), medium in Ca (.98%), and low in titanium (.54%). On the other hand, bentonite C is low in potassium (.42%), medium in Ca (.78%), and high in titanium (.88%), while bentonite E is relatively high in Ca (1.6%), and medium in titanium (.94%) and potassium (.87%). These variations suggest that some combination of these elements might successfully correlate the bentonites.

Trace elements have a strong diadochic substitution for major elements, e.g., Mn-Fe, Sr-Ca, Rb-K, Mn-Ca and so on. It was therefore thought that geochemically similar pairs of elements would constitute

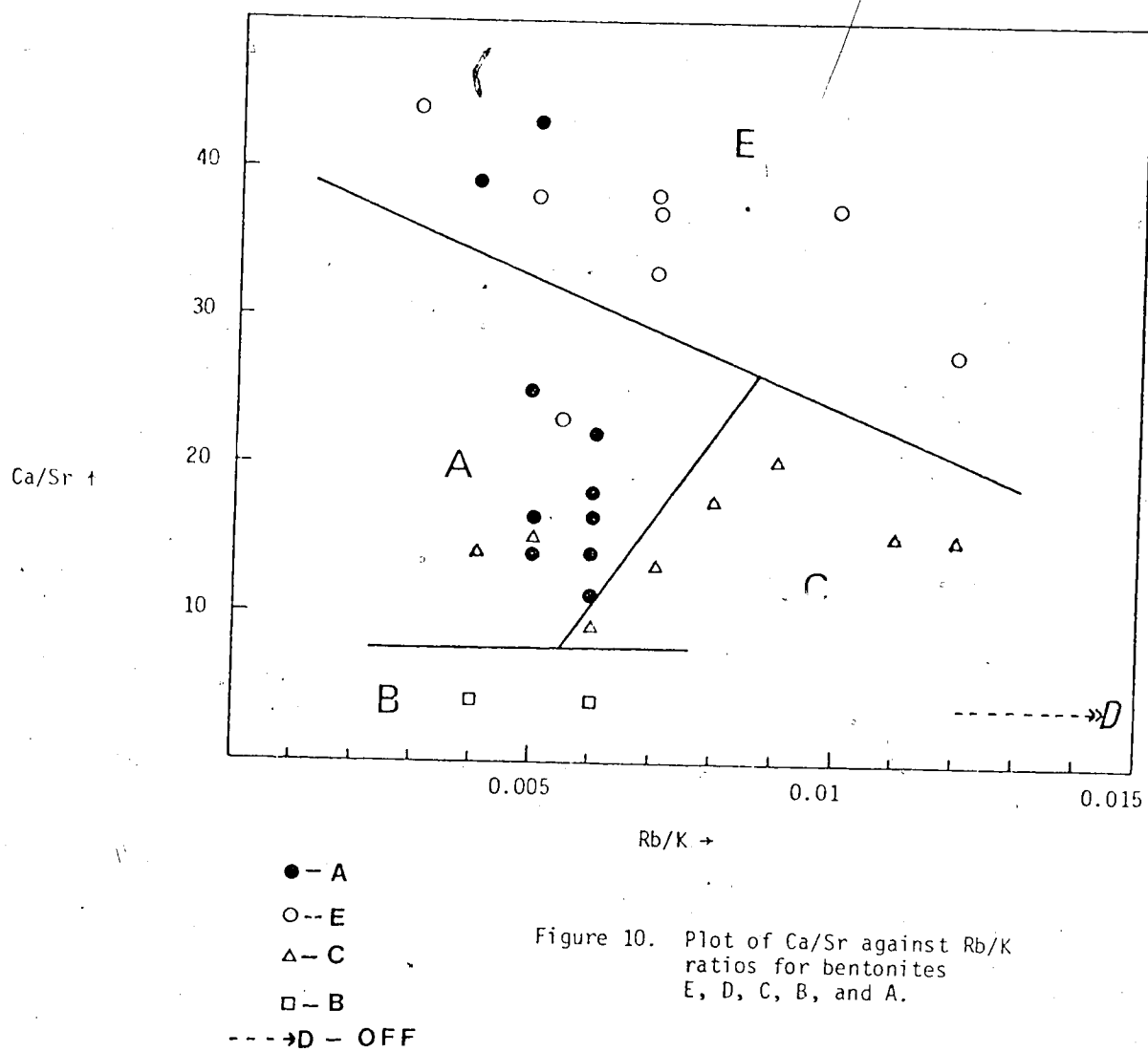


Figure 10. Plot of Ca/Sr against Rb/K ratios for bentonites E, D, C, B, and A.

a useful correlation tool. Any variation in the origin of either of the two elements as a function of time should be apparent. However, possible variations in mineralogy related to the environment of deposition and diagenesis should also affect the degree of substitution and should be expected, assuming a high degree of analytical precision was obtained. Reasoning along these lines, element ratios of Ca/Sr and Rb/K for 31 samples were plotted on an X-Y coordination system to see if the bentonites would be differentiable. Figure 10 shows the scatter plot. It differentiates the 5 bentonites fairly well, but 6 samples overlap, representing approximately 19% of the total. Samples VB2785A and VB3042A fall into the field of bentonite 'E'; VB1861E falls into the field of bentonite 'A'; and VB2684C, VB3246C and 3455C fall into the field of bentonite 'A' (see Tables I-III for sample locations). Furthermore, individual groups show considerable scatter, especially bentonite 'E'. Diagenetic effects and analytical errors are possible sources of scatter.

Relative concentrations of Ca, K, and Ti were converted to relative percent and plotted on a triangular diagram, Figure 11. This diagram differentiates the bentonites better than the above element ratios. However, three discrepancies occur, representing 13% of the samples. Potassium content of the bentonites appears generally to increase with decrease in geologic age. Bentonites 'E', 'D', and 'C' are the oldest and lowest in K content, while bentonites 'A' and 'B' are younger and higher in K content. In this diagram, the fields show relatively smaller scatter.

These two plots were the only ones, among many that were tried, that correlated well with the log correlations of the bentonites (see

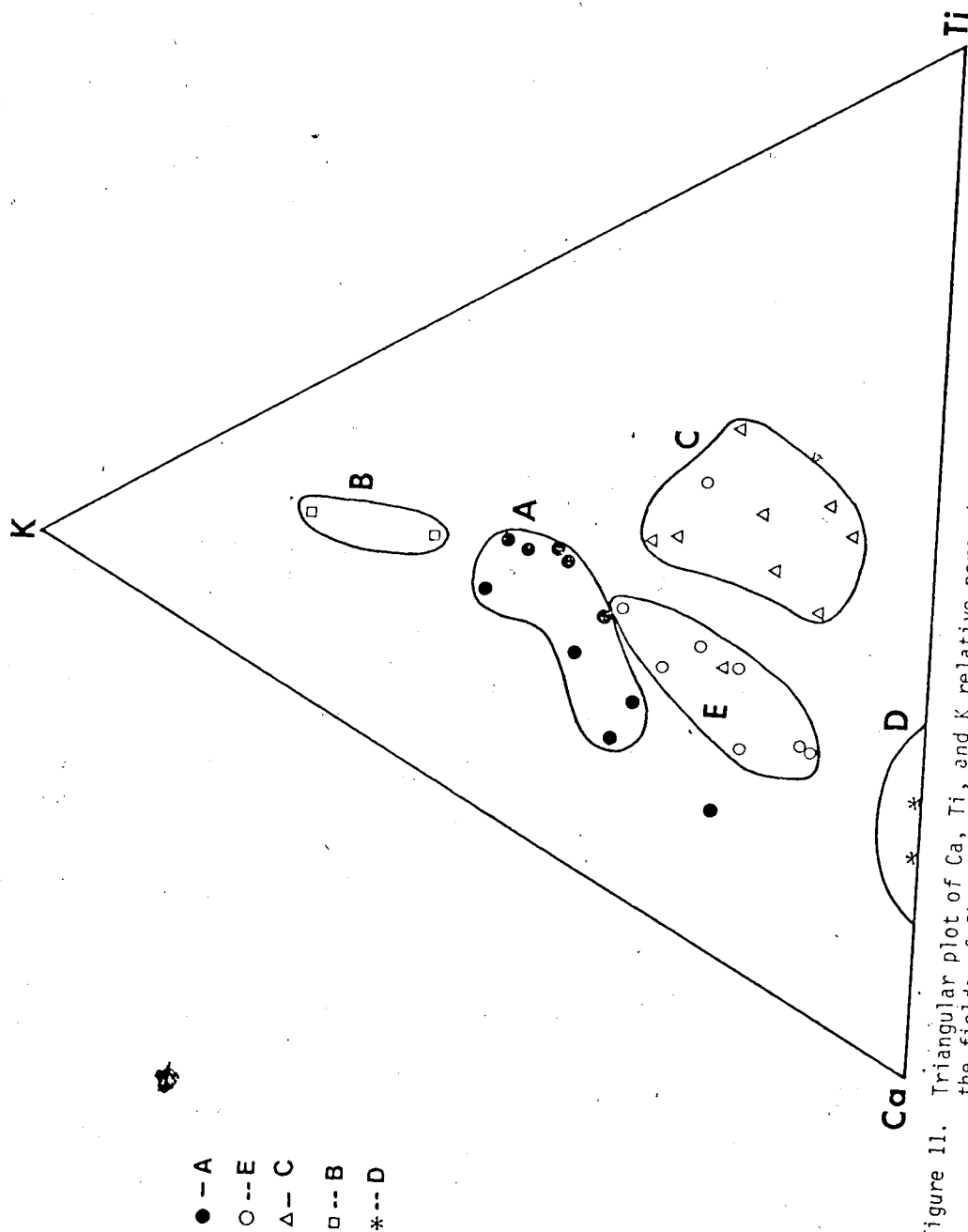


Figure 11. Triangular plot of Ca, Ti, and K relative percent concentrations, showing the fields of five bentonite beds: A, B, C, D, and E.

Figures 6, 7 and 8). The agreement between the two correlation schemes satisfies one of the objectives of this exercise and supports the existence of 5 independent bentonite horizons in the Viking Formation. This also makes it possible to establish 3 time planes within the formation. These planes have been used to divide the Viking sandbodies into three basic units: Basal, Lower, and Upper Viking sandbodies (Figure 9).

CHAPTER 6

SOURCE AREA OF THE VIKING BENTONITES

Biotite Grain Size Distribution

Grain size distribution of volcanic products may be useful to characterize them and to infer the direction of the eruption centre. It was hoped that this parameter would be useful in this study but sample limitations allowed only a study of the latter to be attempted. The biotite grain size of seven 'A' and six 'E' bentonite samples was measured.

Method

Samples were crushed in a ceramic mortar, and water and a small quantity of Calgon added. The latter prevents flocculation and facilitates disaggregation of the fine particles. The preparation was left for 5 hours to ensure complete disaggregation. The mixture was then blended for about 3-5 minutes and poured into a beaker. The coarse particles were allowed to settle for three seconds and then recovered wet by decanting off the fine sizes.

The dried samples were sieved through a 200 mesh sieve. The fraction coarser than this size was passed through a Frantz isodynamic separator model L-1 under a moderate magnetic field, so as to separate the magnetic minerals from other non-magnetic minerals. It was observed that the magnetic susceptibilities of this mineral differed from sample to sample, possibly in relation to biotite grain size, as the coarse grains were the most magnetic. Frantz settings for each sample were selected by trial and error.

The biotite separates were mounted on slides with the aid of aroclor, and allowed to dry. A 1/100 mm monochromatic lens was used to calibrate the eye piece of the optical microscope (.01mm = .012mm). The longest diameters of the largest twenty biotite grains in each sample were measured, and the sizes of the largest ten averaged. Table V shows the biotite grain size distribution and Mn/Fe ratios for bentonites 'A', 'C', and 'E'.

Discussion

Biotite grain size distribution for bentonite 'A' is greater than that of 'E'. When plotted on a map, Figure 12, the 'E' bentonite appears to have a roughly southwestern source. The 'A' bentonite grain size variation does not show any recognizable trend.

Figures 13a, b, c show the contoured maps of Mn/Fe ratio for bentonites 'A', 'C', and 'E'. When the map for bentonite 'E' (Figure 13a) is superimposed on the biotite grain size distribution map, an apparent correlation becomes obvious, suggesting that a positive linear relationship exists between maximum biotite grain size and Mn/Fe ratio. If we accept the hypothesis that the source of bentonite 'E' lay roughly to the southwest, then the above relationship also indicates a variation in element chemistry with distance from source. These observations may support the observations of Lerbekmo and Campbell (1969), that the relationship of chemistry to distance from source is a function of particle size, although their size data were not restricted to single mineral components.

If the above relationship is correct, then it could be used to infer the approximate direction to the location of other eruptions.

Table V. Biotite Grain Size (mm) Distribution and Mn/Fe Ratios for Bentonites 'A', 'C', and 'E'.

<u>BENTONITE A</u>			
Well Location	Sample No.	Biotite Grain Size (mm)	Mn/Fe Ratio
11-23-23-14	VB2647A	0.42	0.002
14-26-25-12	VB2785A	0.49	0.006
13-11-28-14	VB3116A	-	0.004
10-36-28-14	VB3097A	0.53	0.003
11-30-29-10	VB2866A	0.38	0.005
7-22-29-14	VB3088A	0.50	0.006
11- 7-30-12	VB3101A	0.47	0.013
7-10-30-12	VB3042A	-	0.015
6-23-30-14	VB3153A	0.50	0.003
10-20-30-12	VB3007A	-	0.011

<u>BENTONITE C</u>			
Well Location	Sample No.	Biotite Grain Size (mm)	Mn/Fe Ratio
11-30-29-10	VB2895C	-	0.02
10-13-30-11	VB2866C	-	0.02
6-12-34-17	VB3479C	-	0.01
6-21-36-17	VB3455C	-	0.01
10- 9-39-10	VB2719C	-	0.002
14- 4-51-22	VB3330C	-	0.01
7-11-46-20	VB3246C	-	0.01
7-16-39-11	VB3684C	-	0.004
8-30-47-10	VB2166C	-	0.002

<u>BENTONITE E</u>			
Well Location	Sample No.	Biotite Grain Size (mm)	Mn/Fe Ratio
10-13-30-11	VB2903E	0.29	0.02
6-34-30- 8	VB2770E	-	0.014
12-19-31- 9	VB2907E	0.37	0.01
11-11-32-11	VB2998E	0.42	0.043
2-22-36-11	VB3023E	0.38	0.01
4-28-41-26	VB4821E	0.30	0.015
10-12-53-12	VB1861E	0.29	0.01
6-12-34-17	VB3516E	-	0.02

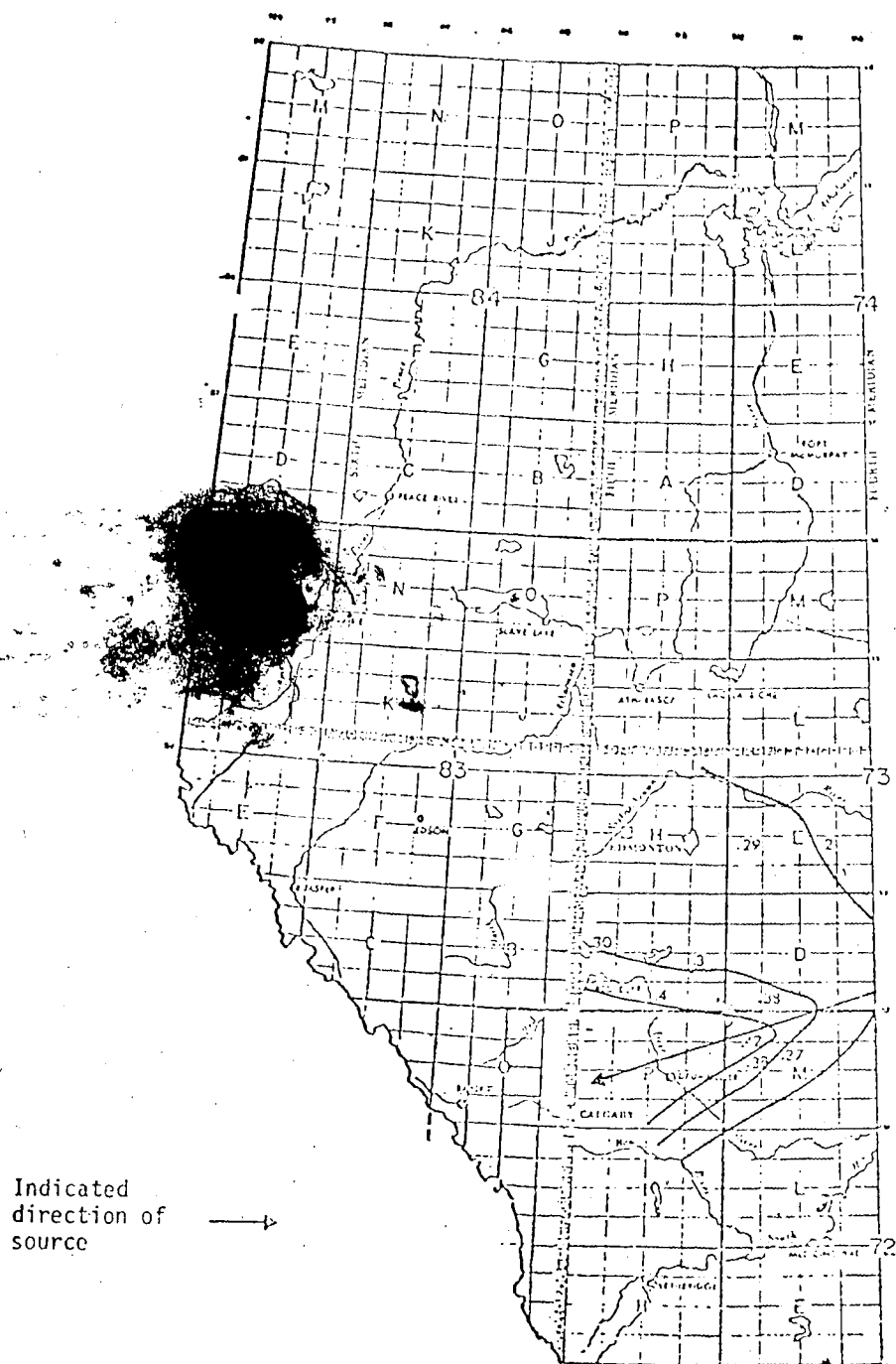
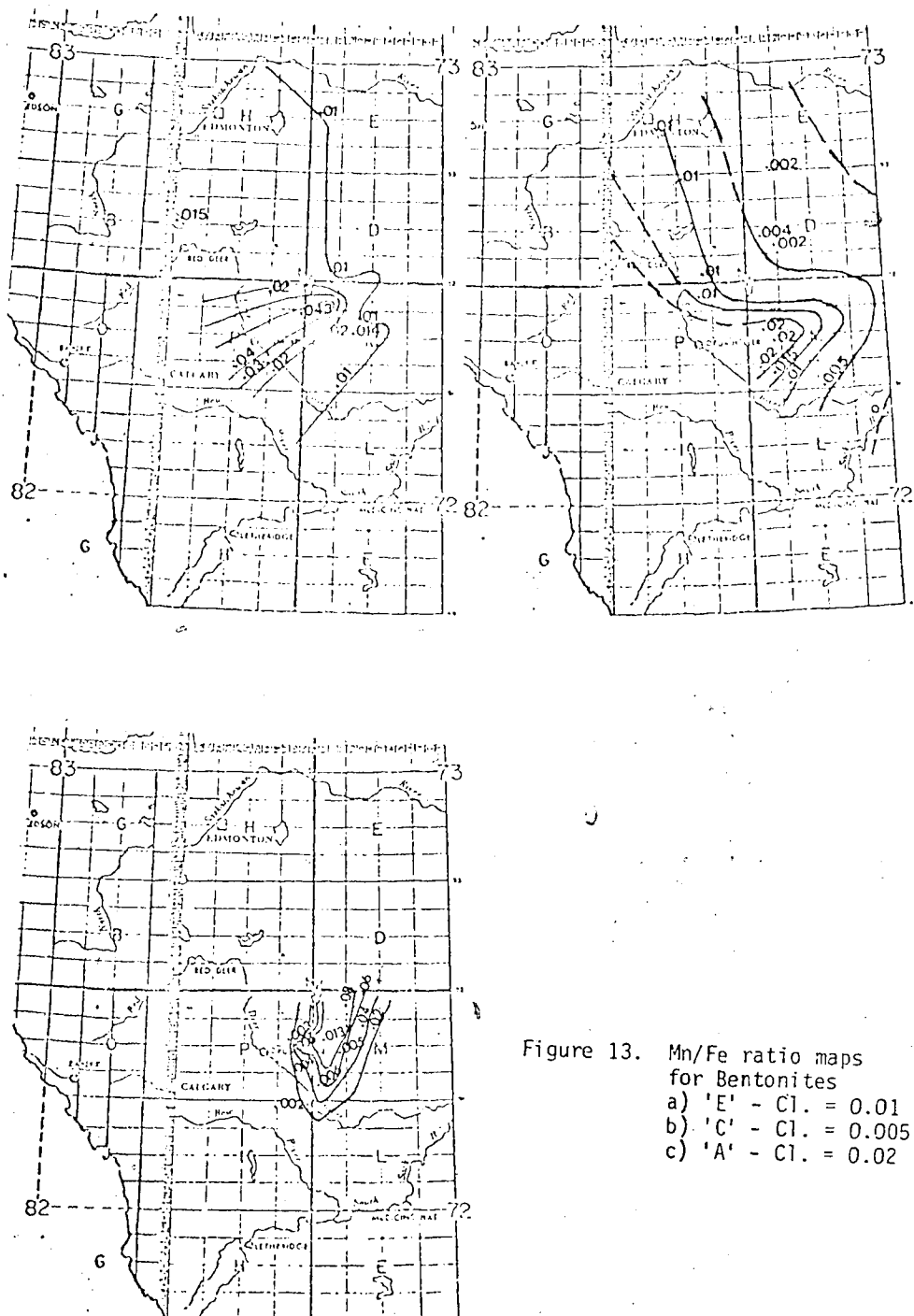


Figure 12. Areal distribution of maximum biotite grain size for Bentonite 'E'. $Cl = .1mm$.

in the absence of any other meaningful criteria. When this idea is applied to bentonite 'C' (Figure 13b), the Mn/Fe ratio map indicates a southwesterly source area. The map for bentonite 'A' tends to suggest a north-northeasterly source for the volcanic ash, (Figure 13c), but such a source area is at present unknown. The southwestern source area deduced for bentonites 'E' and 'C' is consistent with the known tectonic events in the area during deposition of the Viking Formation (Eisbacher, 1977; Wheeler *et al.*, 1972) (Figure 14).

The plot of Ca/Sr ratio against biotite grain size for bentonite 'A' (Figure 15) may also indicate a positive linear relationship, but is very uncertain because of the single mineral component used in the analysis. In general, a larger sample size would be required before any great weight could be placed on the above interpretations.



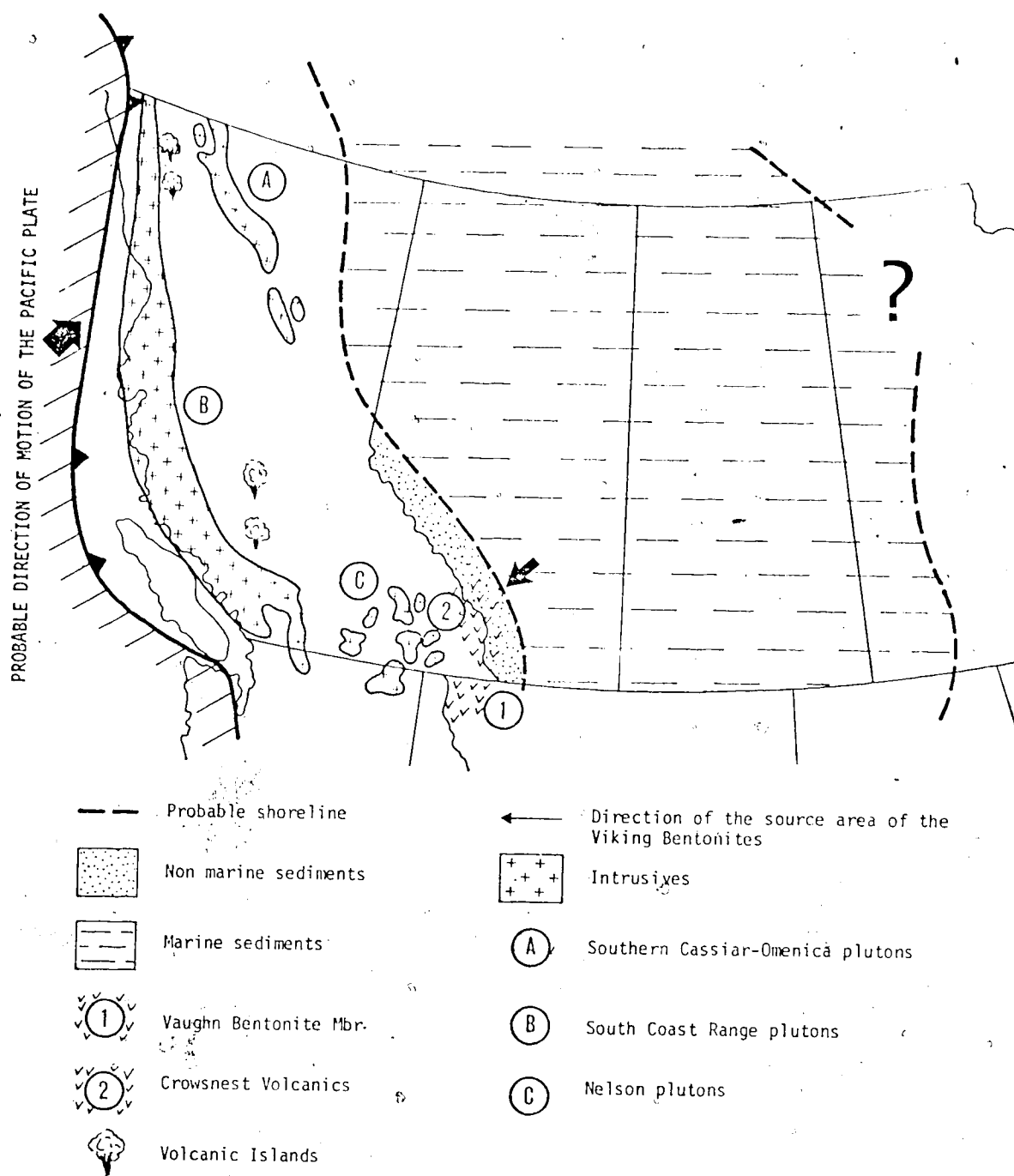


Figure 14. Paleogeographic map of the Lower Cretaceous of Western Canada. (Modified from (Wheeler et al., 1972; Stelick and Williams, 1975; Rudkin, 1964; Kauffman, 1977; Eisbacher, 1977.))

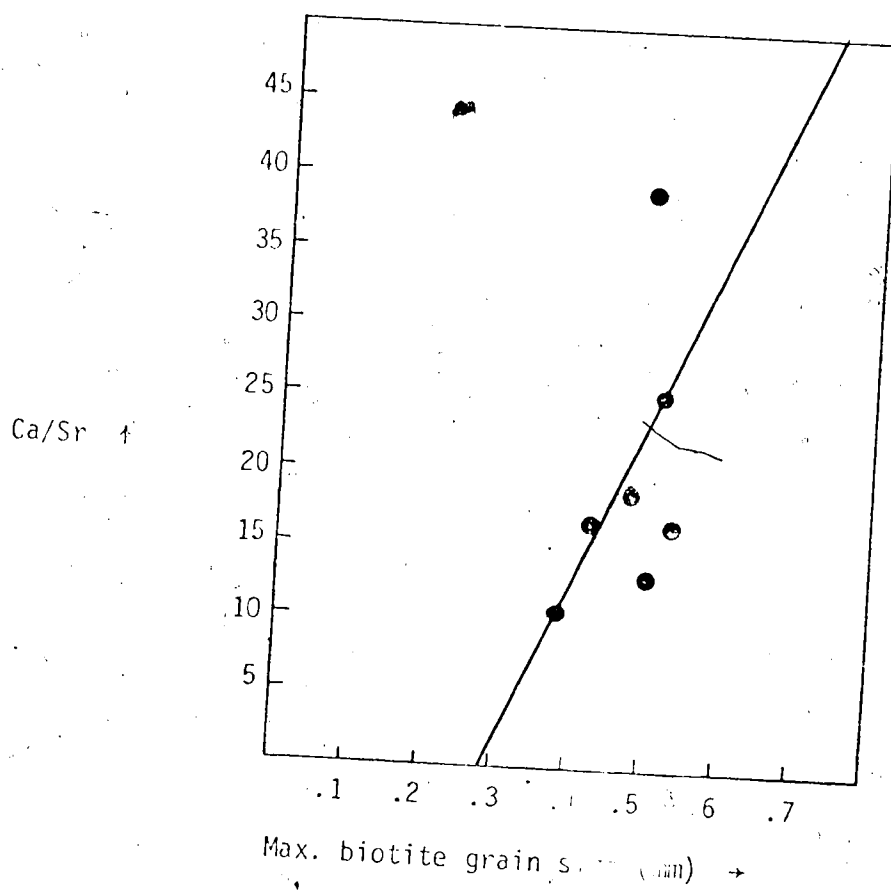


Figure 15. Plot of Ca/Sr ratio against maximum biotite grain size for bentonite 'A'.

CHAPTER 7

DEPOSITION OF THE VIKING SANDBODIES

Geologic cross sections are used to illustrate and depict interpreted conditions within a portion of the earth's crust. Stratigraphic sections use time-markers where possible to correlate and interpret the depositional history of the lithologic units.

Well log studies and chemical analyses have differentiated three different bentonite horizons in the Viking Formation. These in turn subdivide the Viking sandbodies into three units as earlier indicated. The depositional behavior of these sandbodies in relation to the time planes will now be discussed.

Cross Sections

Eight stratigraphic sections (Figures 16-28) were constructed across the study area using the Viking bentonite time planes; Figure 16 shows their locations. The 'A' bentonite horizon was depended upon because it is the most recognizable and easiest to identify in well logs. However, discussion will involve the other two bentonite time planes where possible. In general, the sections show the stratigraphic position of the Viking Formation relative to the time planes so that its depositional pattern can be more easily visualized.

Section D-D' (Figure 17) is an east-west section taken along township 27 between ranges 10 and 28W4M, constructed with the 'A' bentonite as datum. It is oriented at a high angle to the northwest-southeast Viking strandline.

Along the line of cross-section, the basal bentonite can be

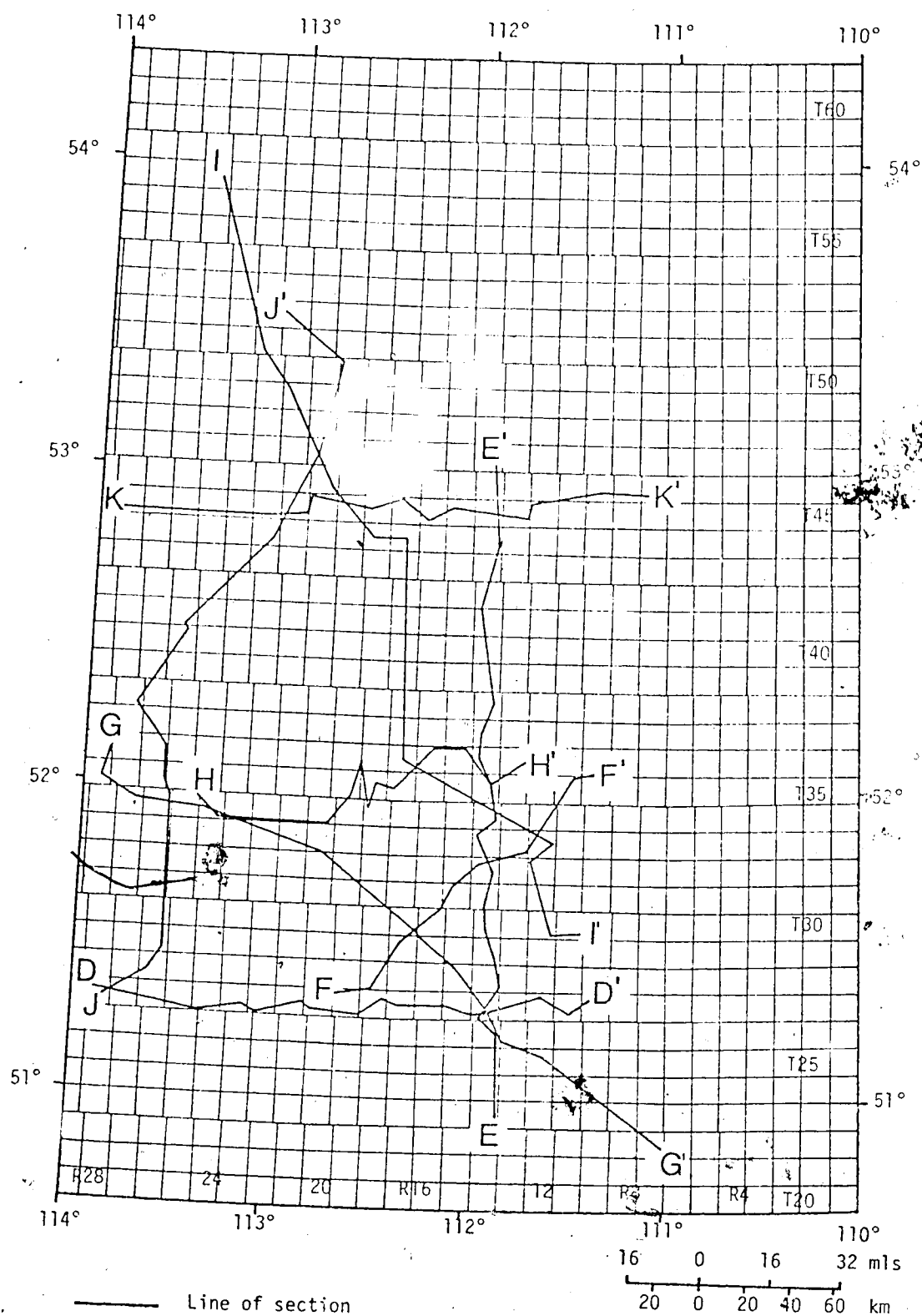


Figure 16. Location map of cross sections.

reliably picked in most well logs. To the west in well 6-26-27-21W4M, it occurs in shale about 56 ft. below the base of the Upper sand. In well 7-10-27-11W4M to the east it occurs in silty shale about 6 ft. below the base of the Lower sand.

Using the Basal bentonite as a time datum it is seen that the first clean sandstone development occurred in the east. This is called the 'Lower Viking sandstone'. Its base prograded westward as evidenced by the westward increase in thickness of the shale and silty shale interval between it and bentonite 'E', which increases from 6 ft. in well 7-10-27-11W4M to 40 ft. in well 10-24-27-16W4M. This sandstone pinches out into shale west of well 10-21-27-17W4M and to the east of well 11-29-17-10W4M. Maximum thickness of 50 ft. to 60 ft. occurs in wells 7-9-27-14W4M and 6-22-27-13W4M. Although the latter contains some shale interbeds indicative of intermittent progradation in this area, in general, the axis of maximum sand development lay between wells 7-9-27-13W4M and 6-22-27-13W4M.

A marine deepening arrested this sand development and allowed accumulation of the volcanic 'A' bentonite and silty shale deposits. East of well 10-21-27-17W4M, the 'A' bentonite shows up very well in logs, but becomes indistinct to the west. Relative to this datum, western and eastern Upper sand units appear to have developed about the same time. However, the western sand developed first and prograded eastwards relatively quickly. This is deduced from the fact that the sand was being deposited at the same time as bentonite 'A' in well 2-29-27-28W4M, but to the east the base of the sand maintains a fairly constant position a few feet above the bentonite up to well 10-21-27-17W4M, where the sand begins to shale out. In well 2-29-27-28W4M this western

Upper sand attains its maximum thickness of 53 ft.

At the same time, an eastern Upper sand was rapidly prograding westward. The silty shale interval between the Lower and Upper sands is absent in well 7-10-27-11W4M, and about 20 ft. thick between wells 6-22-27-13W4M and 10-24-27-16W4M. Its maximum thickness of 40 ft. occurs in well 7-10-27-11W4M. In well 10-21-27-17W4M, the siltstone facies of the eastern sand appears to overlap the western sand. In general, the base, and probably the top, of the Viking sand units along this section is diachronous.

Figure 18 shows section E-E' taken in a north-south direction through townships 23 to 47, range 14W4M, and constructed with the 'A' bentonite time plane as datum. It is roughly at 45° to the paleo-strandline.

In the southern part of the cross-section, in wells 14-23-26-14W4M and 10-16-31-14W4M, for example, the basal bentonite is 16 ft. and 18 ft., respectively, below the base of the lower Viking sand. To the north, it is 4 ft. and 20 ft. below the sand in wells 11-28-35-14W4M and 10-27-38-14W4M, respectively. Therefore, a thin basal sand was first deposited in the vicinity of well 11-28-35-14W4M, where it is about 6 ft. thick. This sand unit extended southward to the vicinity of well 11-31-33-14W4M, beyond which it disappears. In well 11-28-35-14W4M, it is overlain by 12 ft. of silty shale.

Following the formation of this sand, two sandbodies began to form, one in the south and one in the north, at about the same time. Relative to the basal bentonite, the base of the lower southern sand appears to have prograded rapidly northward between wells 14-23-26-14W4M and 3-14-29-14W4M, as it maintains a fairly constant position of

approximately 15 ft. above the bentonite. Between wells 10-16-31-14W4M and 11-31-33-14W4M, intermittent progradation is suggested by the multiple sand development. This sand body pinches out rapidly immediately north of well 6-22-32-14W4M, as it seems absent in well 14-7-34-14W4M. A southward pinchout also occurs beyond well 11-23-23-14W4M. This suggests that the axis of maximum sand thickness lay between wells 14-23-26-14W4M and 3-14-29-14W4M, where the thickness ranges from 45 to 50 ft.

Localized multiple sand development appears to characterize the Lower northern sand. In well 10-20-36-14W4M there is a 26 ft. thick sand (above the Basal sand) which appears to pinchout rapidly to the immediate south, while it seems to have prograded rapidly northward beyond well 13-11-47-14W4M. Another thin sand about 12 ft. thick in well 10-21-37-14W4M prograded southward and possibly overlapped the southern sand in well 11-31-33-14W4M.

A marine incursion during which the 'A' volcanic ash was deposited terminated deposition of the southern and northern Lower sand bodies. To the north of well 6-22-32-14W4M, the transgression brought sand deposition to an end, while to the south an Upper Viking sand succeeded it.

Relative to the 'A' bentonite, the Upper sand, which is 13 ft. thick in well 14-23-26-14W4M, prograded rapidly northward to the vicinity of well 10-16-31-14W4M. In these wells its base is 18 ft. and 22 ft., respectively, above the time horizon.

In general, the base of the Viking Formation in this cross-section is slightly diachronous, as opposed to its top, which is very diachronous and older to the north. This supports Evans (1970) observation that

the top of the Viking Formation is older to the northeast and younger to the south. Figure 19 is a generalized sketch showing the depositional behaviour of these sand units relative to the 'A' and 'E' time planes for sections a) D-D' and b) E-E'.

Section F-F' is oriented approximately in a southwest-northeast direction from townships 27 to 36 and ranges 19 to 10, and constructed with the Basal bentonite 'E' as datum (Figure 20). It runs almost perpendicular to the Viking strandline and should show the greatest diachroneity if the sand unit is regressive (Jones, 1961).

Relative to the Basal bentonite, a Basal sand first developed between wells 10-3-36-104M and 6-12-33-13W4, pinching out southwestward before well 10-29-32-14W4M. Another local Basal shaly sand developed between wells 1-33-29-17W4M and 10-1-30-18W4M. In these wells the sand is underlain by the Basal bentonite. The northeastern Basal sand is overlain by silty shale while the southwestern one was overlain almost immediately by the Lower sand unit.

In wells 1-33-29-17W4M and 10-1-30-18W4M to the west, the base of the Lower sand is about 15 ft. above the Basal bentonite; whereas between wells 4-1-31-16W4M and 6-12-33-13W4M, it occurs approximately 28 ft. above the datum. This indicates rapid northeastward progradation after localized development for some time, and shows maximum diachroneity of the base of this sand in this section. Maximum thickness varies from 65 to 70 ft. and occurs in wells 1-33-29-17W4M and 10-1-30-18W4M, respectively. The Lower sand unit shales out southwest of well 11-5-28-18W4M. To the east, around wells 10-29-32-14W4M and 6-12-33-13W4M, it becomes a distinct multiple sand and finally is restricted to a single 10 ft. thick sand unit in wells 10-35-35-11W4 and 10-3-36-10W4.

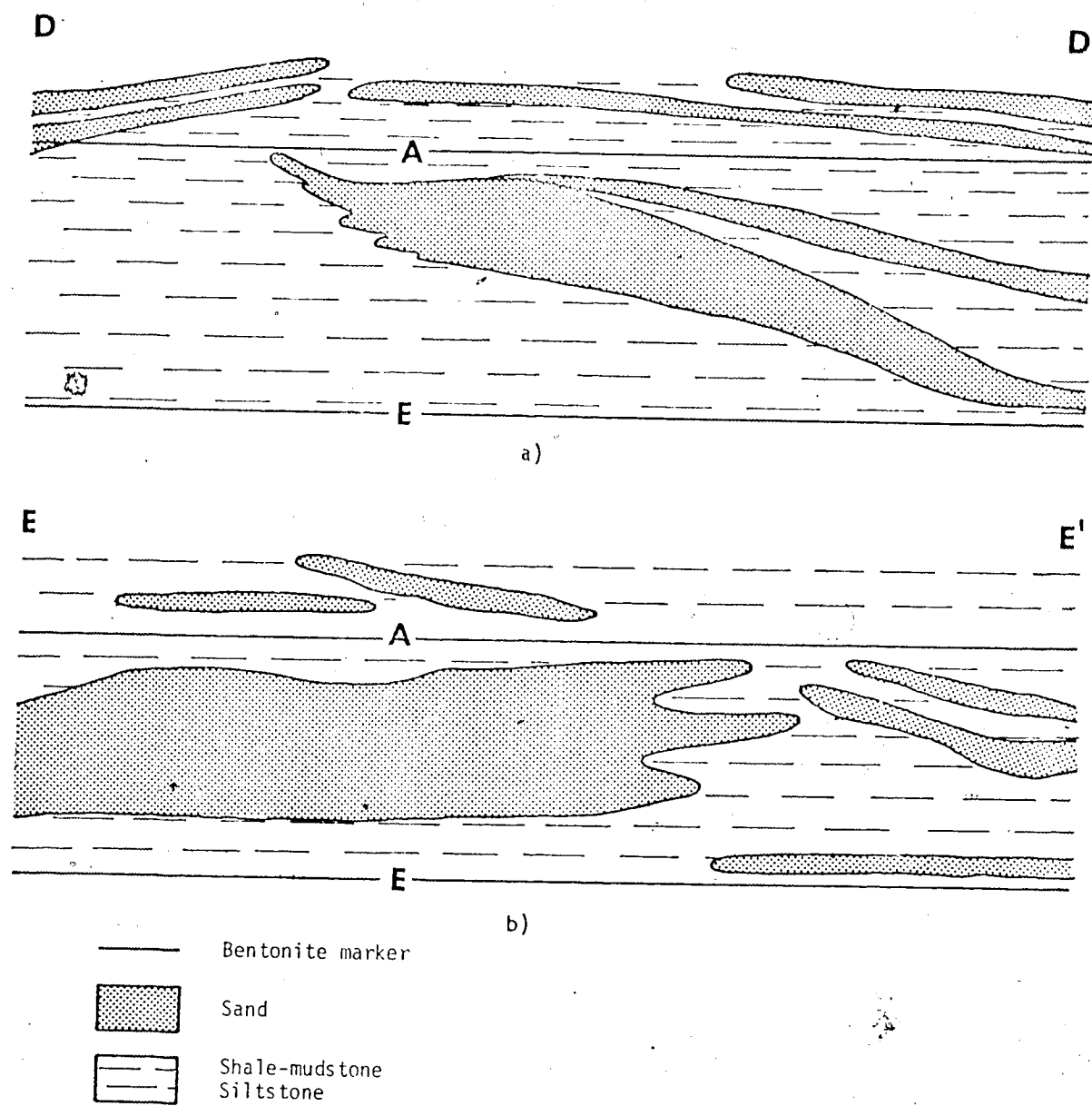


Figure 19. Sketch of gross lithologic distribution for sections:
 a) D-D'
 b) E-E'

It shales out northwestward in the immediate vicinity of well 16-21-34-12W4, and northeasterly beyond well 10-3-36-10W4. Since the stratigraphic position of the bentonite 'A' is inferred in these wells, it is equally probably that the 10 ft. thick sand in well 10-3-36-10W4 developed locally at about the same time as the lower southwestern sand, as the silty shale interval between its base and the top of the basal sand appears to increase toward well 10-35-35-11W4. This interpretation implies that it pinches out around well 10-35-35-11W4.

The 'A' bentonite occurs in silty shale deposited by a marine deepening which terminated the development of the lower sand. An upper sand prograded southwestward relative to this time plane from well 10-32-31-15W4M toward well 6-31-27-19W4 where it may overlap another local thin sand unit. To the east of well 10-29-32-14W4, the 'A' bentonite is not distinct and appears to lie in the overlying shale unit. This again suggests that the top of the Viking sand is younger to the west, implying that it is diachronous and that the lower part of the overlying shale to the east formed during Viking time.

Section G-G' is oriented approximately in a southeast-northwest direction through townships 22 to 36 and ranges 8 to 28W4M (Figure 21). It is almost parallel to the paleo-strandline, the axis of maximum sand development; the 'A' bentonite is the datum.

Along this section the first sand to be deposited is the lower sand unit. Maximum sand development occurs in wells 7-13-22-8W4M and 7-21-32-19W4M where it reaches a thickness of 90 and 70 ft., respectively. A fairly constant thickness of about 50 ft. occurs in the intervening area. It thins towards the west and shales out in well 3-22-39-27W4M.

Between wells 7-13-22-8W4M and 11-12-30-17W4M to the west, the

basal bentonite lies almost at the base of the Lower sand. This relationship suggests non-diachroneity of the base of this unit in this area, and that the Lower sand developed here at about the same time as the Basal sand in townships 33 and 34, ranges 12 to 14W4M. In wells 11-7-26-13W4M and 11-15-28-15W4 the base of the sandstone occurs about 13 ft. and 17 ft. above the basal bentonite. However, these wells are slightly off the axis of main sand development.

West of well 11-12-30-17W4, the basal bentonite is not quite as distinct in well logs. Between wells 6-20-34-24W4 and 4-29-31-18W4, it appears to lie between 15 and 10 ft. below the base of this sand and 30 to 35 ft. between wells 6-27-34-27W4 and 7-24-36-28W4. This implies that this sand may be slightly diachronous in this area and therefore older to the east. The relationship of the top of this sand to the 'A' bentonite supports this inference, as the silty shale interval between them increases in thickness eastward from 8 ft. in well 7-24-36-28W4 to 24 ft. in well 7-20-32-19W4. East of this well, the interval is fairly constant (20 to 22 ft.), except in wells 10-33-28-15W4 to 11-7-26-13W4 which, as earlier mentioned, are on the flanks of this sand unit.

Relative to the 'A' bentonite the base of the thin Upper sand appears to have prograded eastward from well 7-3-33-20W4 as the silty shale interval increases in thickness in this direction. It is 4 ft. in the above well and 25 ft. in well 11-7-26-13W4M. It is about 20 ft. thick in well 7-31-29-16W4M. Another eastern Upper sand appears to prograde westward from well 7-13-22-8. to well 10-33-28-15W4.

These relationships show that the top of the Upper sand is diachronous in this section. In general, diachroneity of the base of the Viking sand in this section appears minimal. This possibly agrees

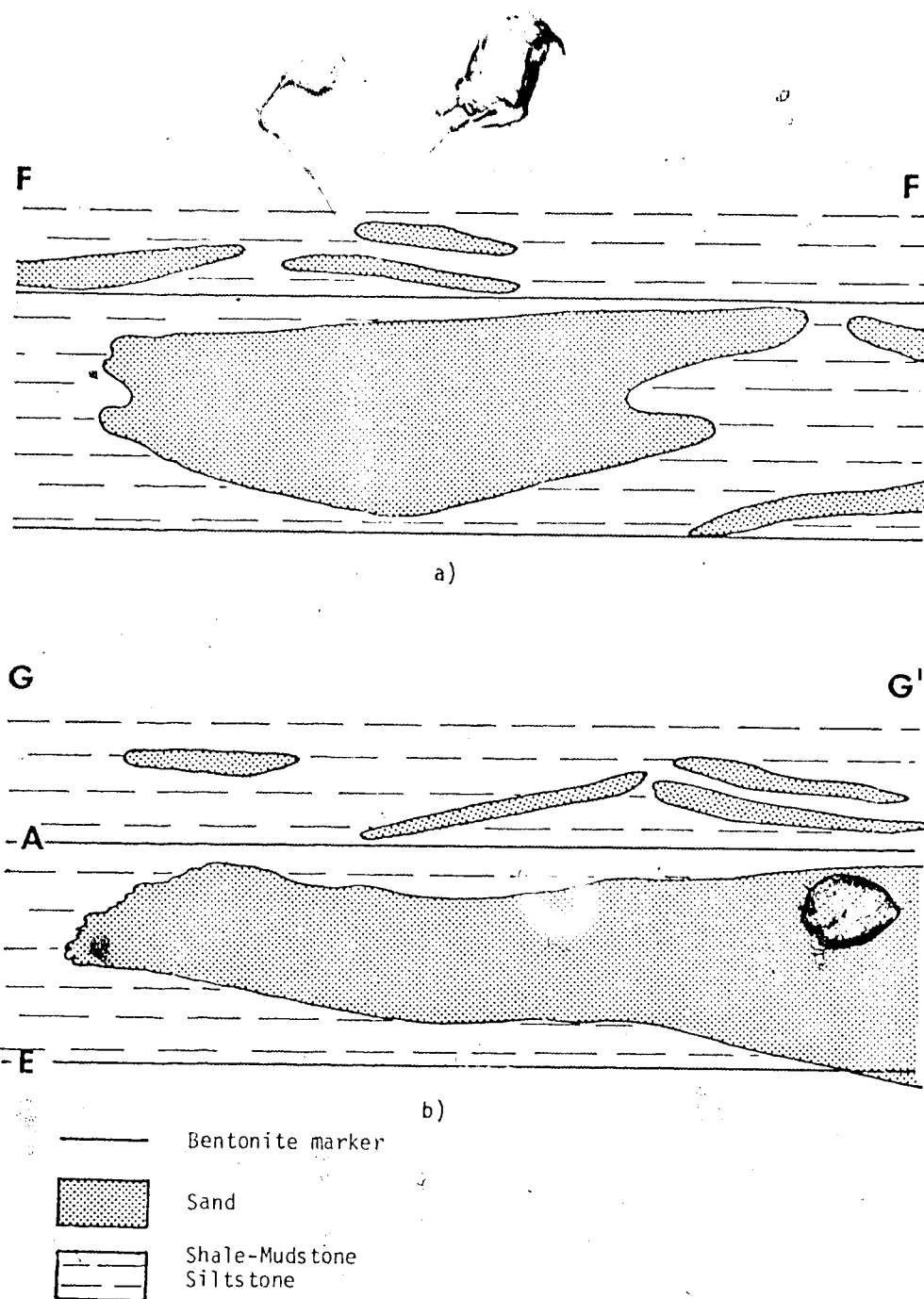


Figure 22. Sketch of gross lithologic distribution for sections:
 a) F-F'
 b) G-G'

with the observations of Jones (1961) and Tizzard (1974), that parallel to the Viking strandline, we should expect only slight diachronism. Figure 22 shows the sketched distribution of these sand units relative to the 'A' and 'E' time planes for section a) F-F' and b) G-G'.

Section H-H' is oriented roughly in a southwest-northeast direction along townships 34 to 36, ranges 13 to 25W4M (Figure 23). It is constructed with the 'A' bentonite as datum.

The bentonite horizons are not very distinct in these well logs. However, the basal bentonite has been correlated in wells 7-35-36-15W4 and 11-28-35-14W4. Here it underlies the Basal sand. West of well 15-3-35-19W4, the 'A' bentonite shows up fairly well in the well logs.

The Lower sand appears in the western three wells and attains maximum thickness of about 50 ft. East of well 11-2-34-10W4, this sand rapidly pinches out as sand development is very poor and lacking in some wells.

To the east of well 4-30-34-18W4, a multiple sand development appears to have occurred during the same time span as the western Lower sand. These eastern sand units appear to shale out west of well 7-30-35-17W4M and east of well 6-25-36-13W4M, respectively. The Upper sand is poorly developed in this section. In this area the 'A' bentonite therefore overlies the Viking sand.

Section I-I' goes through townships 59 to 30 and ranges 27 to 11W4M in a northwest-southeast direction (Figure 24). It is constructed with the 'C' bentonite as datum.

The basal bentonite can be picked with confidence in well logs to the east of well 9-9-44-17W4M. In this area it underlies the Basal sand. In well 6-31-32-12W4M it lies in silty shale 2 ft. below the Basal sand.

while in well 7-10-30-12W4M it occurs in silty shale 30 ft. below the base of the Lower sand. To the west of well 9-9-44-17W4M it becomes indistinct and difficult to locate in well logs. However, should it extend westward, it should underlie the Basal sand.

The thin Basal sand was the first to develop in this section. In wells 9-9-44-17W4M and 6-31-32-12W4M, it is respectively 25 and 4 ft. thick. It appears to have prograded westward relative to the datum as its top is 25 ft. below the datum in well 6-31-32-12W4M and 20 ft. in well 8-16-47-20W4M. Progradation appears to have been rapid between wells 6-31-32-12W4M and 11-16-46-20W4M, as the silty shale interval between its top and the datum maintains a fairly constant thickness of about 25 ft. It pinches out into silty shale to the east of well 6-31-32-12W4M.

The 'C' bentonite underlies the Lower sand throughout the section. This suggests that the base of this sand unit constitutes a good time marker. Between wells 10-13-30-11W4M and 10-24-33-12W4M, a multiple Lower sand development occurred. It is about 25 ft. thick in well 7-10-30-12W4M, but pinches out to the immediate west to well 10-24-33-12. This sand unit is the terminal part of the main Lower sand to the south of the study area.

As the Lower eastern sand was being deposited, a western sand began to form west of well 10-24-33-12W4M. It is about 40 ft. thick in well 11-33-59-27W4M. It pinches out to the east of well 6-21-36-17W4M. This sand is an independent northwest-southeast trending sand unit to the north of the study area and will be discussed briefly in the sections to follow. It parallels the paleo-strandline.

The 'A' bentonite occurs in silty shale above the Lower sand in

wells 7-10-30-12W4M and 10-13-30-11W4M. To the west of these wells it is indistinct in well logs. However, it appears to lie in the overlying shale unit except in well 11-33-59-27W4M where it is possible that it occurs in the shale interbed between the Lower sand and an upper thin sand. This assumes that its distribution extends to this area.

Along this trend the Viking sand is not diachronous. Figure 25 is a sketch of the probable distribution of the sandbodies relative to the three bentonite horizons for sections a) H-H' and b) I-I'.

Section J-J' encompasses townships 27 to 52 and ranges 28 to 19W4M. It is oriented approximately in a southwest-northeast direction and constructed with bentonite 'A' as datum (Figure 26).

The basal bentonite in wells 15-35-40-25W4M and 10-3-41-25W4M has been reliably correlated to a nearby well (see Figure 7, well 14-28-41-26W4M), where it was observed in the core. In the other wells it is indistinct and difficult to pick. In the above wells (15-35-40-25W4M and 10-3-41-25W4M) it possibly occurs in shale about 5 ft. below the basal sand. The thin Basal sand appears to have prograded rapidly southwestward from well 10-33-51-19W4M, shaling out immediately west of well 15-35-40-25W4M.

Bentonite 'A' was confidently correlated in wells 6-36-34-26W4M and 10-13-35-26W4M. In the other wells its position is less certain, but inferred to lie above the Lower sand east of well 16-25-36-26W4M and in the Lower sand west of well 11-17-28-26W4M.

Relative to the datum the Lower sand gradually prograded westward from well 10-33-51-19W4M where it attains a maximum thickness of about 50 ft. and disappears west of well 6-36-34-26W4M. The shale interval between the top of the sand and the datum decreases in thickness in the

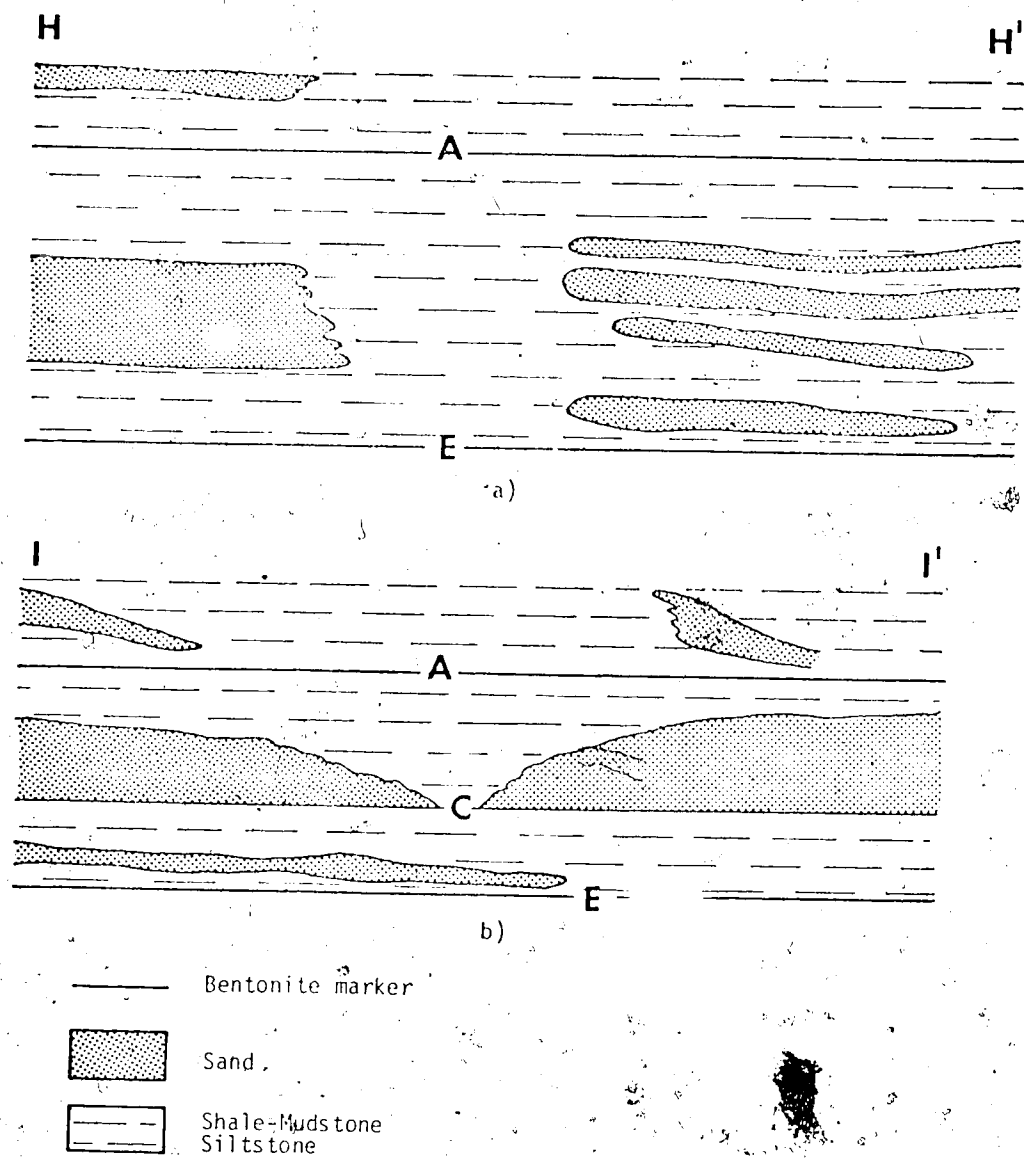


Figure 25. Sketch of gross lithologic distribution for sections:
a) H-H'
b) I-I'

same direction, from about 20 ft. in well 10-3-41-25W4M to 10 ft. in well 6-36-34-26W4M and finally zero in well 10-14-27-28W4M.

The Upper sand prograded northeastward from well 10-14-27-28W4M, and pinches out east of well 10-13-35-26W4M. It is about 45 ft. thick in the former well.

Relative to the top of the underlying Viking Formation, the Base of the Fish Scale Marker is approximately located 64 ft., 104 ft., and 140 ft. respectively in wells 10-14-27-28W4M, 10-13-25-26W4M, and 10-3-41-25W4M above the Viking Formation. This relationship shows that the Lloydminster Shale thickens in a northeast direction along the line of section, which supports earlier interpretation that the Viking Formation is younger to the south. With respect to the 'A' bentonite, the Base of the Fish Scale Marker, the Viking Formation and the base of the Joli Fou Shale are all generally diachronous.

Section K-K' is taken along townships 44 and 45, ranges 8-27W4M in an east-west direction. It is constructed with the basal bentonite as datum (Figure 27), but this bentonite is not very distinct in well logs except in well 6-20-44-15W4M where it occurs in silty shale at a depth of 2751 ft., about 30 ft. below the thin Lower sand unit. East of this well it is reliably correlated and appears to lie in silty to sandy shale beds below the Basal sand. West of well 6-20-44-15W4 it is referred to underlie the thin Basal sand.

Relative to the datum, the Basal sand appears to have prograded westward pinching out beyond well 2-8-44-27W4M. The silty shale to shale interval between the datum and the bottom of the sand appears to increase in thickness in this direction, from almost zero in well 7-12-44-13W4M to about 8 ft. in the former well, where it attains a

maximum thickness of 10 ft.

The Lower sand is thick in the west and thins to the east. In wells 13-2-44-22W4M and 12-24-44-13W4M it is 37 ft. and 12 ft. thick respectively. A rapid progradation appears to have occurred between wells 10-30-44-12W4M and 1-20-44-18W4M. A temporary slow-down in the rate of progradation might account for its thickness between wells 11-30-44-20W4M to 13-2-44-22W4M. It pinches out to the west of well 2-8-44-27W4M.

The position of the 'A' bentonite is inferred to be above the sand in the overlying shale. The base of the Viking sand in this section appears slightly diachronous. Figure 28 is a sketch showing an interpretation of the lithofacies distribution relative to the 'A' and 'E' bentonites, for sections a) 'J-J' and b) 'K-K'.

Fence Diagram

Figure 29 is a fence diagram which embraces the area almost enclosed by townships 21 to 47, ranges 3 to 28W4M (full size fence diagram in pocket). It integrates the cross-sections previously described and synthesizes them in pictorial form. This facilitates visualization of the lithofacies distributions, direction of maximum sand movement, and the general depositional sequence in three dimensions. It was constructed relative to the 'E' and 'A' bentonite time planes.

The Basal bentonite 'E' marks termination of Joli Fou time and the beginning of Viking time in the area. A westward-prograding northwest-southeast trending Basal thin sand was the first sand deposit of this sea. Following it, southern and northern Lower sand bodies began to form almost simultaneously, but earliest in the southeast. The southern sand body trends northwest-southeast and no main direction of

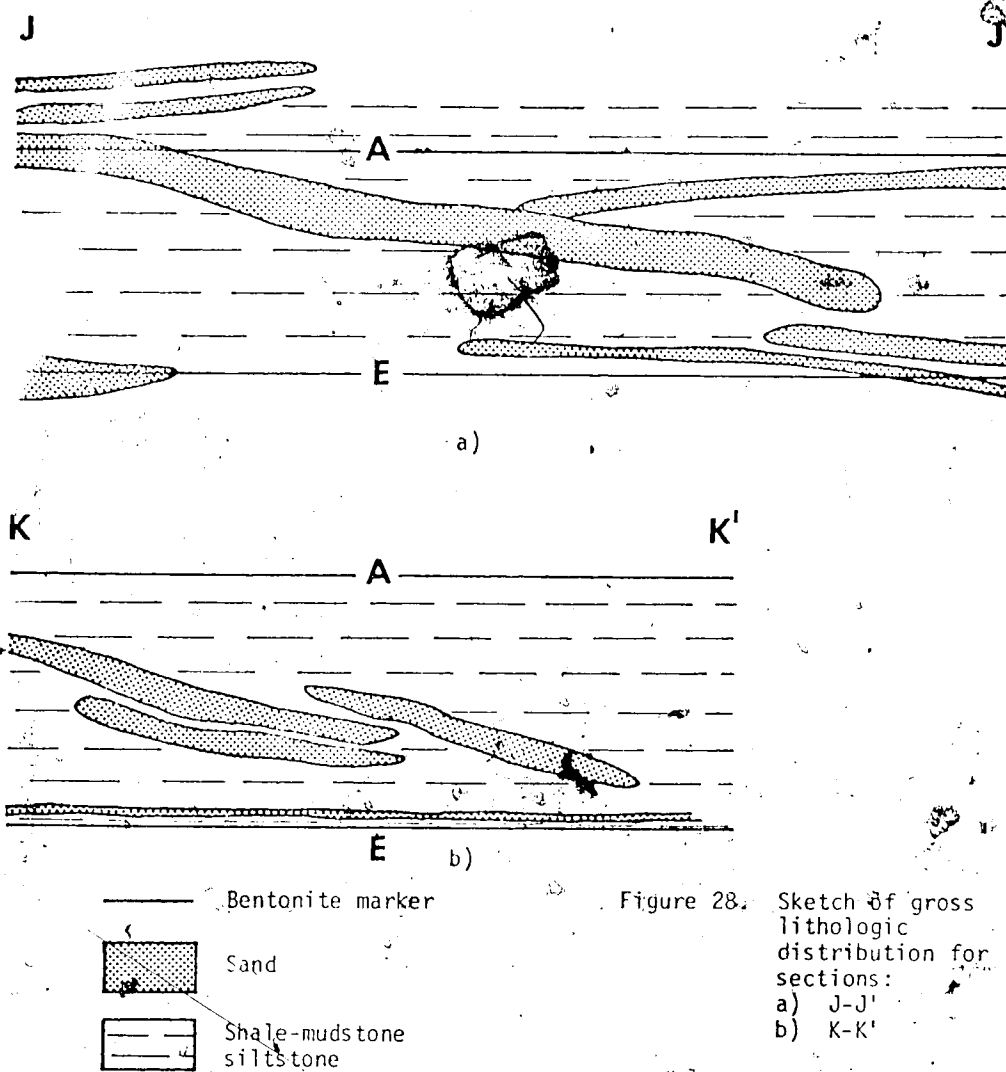


Figure 28. Sketch of gross lithologic distribution for sections:
 a) J-J'
 b) K-K'

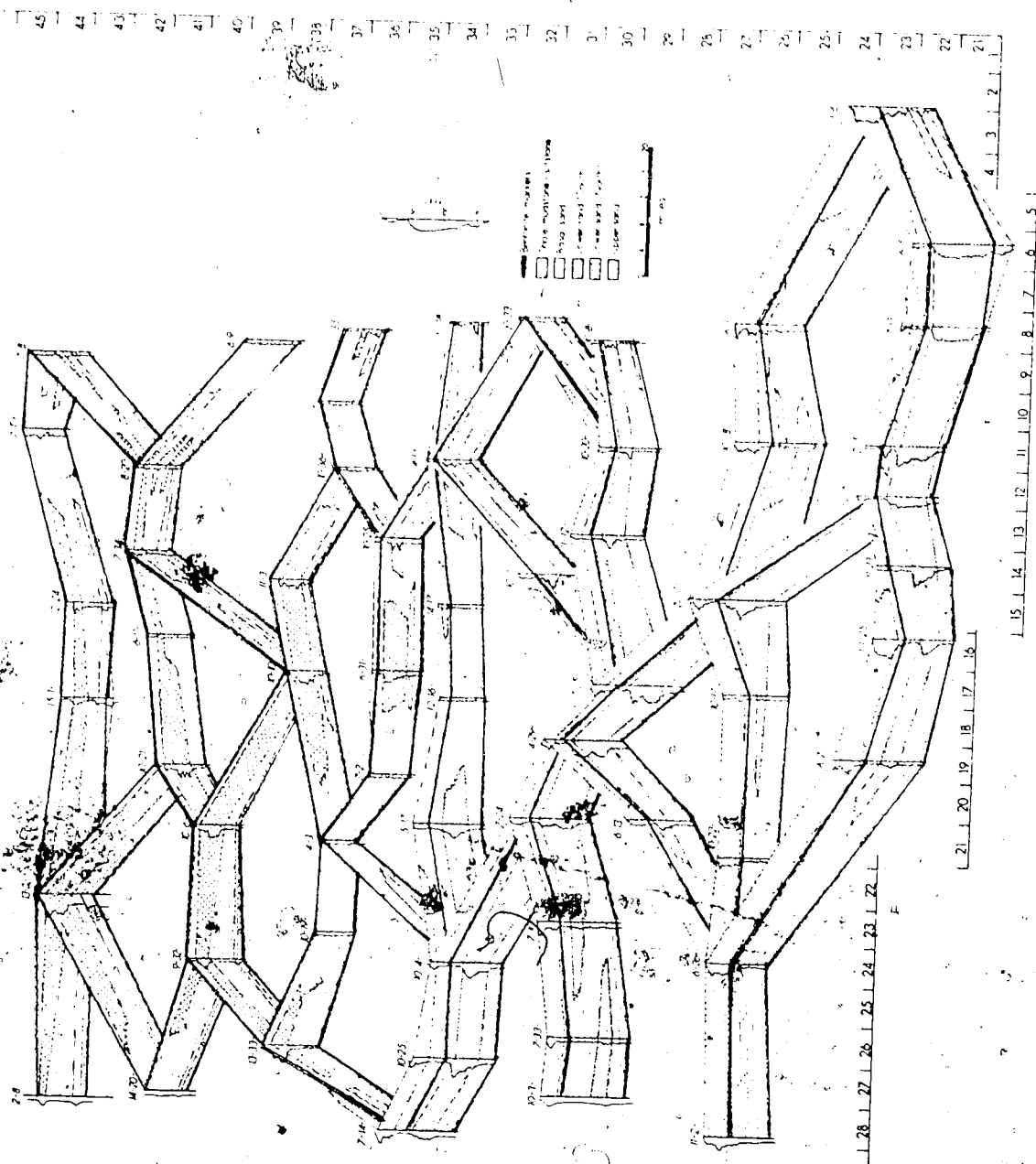


Figure 29. FENCE DIAGRAM OF THE VIKING FORMATION
 Rgs. 21 to 44, Rges. 3 to 28 W4M] (— Bent. 'A', — Bent. 'E')

progradation is obvious, except in the southeast where both westward and eastward progradations are indicated, suggestive of two opposing directions of sand transport. The northern Lower sand trends approximately in the same direction as the southern and appears to have prograded toward the west. Shale development in wells in the centre of the area separates the southern and northern Lower sand bodies.

A probable deepening halted sand formation almost throughout the area, and deposited silty shale, preserving a volcanic ash ('A' bentonite) deposit. This event marks essentially the termination of sand formation in the north, but in the south a final phase of sand deposition followed.

Initial southwestern and southeastern Upper sand bodies prograded towards one another almost at the same time. The latter overlaps the former in the south-central part of the area around townships 27 and 28, ranges 17 to 14W4M. This observation confirms an earlier suggestion of two opposing directions of sand transport during Viking deposition.

These sand bodies also terminate rather abruptly around wells 14-17-34-14W4M and 4-3-37-20W4M in a similar fashion to the underlying Lower sand. This last southern phase of sand development brought Viking deposition to an end in this area.

CHAPTER 8

SUMMARY AND CONCLUSIONS

A study of Viking well logs and cores has revealed the presence of bentonite horizons throughout the study area. A maximum of eight bentonite horizons with differing texture and thicknesses were observed in a single well. Five of these were differentiated chemically using Sr/Ca and Rb/K ratios, and a triangular plot of K, Ca, and Ti. Three of the bentonites have been regionally correlated and in turn used to correlate the Viking Formation in south-central Alberta.

The bentonite time planes show three periods of sand development in the area. A medium- to coarse-grained biotite-rich thick bentonite ('E') marks the beginning of Viking time and underlies the Basal thin sand in places. This sand body trends northwest-southeast and prograded slightly to the west.

Following this, a slight marine deepening deposited shales and silty shales, and preserved a volcanic ash fall ('C' bentonite) in the north, whereas deposition of the Lower sand had already begun in the southern and central parts of the area. This Lower sand body also trends in a northwest-southeast direction, acquiring a maximum thickness of about 80 ft. in the southeast. Both westward and eastward growth of the sand body are indicated.

In the north, a northwest-southeast trending Lower sand developed in places immediately after deposition of the 'C' volcanic ash. This independent sand body prograded westward.

The differential progradation of these sand bodies created a lagoon-like area between them where little or no sand deposition

occurred. Most of the Viking sands in the study area were deposited during this time interval.

Another marine deepening completely terminated sand deposition to the north and preserved another thick coarse biotite-rich volcanic ash ('A' bentonite) and silty shale deposits in the southern and central parts of the area.

Southeastern and southwestern Upper sandbodies followed the marine deepening. They developed at about the same time, but prograded in opposite directions. Deposition of these sandbodies brought Viking deposition to an end in the south and central parts of the area.

This complex sedimentation pattern accounts for the diachronous nature of the formation. The top of the formation is older to the north and younger to the south. This observation is in agreement with Evans (1970) who noted that the top of the Viking Formation in southwestern Saskatchewan is older to the northeast and younger to the south. Parallel to the paleo-strandline the formation is only slightly diachronous.

Biotite grain size distribution and Mn/Fe ratio maps tentatively suggest that the source area for the 'E' and 'C' bentonite beds lay to the southwest, while that of bentonite 'A' lay to the northwest of the study area but is uncertain.

The suggested linear relationship between biotite grain size, Rb/K and Mn/Fe ratios supports the model of change in chemistry of volcanic ash as a function of grain size and distance from source.

South of this area, Tizzard (1974) interpreted the sand units as offshore barrier bars. East of these bars in the Dodsland-Hoosier area in southwest Saskatchewan, Evans (1970) interpreted the sand bodies as

of tidal current origin. In the present study no attempts have been made to evaluate the depositional environment. However, more data are needed to evaluate the depositional environment of these sandbodies.

This work will serve as a framework to be used by later workers to differentiate and correlate the Viking bentonites in other areas of Alberta and Saskatchewan. These may enable an extensive time network datum to be established in the Viking Formation, which is necessary before detailed depositional history can be unravelled.

BIBLIOGRAPHY

- Abbey, S., 1975, Studies in 'standard samples' of silicate rocks and minerals, Part 4, 1974 edition of "usable values": Geol. Surv. Canada, Paper 74-41, 10 p.
- Bartlett, P.R., 1961, Spectrographic analyses for selected minor elements in Pierre Shale: U.S. Geol. Surv. Prof. Paper, 391-B, p. B4-B10.
- Beach, F.K., 1956, Reply to DeWiel on turbidity current deposits: Alberta Soc. Petroleum Geologists, Bull., v. 4(8), p. 175-177.
- Berg, R.R., and Davis, D.K., 1968, Sandstone at Bell Creek field, Montana: Am. Ass. Petroleum Geologists Bull., v. 52, p. 2099-2110.
- Borchardt, G.A., Aruscavage, P.J., and Millard, H.J., Jr., 1972, Correlation of the Bishop Ash, a Pleistocene marker bed, using instrumental neutron activation analyses: J. Sed. Petrology, v. 42(2), p. 301-306.
- DeWiel, J.E.F., 1956, Viking and Canby not turbidity current deposits: Alberta Soc. Petroleum Geologists, Bull., v. 4(8), p. 173-174.
- Eisbacher, G.H., Mesozoic - Tertiary basin models for the Canadian Cordillera and their geological constraints: Can. J. Earth Sci., v. 14(10), p. 2417.
- Evans, W.E., 1970, Imbricate linear sandstone bodies of the Viking Formation in Dodsland-Hoosier area of southwestern Saskatchewan: Am. Ass. Petroleum Geologists, Bull., v. 54(3), p. 469-486.
- Flanagan, F.J., 1973, 1972 values for International Geochemical reference samples: Geochem. Cosm. Acta., v. 37, p. 1189-1200.

- Gammell, H.G., 1955, The Viking Member in Central Alberta: Alberta Soc. Petroleum Geologists, Bull., v. 3(5), p. 63-69.
- Glaister, R.P., 1959, Lower Cretaceous of Southern Alberta and adjoining areas. Am. Ass. Petroleum Geologists, Bull., v. 43(3), p. 590-640.
- Jack, R.N., and Carmichael, I.S.E., 1969, The Chemical 'Fingerprinting' of Acid Volcanic Rocks, in Short Contributions to California Geology, Special Report 100, California Division of Mines and Geology, p. 17-32.
- Jenkins, R., and De Vries, J.L., 1967, Practical X-ray Spectrometry: Springer-Verlag, 190 p.
- Jones, H.L., 1961, The Viking Formation in southwestern Saskatchewan: Dept. of Mineral Resources, Saskatchewan, Rept. No. 65, 79 p.
- Kauffman, E.G., 1977, Geological and Biological Overview: Western Interior Cretaceous Basin: The Mtn. Geologist, v. 14(3 and 4), p. 81.
- Kiley, W.R., 1960, The function and application of counters and the pulse height analyzer. Norelco Report, VII(6), p. 143-149.
- Koldijk, W.S., 1976, Gilby Viking 'B': A Storm Deposit, in Leland, M.M. (ed.), The Sedimentology of Selected Clastic Oil and Gas Reservoirs in Alberta, Can. Soc. Petroleum Geologists, p. 62-77.
- Larson, L.H., 1969, (ed.), Gas Fields of Alberta: Alberta Soc. Petroleum Geologists, p. 5.
- Lerbekmo, J.F., 1968, Chemical and modal analyses of some Upper Cretaceous and Paleocene bentonites from western Alberta: Can. J. Earth Sci., v. 5(6), p. 1505-1511.

- Lerbekmo, J.F., and Campbell, F.A., 1969, Distribution, composition, and source of the White River Ash, Yukon Territory: *Can. J. Earth Sci.*, v. 6(1), p. 109-116.
- Lerbekmo, J.F., Westgate, J.A., Smith, D.G.W., and Denton, G.H., 1975, New Data on the Character and History of the White River Volcanic Eruption, Alaska, in Suggates, R.P., Cresswell, M.M. (eds.), *Quaternary Studies: Roy. Soc. New Zealand*, p. 203-209.
- Merriam, R., and Bischoff, J.L., 1975, Bishop Ash: A widespread volcanic ash extended to southern California: *J. Sed. Petrology*, v. 45(1), p. 207-211.
- Norrish, K., and Chappell, B., 1967, X-ray Fluorescence Spectrography, in Zussman, J. (ed.), *Physical Methods in Determinative Mineralogy: Acad. Press*, p. 161-214.
- Rader, L.F., and Grimaldi, F.D., 1961, Chemical analysis for selected minor elements in Pierre Shale: *U.S. Geol. Surv. Prof. Paper*, 391-A, p. A7-A13.
- Roessingh, H.K., 1959, Viking Deposition in the Southern Alberta Plains: *Alberta Soc. Petroleum Geologists, 9th Annual Field Conf.*, p. 130-137.
- Rudkin, R.A., 1964, Lower Cretaceous, Chapter 11, in McCrossan, R.G. and Glaister, R.P., *Geological History of Western Canada: Alberta Soc. Petroleum Geologists*, p. 156-168.
- Shelton, J.W., 1973, Models of sand and sandstone deposits: a methodology for determining sand genesis and trend: *Viking Sandstone, Cretaceous, Joffre Field, Alberta: Oklahoma Geol. Surv. Bull.*, 118, p. 91-94.
- Slipper, S.E., 1918, Viking Gas Field, Structure of Area: *Geol. Surv. Summ. Rept.* 1917, Part C, p. 8C.

- Smith, D.G.W., and Westgate, J.A., 1968, Electron probe technique for characterizing pyroclastic deposits: *Earth Planet. Sci. Lett.*, v. 5, p. 313-319.
- Stelck, C.R., 1958, Stratigraphic position of Viking sand: *Alberta Soc. Petroleum Geologists, Bull.*, v. 6(1), p. 2-7.
- , 1975, The Upper Albian Miliamina manitobensis zone in north-eastern British Columbia, in Caldwell, W.G.E. (ed.), *The Cretaceous System in the Western Interior of North America*: *Geol. Assoc. Can. Special Paper No. 13*, p. 253-275.
- Tizzard, P.G., 1974, Viking deposition in the Suffield area, Alberta: Unpub. M.Sc. thesis, University of Alberta, p. 54.
- Tizzard, P.G., and Lerbekmo, J.F., 1975, Depositional history of the Viking Formation, Suffield area, Alberta, Canada: *Can. Soc. Petroleum Geologists, Bull.*, v. 23(4), p. 715-752.
- Wheeler, J.O., Aitken, J.D., Berry, M.J., Gabrielse, H., Hutchison, W.W., Jacoby, W.R., Monger, J.W.H., Niblett, E.R., Norris, D.K., Price, R.A., Stacey, R.A., 1972, The Cordilleran Structural Province, in Price, R.A., and Douglas, J.W. (eds.), *Variations in Tectonic Styles in Canada*: *Geol. Assoc. Can. Special Paper No. 11*, p. 1-82.
- White, R.J., 1960, (ed.), *Oil fields of Alberta*: *Alberta Soc. Petroleum Geologists*, p. 5.
- James, G.D., and Stelck, C.R., 1975, Speculations on the Cretaceous palaeogeography of North America, in Caldwell, W.G.E., (ed.), *The Cretaceous System in the Western Interior of North America*: *Geol. Assoc. Can. Special Paper No. 13*, p. 7.
- Yen Fu-Su, and Goodwin, J.H., 1976, Correlation of tuff layers in the Green River Formation, Utah, using biotite compositions: *J. Sed. Petrology*, v. 46(2), p. 345-354.

APPENDICES.

APPENDIX A
WELL NAME, LOCATION, CORED INTERVAL, DEPTH AND THICKNESS OF OBSERVED BENTONITE HORIZONS
IN THE VIKING FORMATION OF THE STUDY AREA

No.	Well Name	Location	Cored Interval (ft.)	Depth (ft.)	Bentonites Thickness (in.)	Type	Remarks
1.	Mobil Matzim	11-23-23-14W4	2630-2716	2647 2665 2680	12 1 1	coarse fine fine	
2.	H.B. Cessford	14-26-25-12W4	2710-2760 2784-2825	2715 2785	1 12	fine coarse	
3.	Oak Ridge oil and minerals #7-21	11-31-27-16W4	3700-3799	3717	1	medium-coarse	
4.	Provo Halliday	13-11-28-14W4	3065-3160	3116 3131	9 2	coarse fine	
5.	Calstain Handhills	10-36-28-14W4	3062-3164	3097 3107	6 4	coarse coarse	
6.	TGT Mobil Oil CPR Nacime #6-1	11-6-28-21W4	4161-4221	4178	<1/2	fine	

APPENDIX A (cont'd)

No.	Well Name	Location	Cored Interval (ft.)	Depth (ft.)	Bentonites Thickness (in.)	Type	Remarks
7.	West Coast Sun Petro Smole	11-30-29-10W4	2769-2895	2856 2876 2895	6 6 6	coarse fine medium	
8.	Fina Handhills	7-22-29-14W4	3051-3113	3038	12	coarse	
9.	CDR Handhills	1-33-29-17W4	4210-4224.5	4224	<1	fine	
10.		7-1-29-10W4	3645-3765	3651	2	fine	
11.	Oak Alta. Can. Pet. Richdale	7-10-30-12W4	3025-3058	3012	2	coarse	
12.		10-13-30-11W4	2831-2920	2851 2861 2871 2876 2882 2903		fine medium fine fine medium coarse	
13.	Amoco B-1 Youngstown	6-34-30-8W4	2700-4800	2750 2770	6 12	medium coarse	

APPENDIX A (cont'd)

No.	Well Name	Location	Cored Interval (ft.)	Depth (ft.)	Bentonites Thickness (in.)	Type	Remarks
14.		10-20-30-12W4	2987-3060	3007	3	coarse	
15.	Westlock et al. Rochdale	11-7-30-12W4	3040-3150	3098 3101	3 3	coarse coarse	
16.	* Dome IOE Willdunn	6-23-30-14W4	3088-3210	3118 3153 3154	2 3 3	coarse coarse coarse	
17.	Ponderay et al. Youngs Bluff	12-19-31-9W4	2860-2913	2868 2875 2896 2907	2 4 2 24	fine medium fine fine/coarse	fine 12"/coarse 12"
18.	West Coast et al. Richdale	10-4-31-13W4	3165-3225	3216 3217	2 1	fine coarse	
19.	C.S. Fenner	11-11-32-11W4	2918-2996	2956 2988 2996	3 3 12	fine medium medium	
20.	C.S. Sulpetro et al. Farrel	6-12-34-17W4	3390-3550	3465 3471 3479 3516	<1 <1/2 3 12	fine fine fine/coarse fine/coarse	

APPENDIX A (cont'd)

No.	Well Name	Location	Cored Interval (ft.)	Depth (ft.)	Bentonites Thickness (in.)	Type	Remarks
21.	SED Banff Wimboine #7-9	7-9-34-26W4	5273-5293 5313-5400	5350	9	fine/coarse	
22.	Chapman Hame1	4-13-34-11W4	2941-2986	2942 2964 2971 2984	2 3 2 2	fine fine fine fine	interlaminated with shale
23.	Mapco Provost	2-5-34-9W4	2893-2944	2908 2916	12 <1/2	fine fine	
24.	Triad BP Sullivan	7-2-35-14W4	3170-3255	3254	2	coarse	
25.	CEJA Gulf KPL Maple Glen	10-34-36-16W4	3316-3366	3340 3352	3 <2	fine fine	interlaminated with shale
26.	GRT Plns. BA Louisiana	10-15-36-22W4	4427-4482	4447 4470 4472	1 1/2 2 1	medium coarse	pieces of coarse bentonite
27.	Mosbacher et al. Provost	2-22-36-11W4	2980-3027	2981 3008 3023	1 3 3	coarse medium medium	
28.	Sohio Leslie Underwood I	16-25-36-26W4	5165-5214	5131	3	fine	interlaminated with shale

APPENDIX A (cont'd)

No.	Well Name	Location	Cored Interval (ft.)	Depth (ft.)	Bentonites Thickness (in.)	Type	Remarks
29.	Cabeen Expl. Pine Lake	10-25-36-24W4	4773-4823	4780 4794 4804	3 <1 9	coarse fine fine	interlaminated with shale.
30.	Cesa PCP LEO	6-21-36-17W4	3399-3459	3452 3455	1 1/2 12	coarse fine-medium	
31.		6-13-38-13W4	279-2900	2853 2855 2864	3 2 3	fine fine fine	interlaminated with shale
32.	California Std. Burbank	3-22-39-27W4	5145-5235	5184 5191	6 2	coarse coarse	
33.	Sharples Kessler	6-9-39-8W4	2520-2555 3000-3027	2554	<1	fine	
34.	Provo Brown field	7-16-39-11W4	2642-2702	2677 2680 2684 2688	2 1/2 4 2 3	coarse fine coarse medium	
35.	BA Ratdan Erskine	7-29-39-20W4	3778-3848	3816	2	fine	

APPENDIX A (cont'd)

No.	Well Name	Location	Cored Interval (ft.)	Depth (ft.)	Bentonites Thickness (in.)	Type	Remarks
36.	Dome HBOG Provost	10-9-39-10W4	2710-2747	2718 2719	<1/2 15	fine fine/medium	
37.	Quasar Alliance	2-13-40-13W4	2688-2748	2714 2719 2720 2740	1 3 3 3	coarse coarse coarse fine	
38.		7-5-40-17W4	3305-3415	3389	2	fine	
39.	Grt. Plns. Cdn. Sup. Lacombe	14-28-41-26W4	4743-4843	4790 4821	2 4	fine/coarse	
40.	HB et al. Schneider Lake	4-33-41-13W4	2545-2638	2580 2586 2598 2608	<1 <1 >3	fine coarse fine	pieces of medium-coarse; 9" interval not cored
41.	Imperial Clive North	11-8-41-24W4	4425-4621	4480	?	fine	
42.	Grt. Plns. Cdn. Sup. Lacombe	1-22-41-26W4	4741-4855	4807 4845	3 1	fine	

APPENDIX A (cont'd)

No.	Well Name	Location	Cored Interval (ft.)	Depth (ft.)	Bentonites Thickness (in.)	Type	Remarks
43.	Bluemont Rosaline	11-16-44-18W4	3050-3110	3068 3074 3076 3094	2 1 1/2 2 3	fine fine coarse fine	
44.	Calston Daysland	11-19-44-16W4	2811-2895	2869 2870	<1/2 2	fine fine	
45.	Imperial Rosaline	9-9-44-17W4	2900-2953	2924 2940 2942	3 3 4	fine medium coarse	
46.	Anglo Krdy C and E Edberg	1-1-45-20W4	3250-3290	3253 3271 3276	4 1 15	fine fine fine-medium-coarse	
47.	Crown Tanner	7-11-46-20W4	3215-3255	3240 3246	3 14	fine fine-medium-coarse	
48.	G. Basins et al. Bruce	10-13-47-16W4	2520-2580	2521 2530 2533 2539 2542 2549 2556 2567	<1 <1 2 1/2 2 3 1/2 1 1/2 3 <1	fine fine coarse medium-coarse medium-coarse coarse medium-coarse fine	

APPENDIX A (cont'd)

No.	Well Name	Location	Cored Interval (ft.)	Depth (ft.)	Bentonites Thickness (in.)	Type	Remarks
49.		8-30-47-10W4	2150-2199	2166 to 2168 2184	20 1 1/2	fine/coarse fine	small intercalations of sandy shale
50.	Chief Blue Crown Holden	6-36-49-14W4	2185-2240	2220	3/4	fine	
51.	S0BC C.S. W10-13	10-13-49-22W4	3280-3340	3298 3329 3336	<1/2 1 1/2	fine fine-medium	
52.		8-30-49-10W4		2543 2556 2558 2559 2561	1 1 3 2 1	fine fine fine fine fine	
53.	Texas Pacific Patterson #1	14-4-51-22W4	3270-3340	3294 3330 3334	4 6 12	medium fine coarse	shale interbedded with shale
54.	Colorado Oil and Gas #7-36	7-36-51-19W4	2490-2584	2537	2	coarse	
55.	Null Beaverhill Lake	10-21-52-20W4	2772-2824	2782	<1	fine	

APPENDIX A (cont'd)

No.	Well Name	Location	Cored Interval (ft.)	Depth (ft.)	Bentonites Thickness (in.)	Type	Remarks
56.	Husky Union Imperial Cooking Lake	11-21-52-22W4	3015-3103	3019 3027	3/4 1	fine fine	
57.	Minerals Plains	10-12-53-12W4	1810-1870	1849 1861	<1 1	coarse coarse	
58.	Imperial Peavy 16-30	16-30-56-24W4	2763-2832	2768	1		
59.	Imperial Moronville	6-32-56-24W4	2678-2839	2756 2773 2821	2 1/2 1	coarse fine	
60.	Imperial Fairy Dell	10-8-57-24W4	2647-2770	2701	2		Bentonitic shale; poor core recovery
61.	Imperial FBA 10-9V	10-9-57-23W4	2419-2488	2444 2447 2454	<1/2 2 6	fine fine fine	shale interlamination
62.	Imperial Eastgate	1-34-57-22W4	2150-2239	2215 2232	2 1/2 2	fine fine	

APPENDIX A (cont'd)

No.	Well Name	Location	Cored Interval (ft.)	Depth (ft.)	Bentonites Thickness (in.)	Type	Remarks
63.	Imperial Union FBA #6-23V	6-23-58-25W4	2500-2583	2550	<1	fine-medium	
64.	Miami Anoco SE Clyde	10-11-59-24W4	2185-2235	2235	>6	coarse	
65.	Imperial Westlock	6-3-60-27W4	2466-2586	2491 2493	2 1/2 2	fine medium-coarse	

APPENDIX B

OPERATING CONDITIONS FOR XRF ANALYSES

Element	Tube Type	Analyzing Xtal	Peak Position (2 θ)	Background (2 θ)	Detector	Detector Voltage (Volts)	Pulse Height Analyzer Level	Window
Al	W	PET	145.13°	144°	Flow	1600	2	5
K	W	PET	50.68°	49.5°	Flow	1600	2	5
Ca	W	PET	45.18°	44.1°	Flow	1600	2	5
Ti	W	PET	36.65°	35.8°	Sc	1000	2	5
Mn	Mo	Lif 220	95.12°	94.6°	Sc	1000	2	5
Fe	Mo	Lif 220	85.65°	84.6°	Sc	1000	2	5
Rb	Mo	Lif 220	37.93° 37.4°	37.4°	Sc	1000	2	5
Sr	Mo	Lif 220	35.8°	35.2°	Sc	1000	2	5
Zr	Mo	Lif 220	32.04°	31.55°	Sc	1000	2	5

APPENDIX C.

PERCENTAGE CHEMICAL ANALYSES FOR STANDARDS EMPLOYED FOR CALIBRATION CURVES

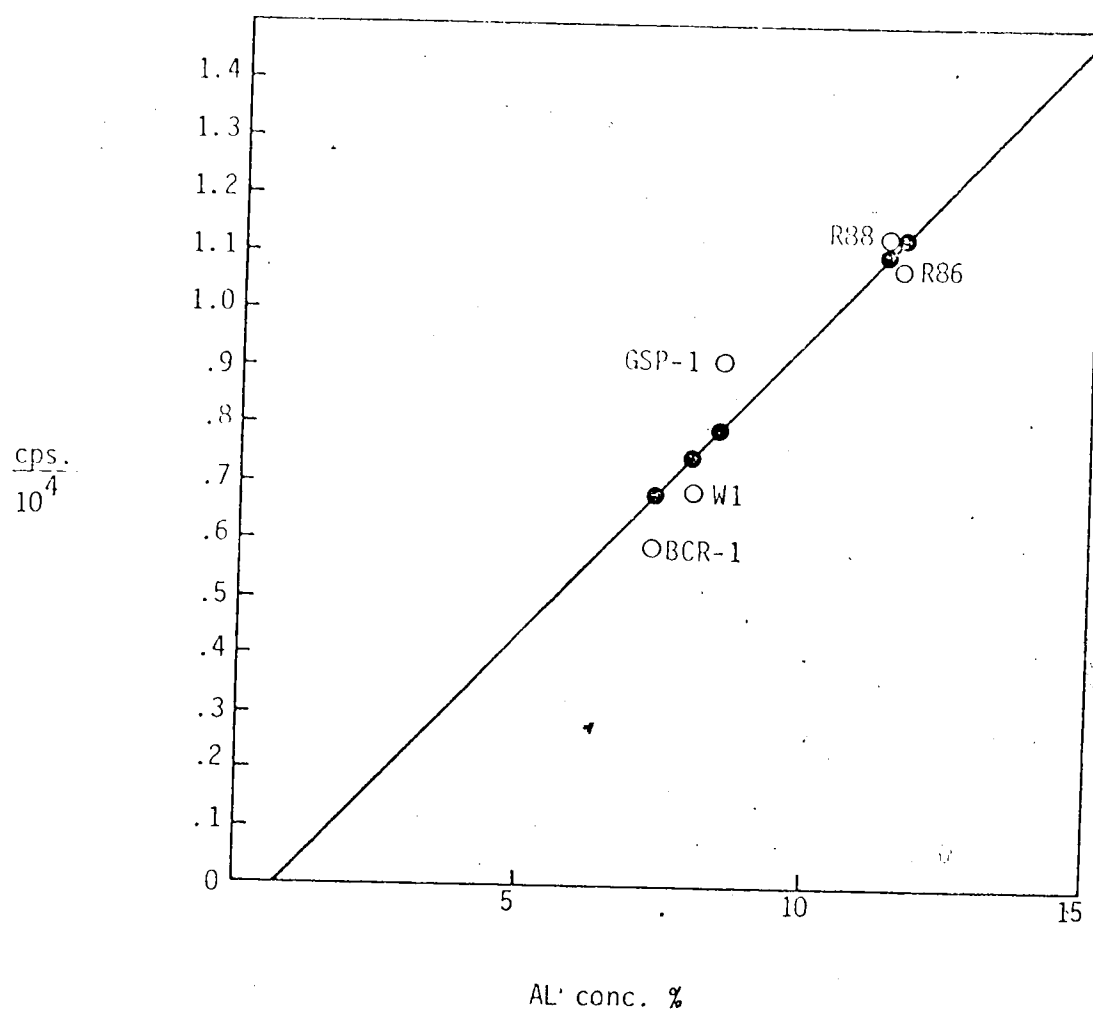
	R ₁₈		R ₅₃		R ₈₆		R ₈₇		R ₈₈		4132 ¹		4156 ¹	
	Oxide Conc. %	Elem. Conc. %	Oxide Conc. %	Elem. Conc. %	Oxide Conc. %	Elem. Conc. %	Oxide Conc. %	Elem. Conc. %	Oxide Conc. %	Elem. Conc. %	Oxide Conc. %	Elem. Conc. %	Oxide Conc. %	Elem. Conc. %
Al					21.71	11.5			21.3	11.3				
K	4.95	4.11			2.65	2.2	1.33	1.1	2.85	2.37				
Ca	4.7	3.36	.8	.57	3.67	2.62	2.75	1.97	3.37	2.41				
Ti	.19	.12												
Mn					.12	.093	.04	.031	.52	.31	.15	.09	.54	.39
Fe ⁴														
Fe ₂ O ₃			2.86	(3.034)	2.56	(3.0)	2.04	(1.7)	2.15	(3.06)				
FeO			1.33		1.55		.35		2.01					

R samples = Bentonites (chemical analyses)
 1 = Bentonites (chemical analyses)
 4 = Used Fe₂O₃ and FeO for conversion

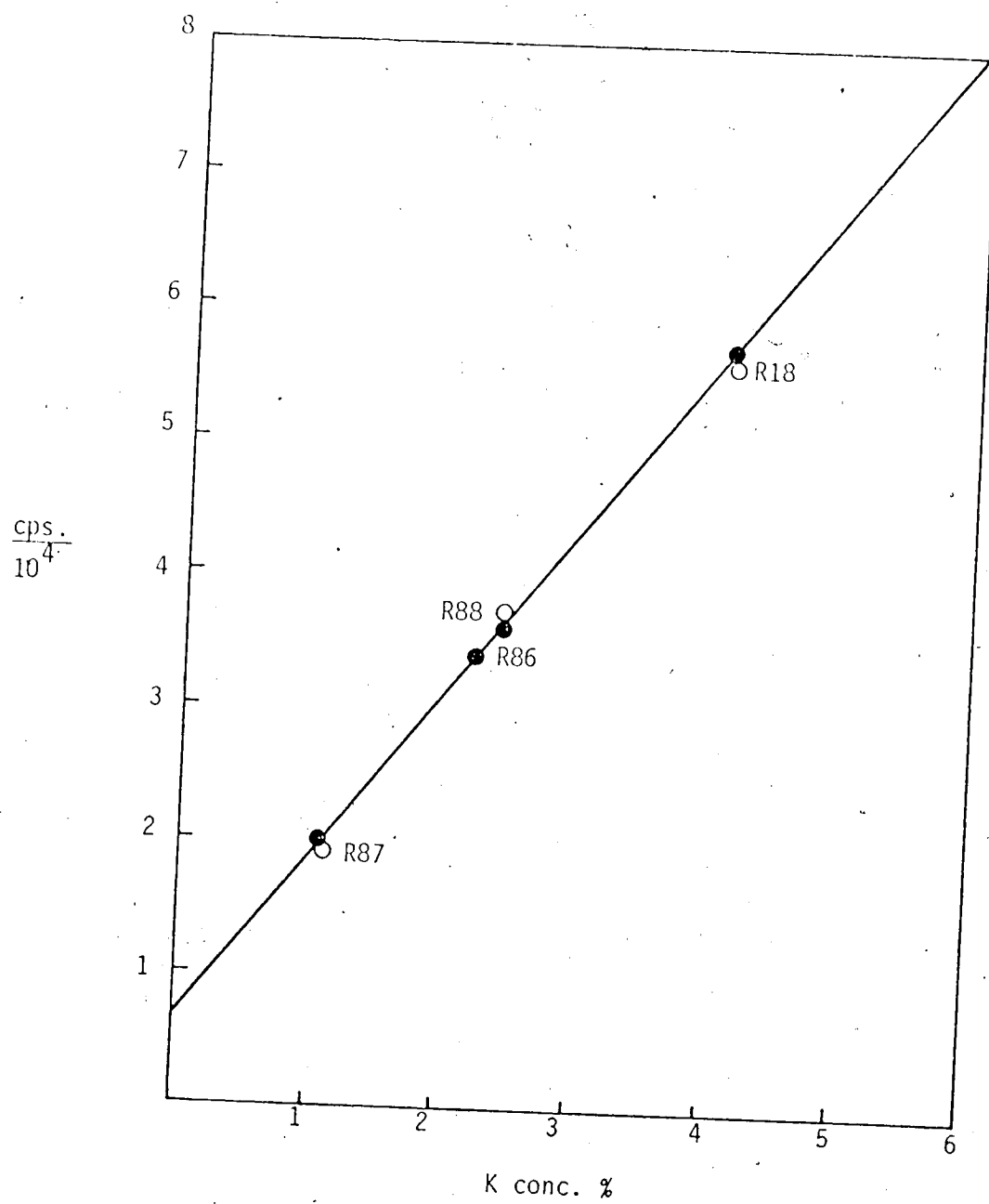
APPENDIX C (cont'd)

259563 ²	259533 ²	G ₁ *		G ₂ *		GSP-1*		AGV-1*		W-1*		BCR-1*	
		Oxide Elem. Conc. %	Oxide Elem. Conc. %	Oxide Elem. Conc. %	Oxide Elem. Conc. %	Oxide Elem. Conc. %	Oxide Elem. Conc. %	Oxide Elem. Conc. %	Oxide Elem. Conc. %	Oxide Elem. Conc. %	Oxide Elem. Conc. %	Oxide Elem. Conc. %	Oxide Elem. Conc. %
Al													
K													
Ca													
Ti													
Mn													
Fe ⁴													
Rb													
Sr													
Zr													

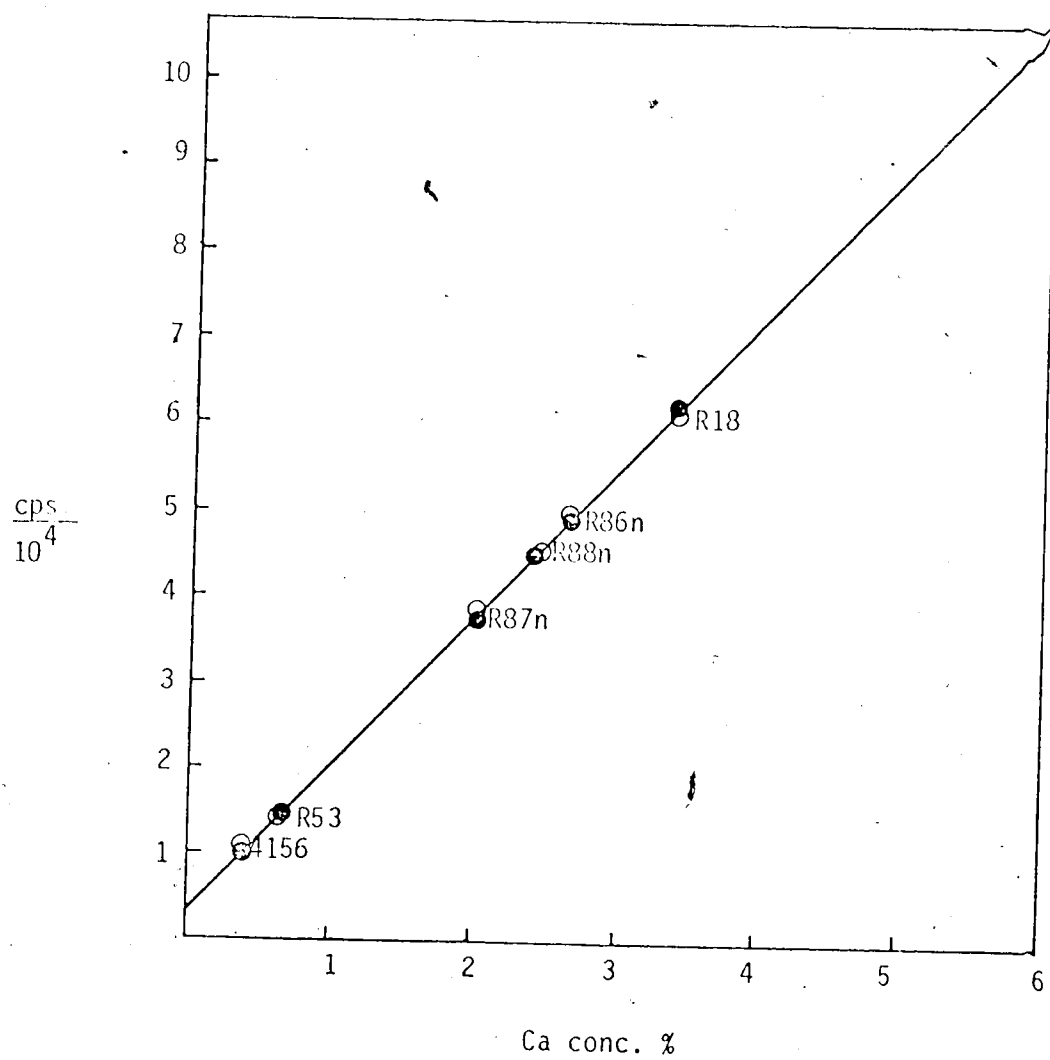
2 = Pierre shales (spectrographic analyses, Rader and Grimaldi, 1961)
3 = Corrected values of USGS standards (Abbey, 1975)
4 = Used Fe₂O₃ and FeO for conversion
* = USGS standards G₁ & G₂ - Granites; GSP-1 - Granodiorite;
AGV-1 - Andesite; W-1 - Diabase; BCR-1 - Basalt
(Flanagan, 1972)

AL Standard

Regr. Equat. = $Y = .103X - .06$

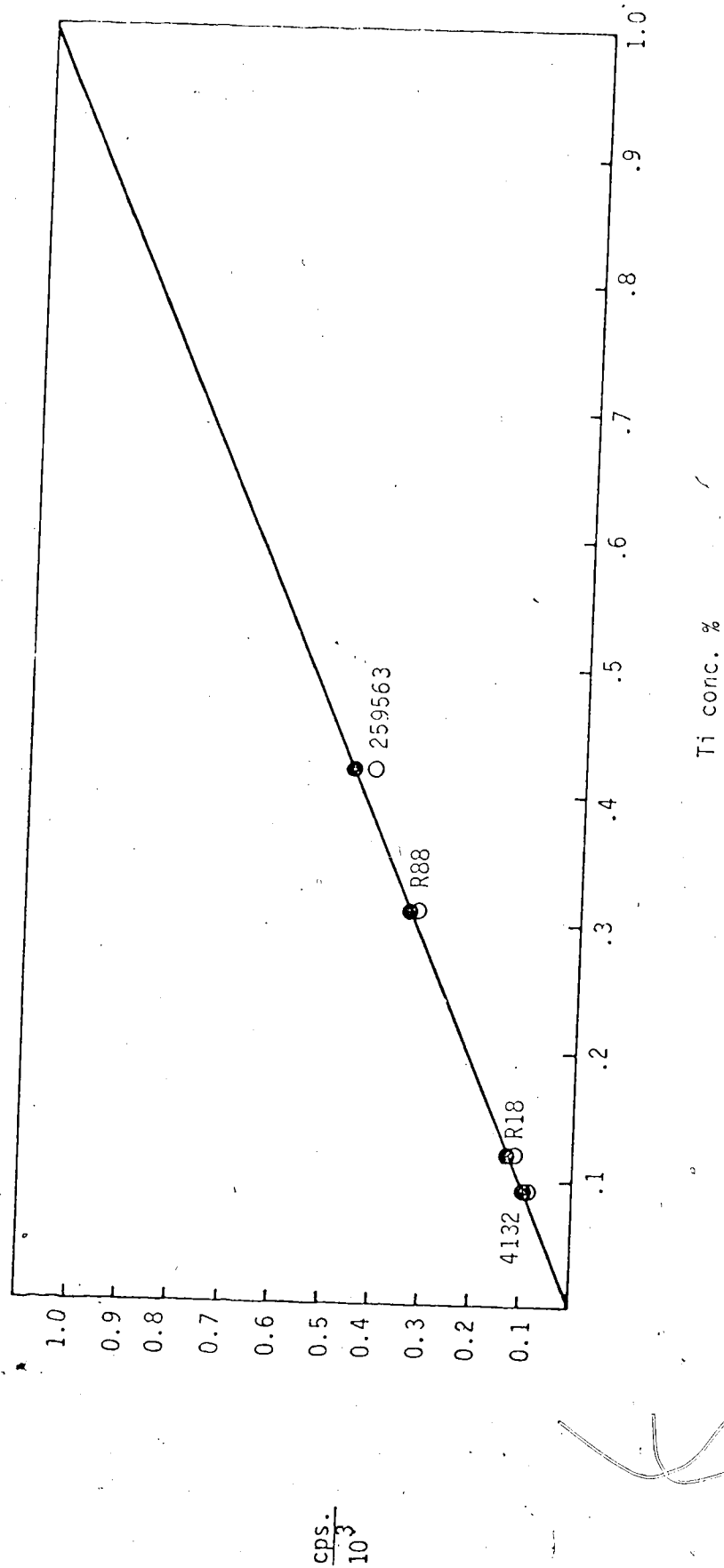
K Standard

$$Y = 1.22X + .67$$

Ca Standard

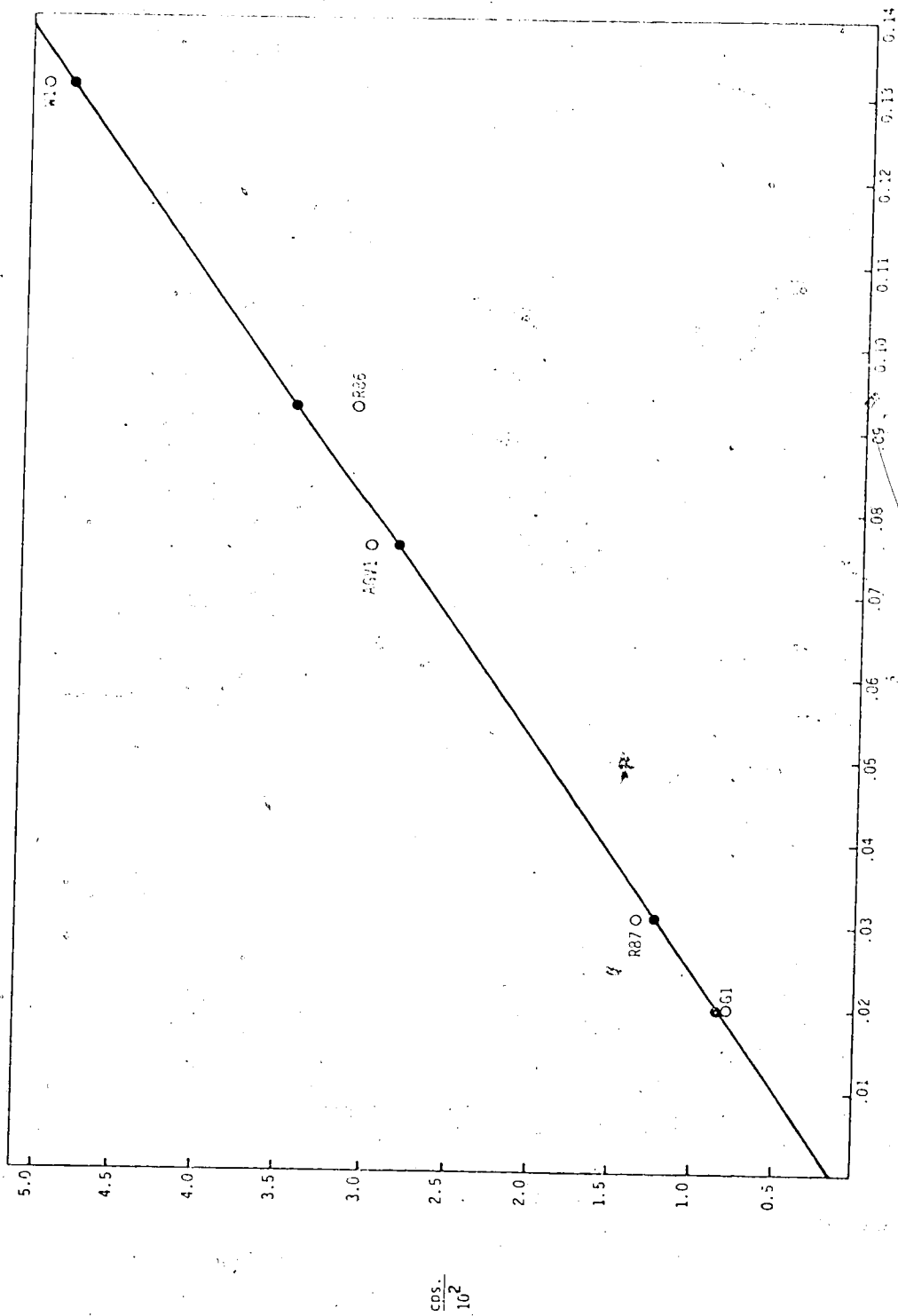
$$Y = 1.69X + .46$$

Ti Standard

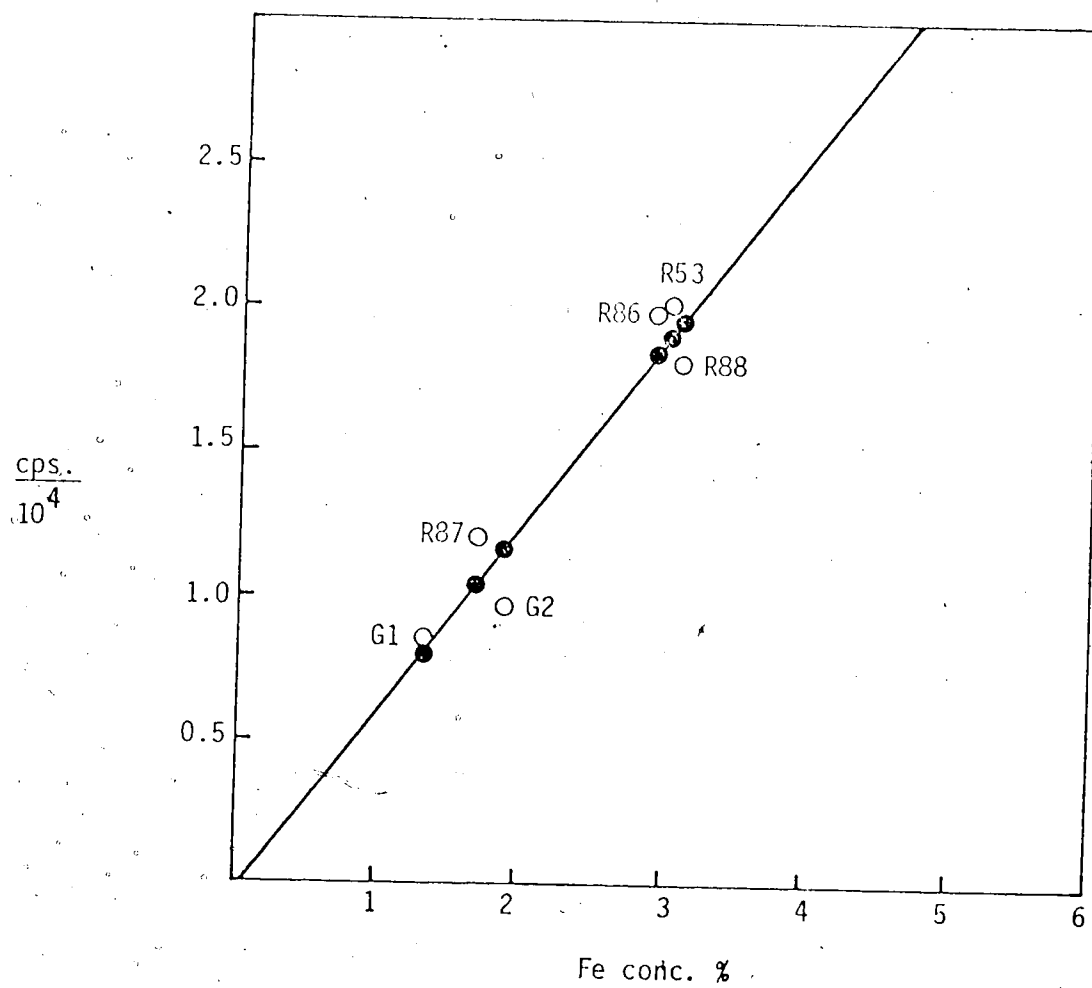


$Y = 1.1X - .002$

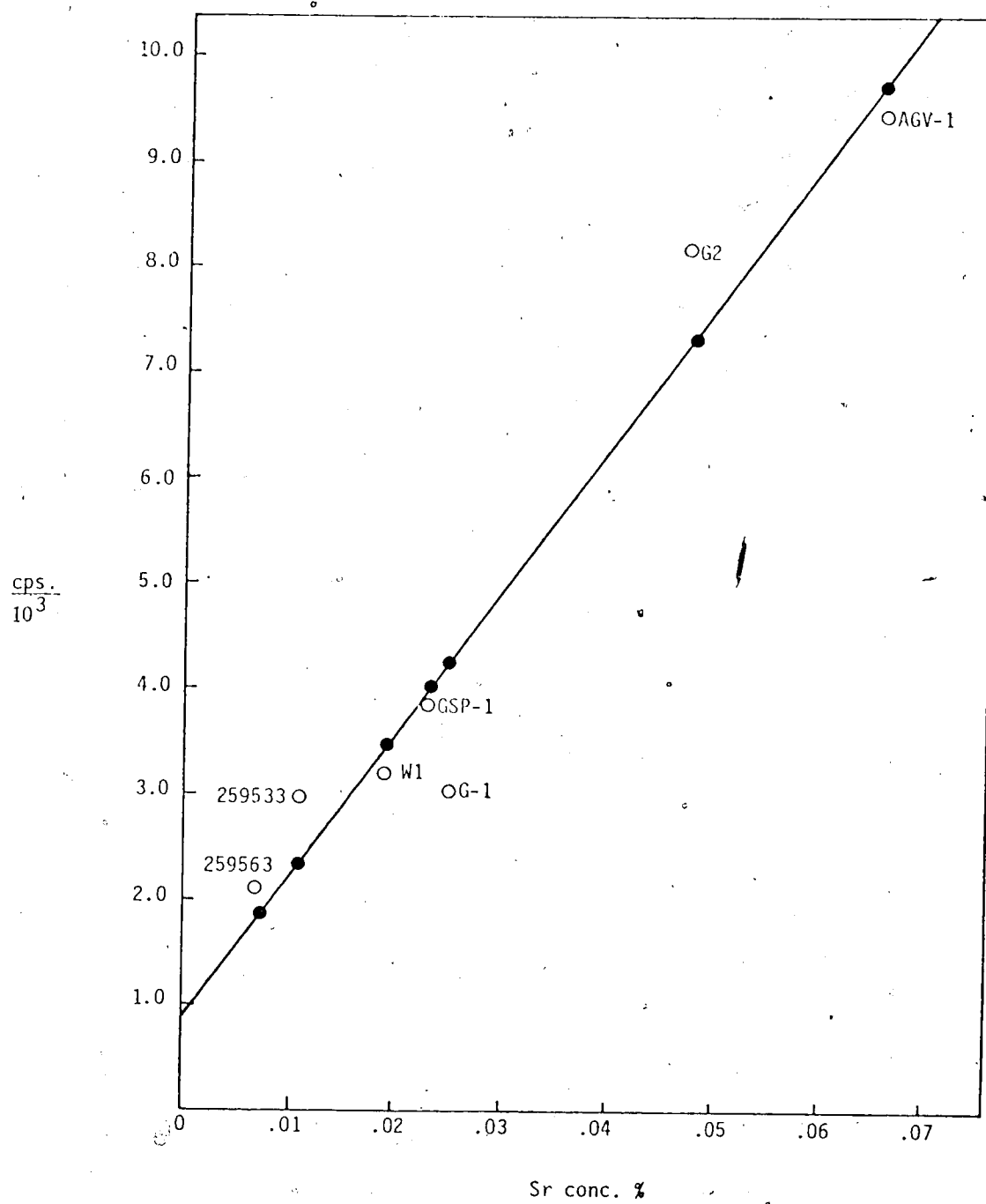
Mn Standard



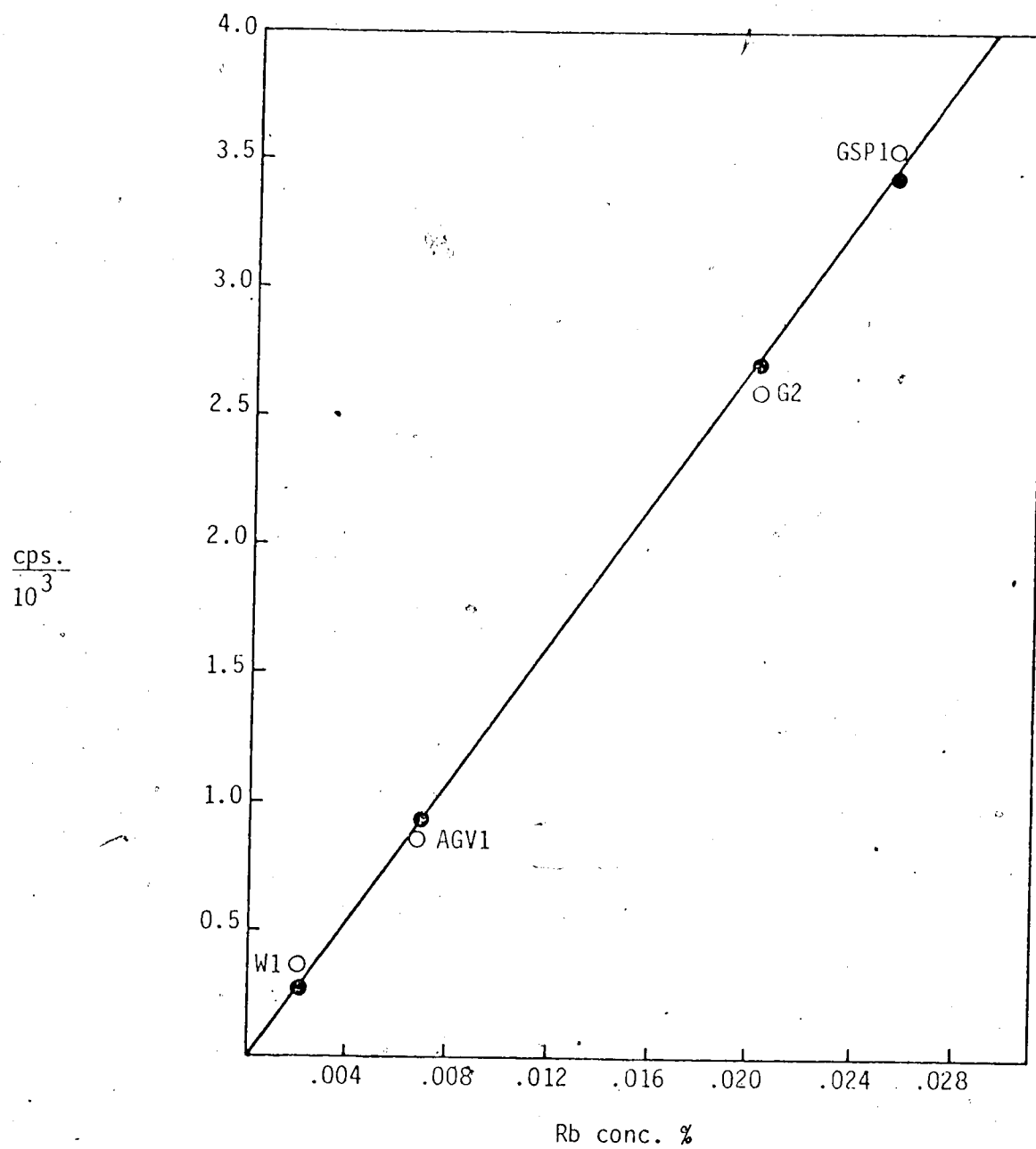
$$Y = 35.8X + .12$$

Fe Standard

$$Y = .66X - .092$$

Sr Standard

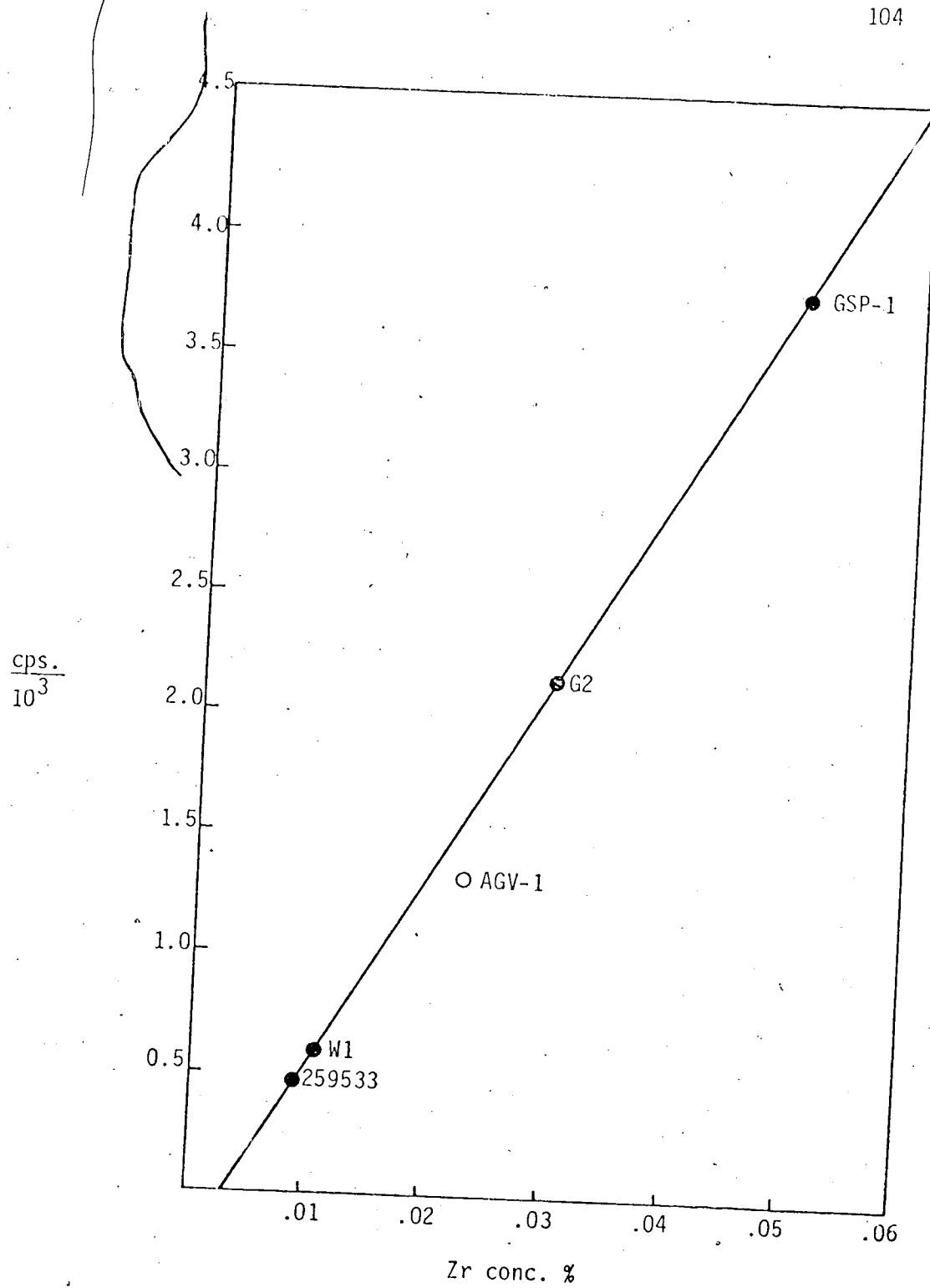
$$Y = 134.91X + .88$$

Rb Standard

$$Y = 136.24X - .016$$

Zr Standard

104



$$Y = 80.98X - .27$$

D

2-29-27-28W4

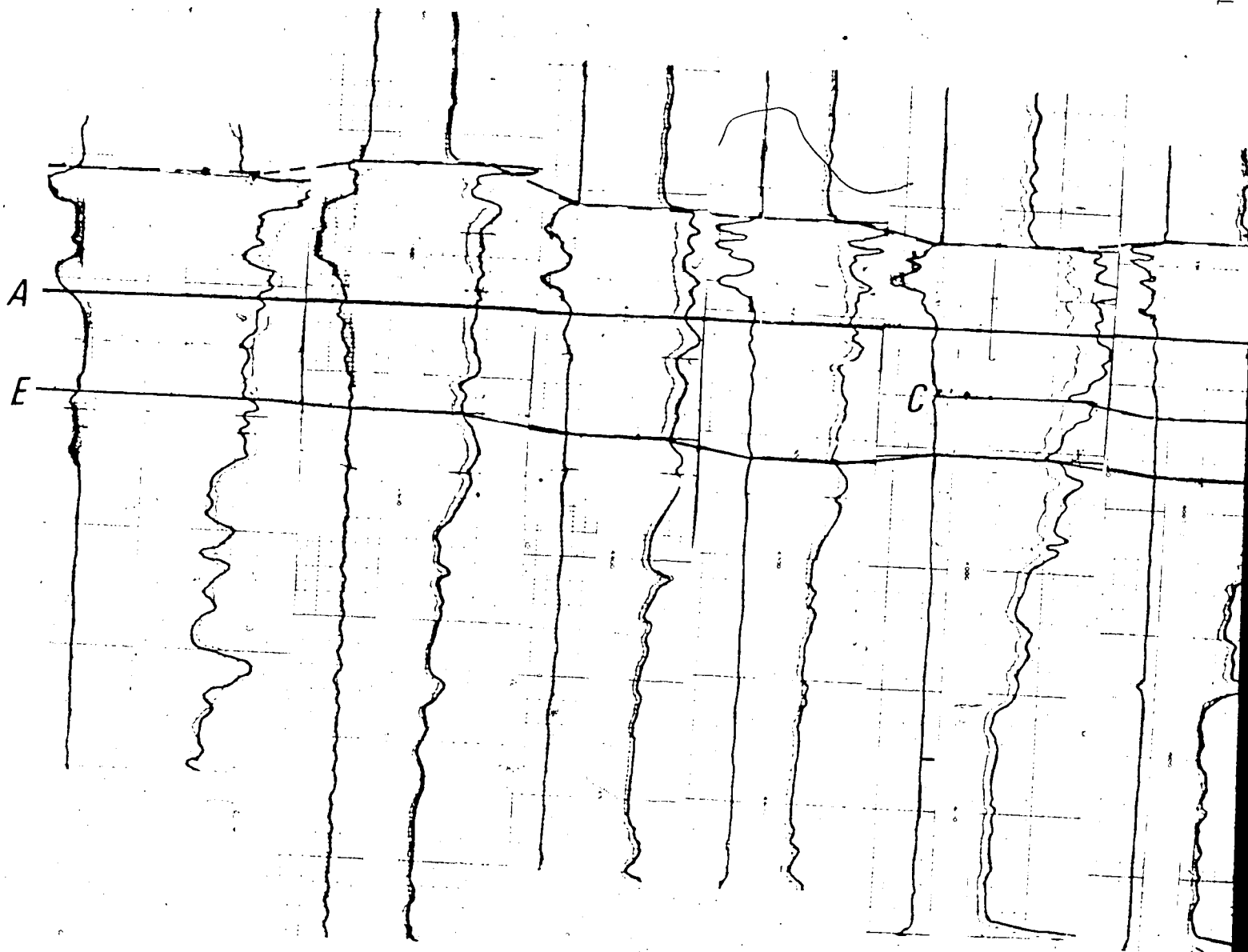
11-6-27-24W4

6-15-27-23W4

10-5-27-22W4

6-26-27-21W4

11-12-27-20W4



E

11-23-23-14W4

14-23-26-14W4

16-5-27-14W4

6-12-28-14W4

3-14-29-14W4

7-16-30-14W4

11-12-27-20W4

7-1-27-19W4

6-27-27-18W4

10-21-27-17W4

10-24-27-16W4

6-12-27-15W4

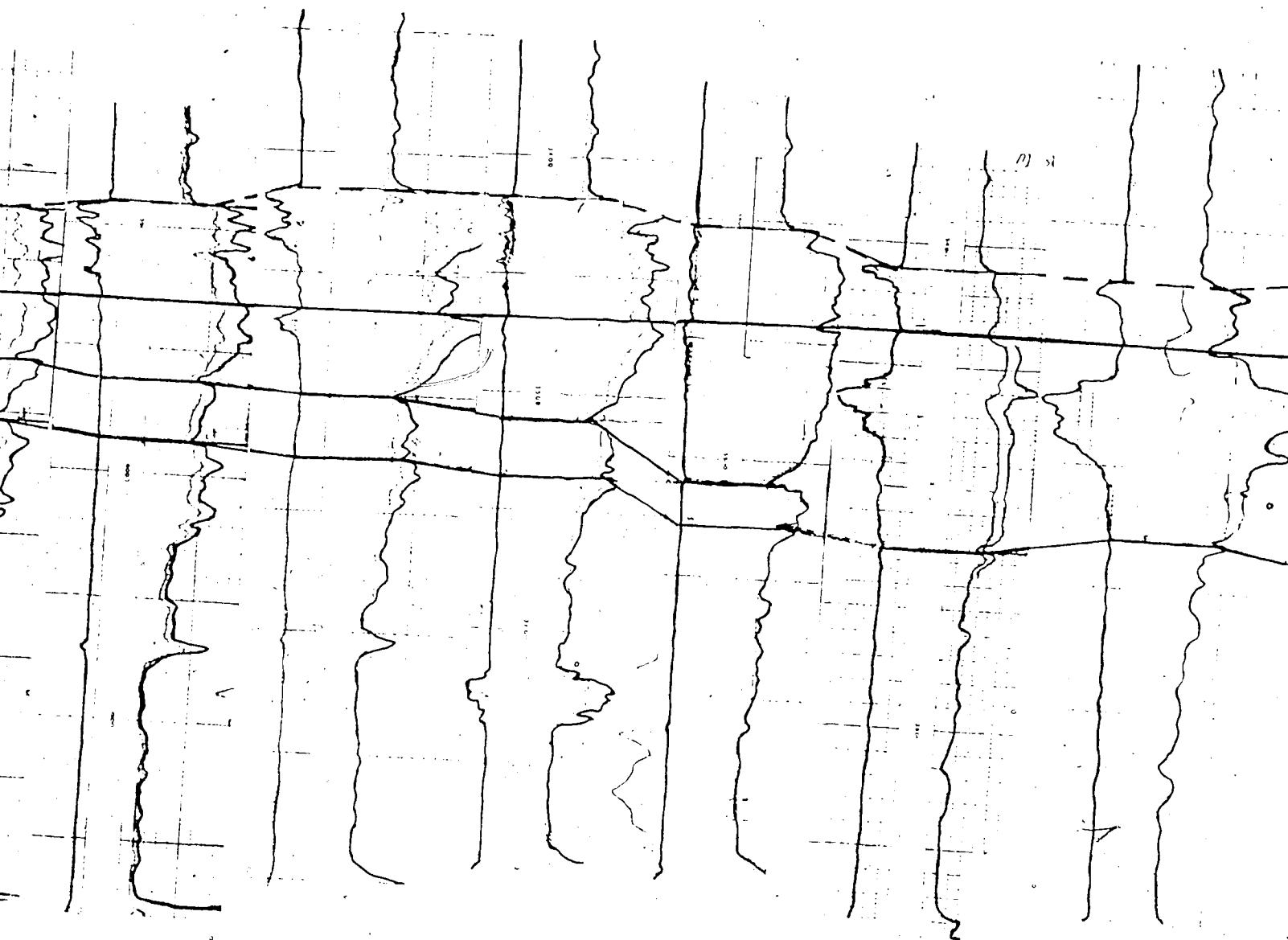


Figure 17. Cross Section D-D'.

7-16-30-14W4

10-16-31-14W4

6-22-32-14W4

11-31-33-14W4

14-7-34-14W4

11-23-34-14W4

11-28-35-14W4

10

D'

7-9-27-14W4

6-22-27-13W4

10-34-27-12W4

7-10-27-11W4

11-29-27-10W4

A

E

34

0-20-36-14W4

10-21-37-14W4

10-27-38-14W4

16-5-42-14W4

10-13-44-15W4

13-11-47-14W4

E'

E

11-23-23-14^{W4}

14-23-26-14^{W4}

16-5-27-14^{W4}

6-12-28-14^{W4}

3-14-29-14^{W4}

7-16-30-14^{W4}

B



Figure

Figure 17. Cross Section D-D'.

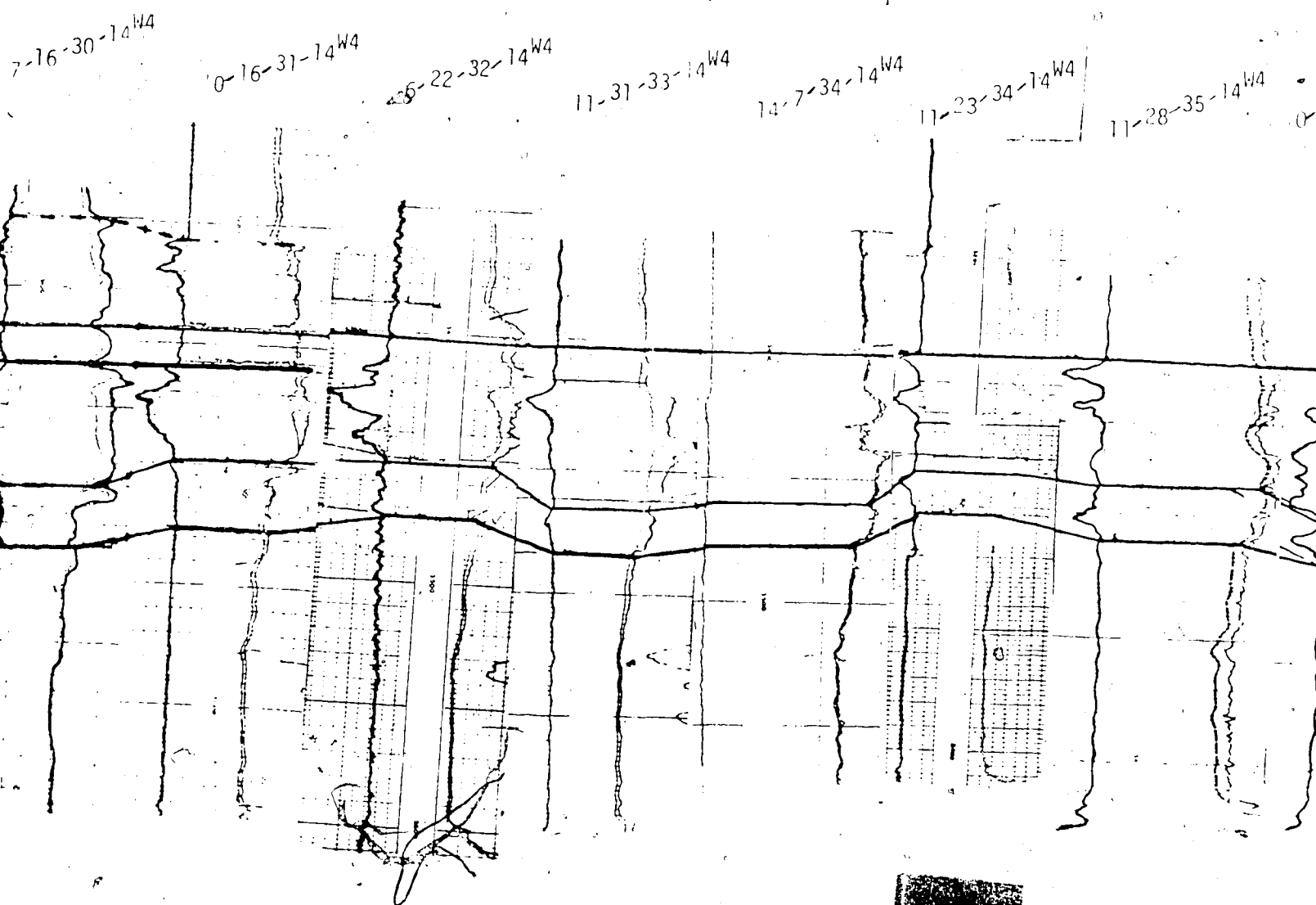
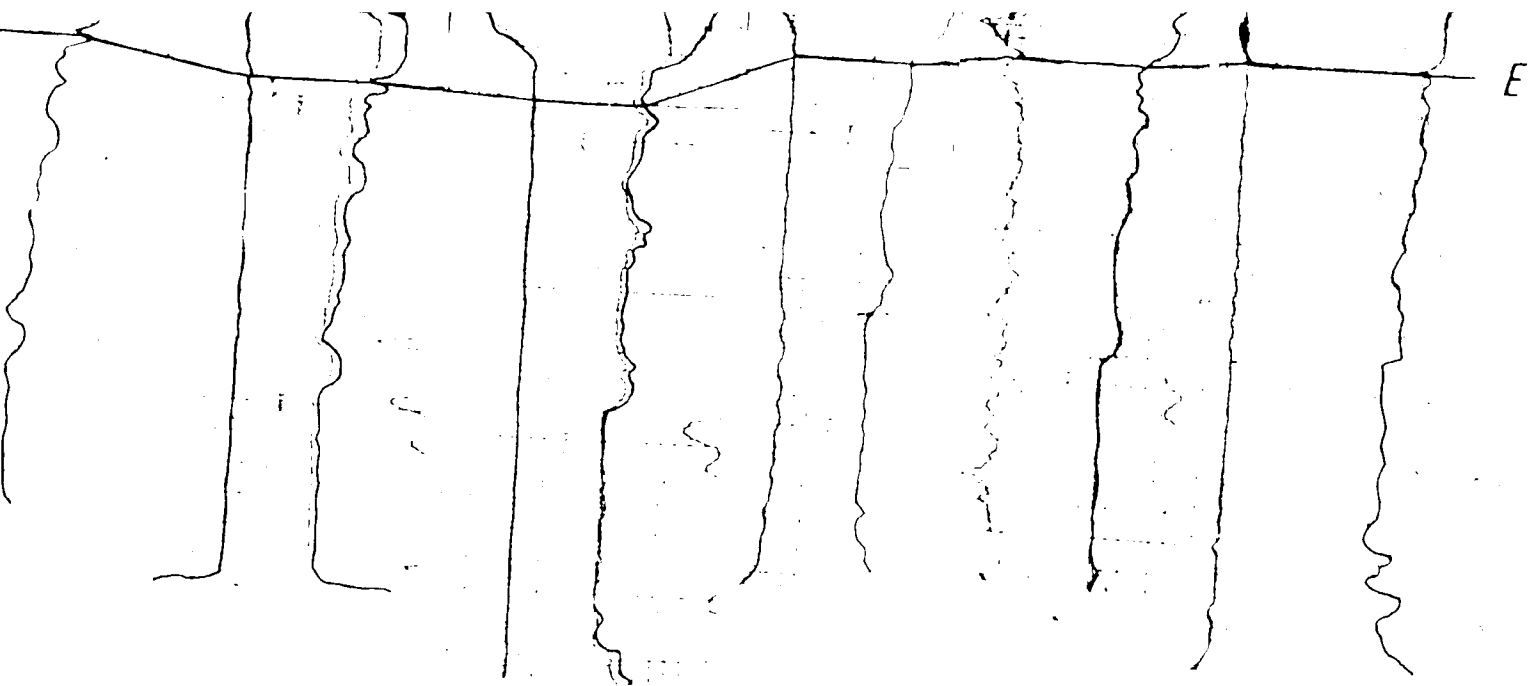


Figure 18. Cross Section E-E' -
 (—— Bentonite Marker, ----- Top Viking Formation)



35-14^{W4} 10-20-36-14^{W4} 10-21-37-14^{W4} 10-27-38-14^{W4} 16-5-42-14^{W4} 10-13-44-15^{W4} 13-11-47-14^{W4} E'



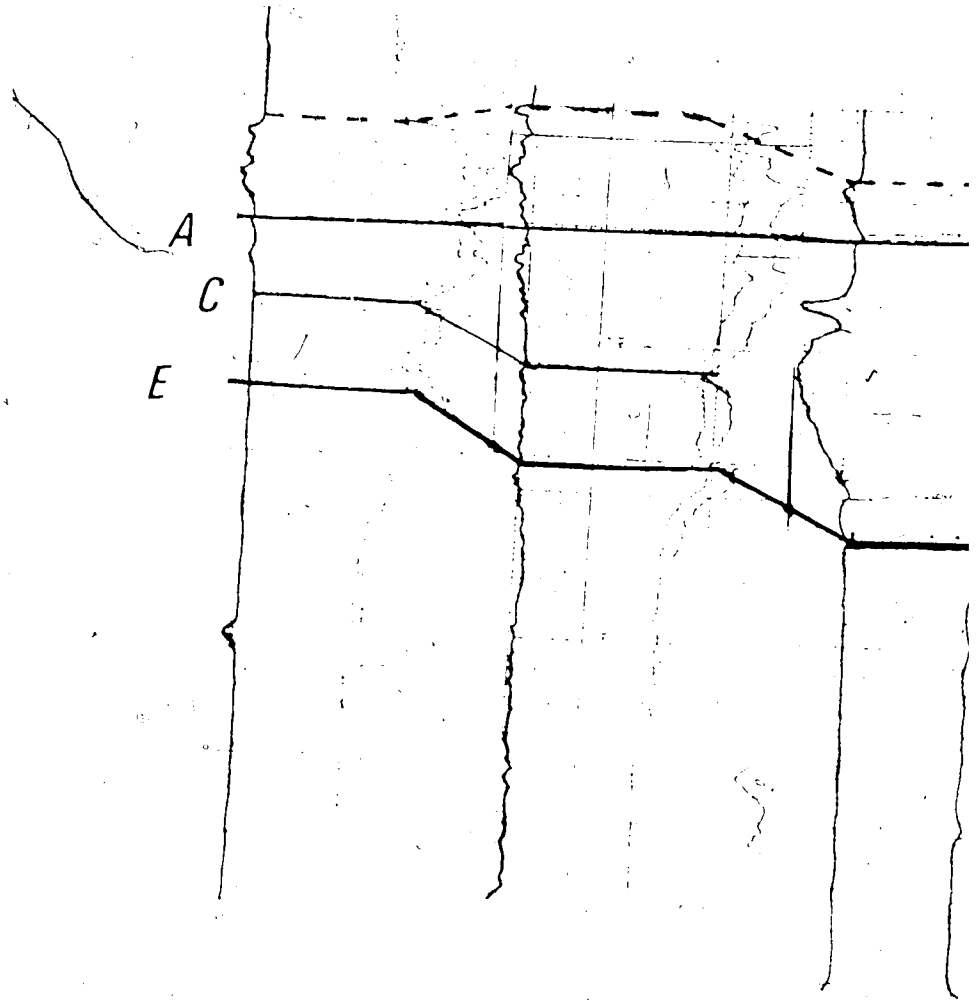


Figure 20 Cross Section F-F'.

6-20-34-24W4

6-20-34-24W4

7-3-33-20W4

7-20-32-19W4

4-29-31-18W4

11-12-30-17W4

1-33-29-17W4

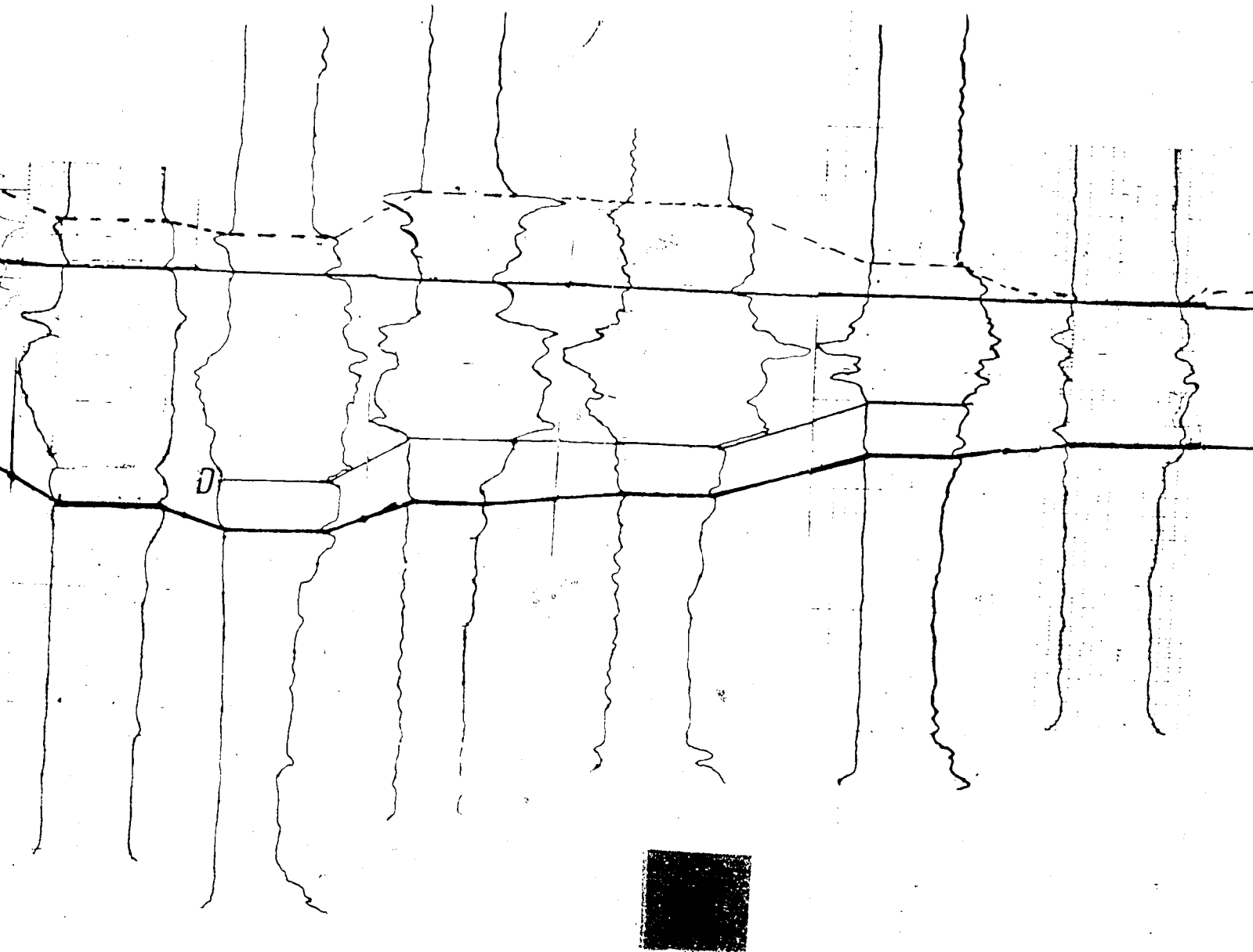
10-1-30-18W4

4-1-31-16W4

10-32-31-15W4

10-29-32-14W4

6-12-33-13W4



F'

(Figs. 20 & 2

10-21-34-12W4

10-35-35-11W4

10-3-36-10W4



34

7-31-29-16W4

10-33-28-15W4

11-15-27-14W4

11-7-26-13W4

14-26-25-12W4

7-13-22-8W4

G'

Figure 20. Cross Section F-F'.

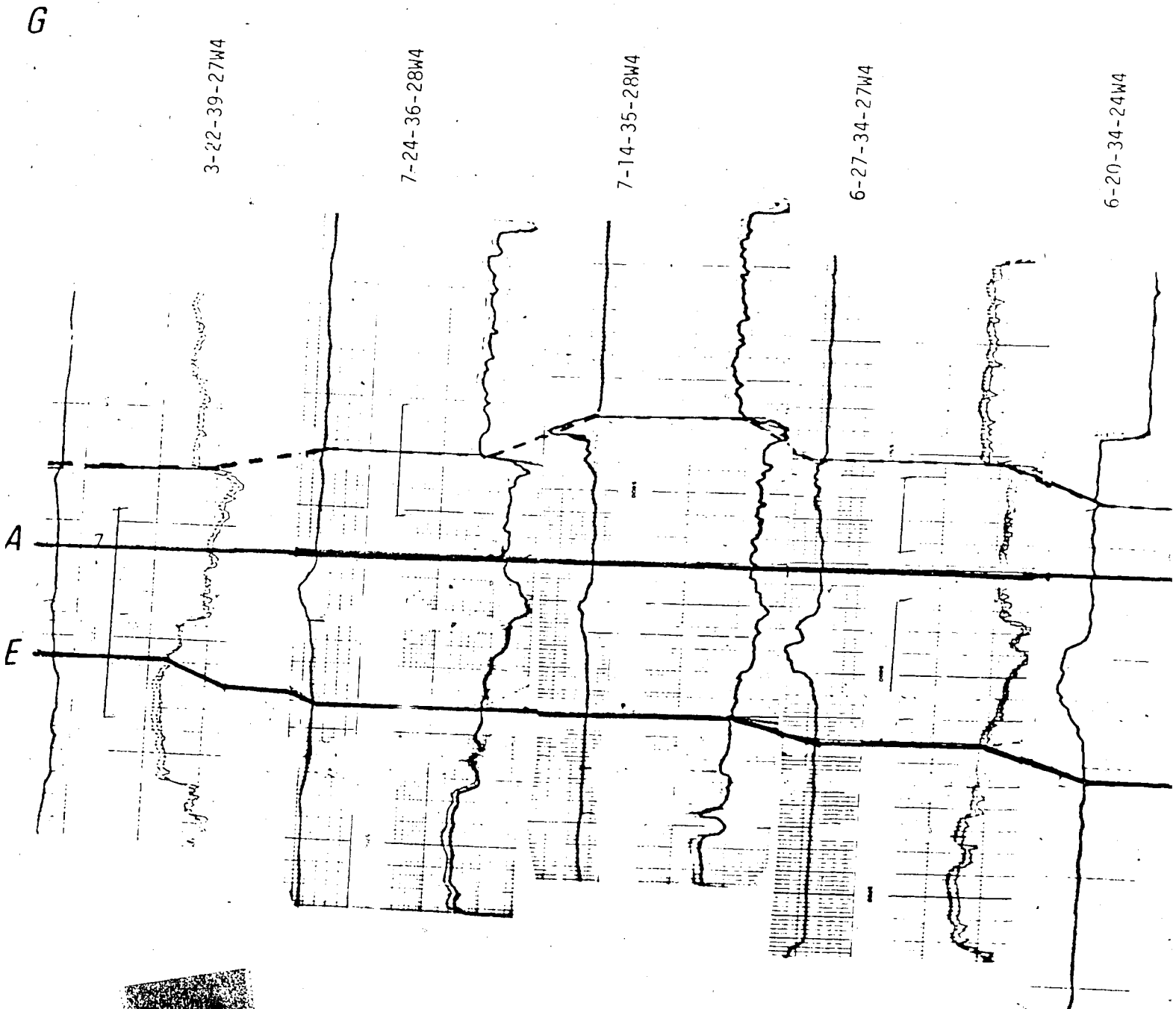
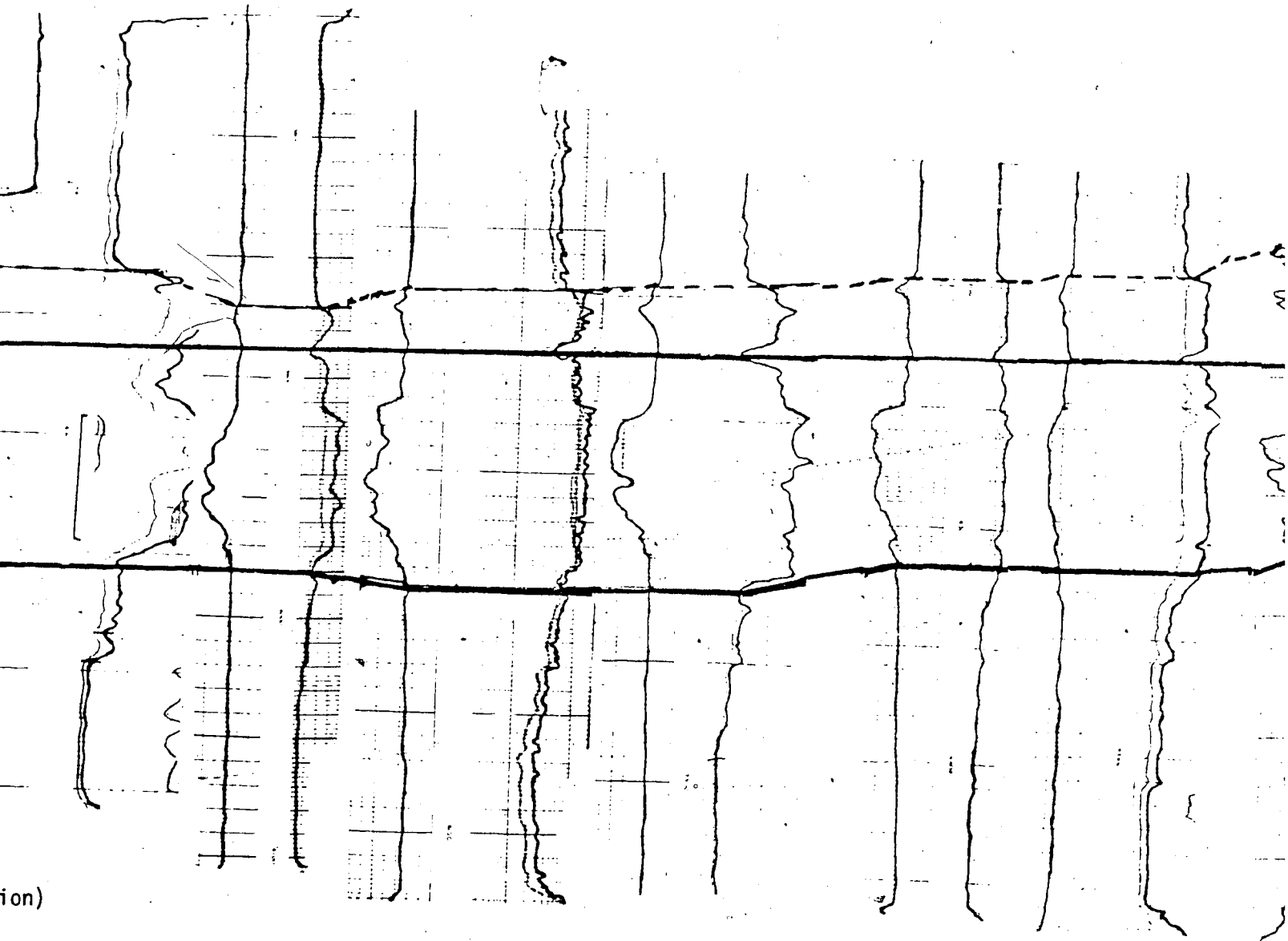


Figure 21. Cross Section G-G'.
(—— Bentonite Marker, ---- Top Viking Formation)



7-3-33-20W4

7-20-32-19W4

4-29-31-18W4

11-12-30-17W4

7-31-29-16W4

54

7-31-29-16W4

10-33-28-15W4

11-15-27-14W4

11-7-26-13W4

14-26-25-12W4

7-13-22-8W4

G'



H

6-36-34-26W4

6-36-34-25W4

10-2-34-24W4

11-2-34-20W4

15-3-35-19W4



Figure 23...

15-3-35-19W4

6-23-36-19W4

11-28-35-18W4

4-30-34-18W4

7-30-35-17W4

6-17-36-16W4

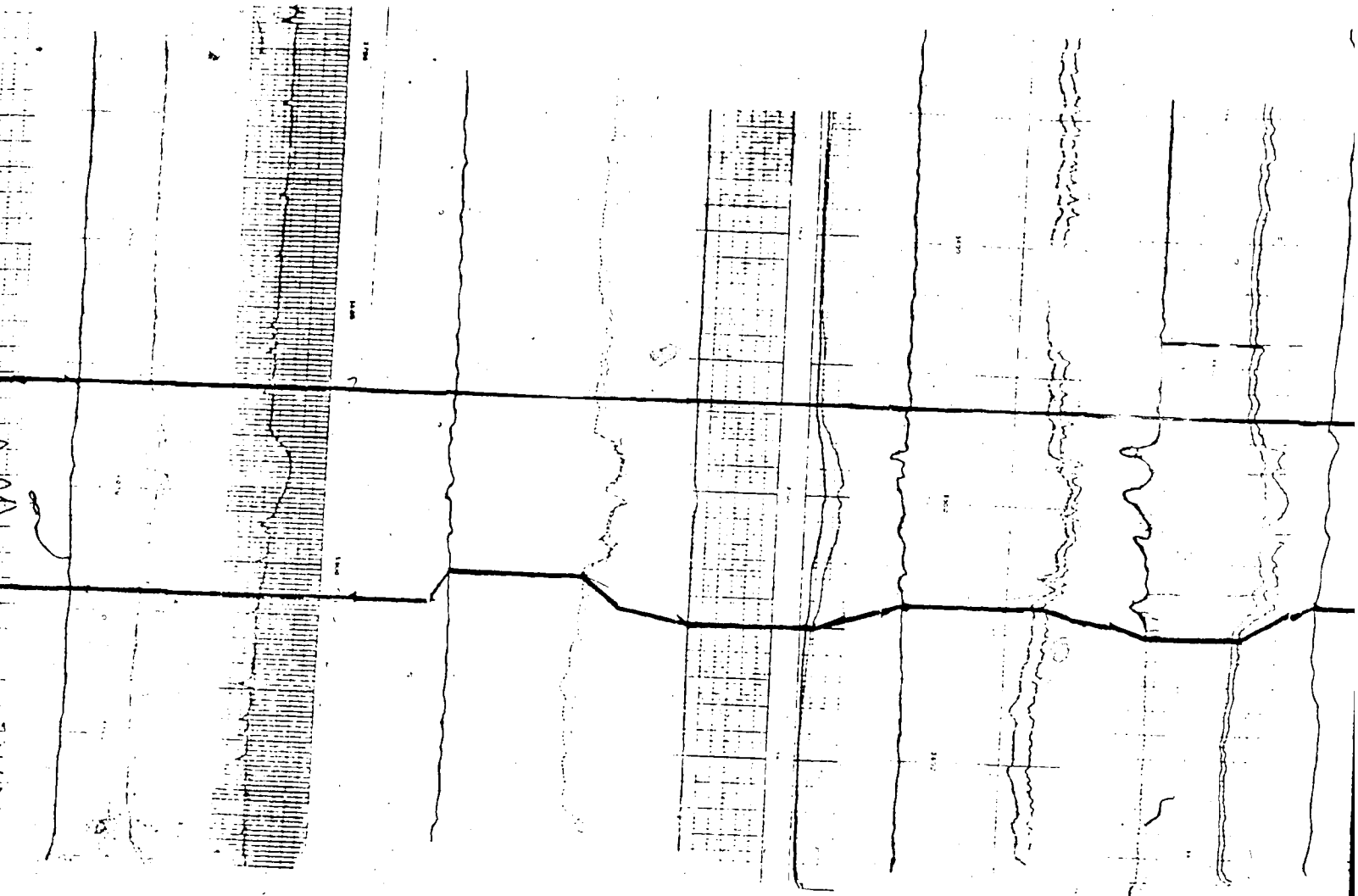


Figure 23. Cross Section H-H'



20W4

20W4

18W4

W4

W4

W4

H'

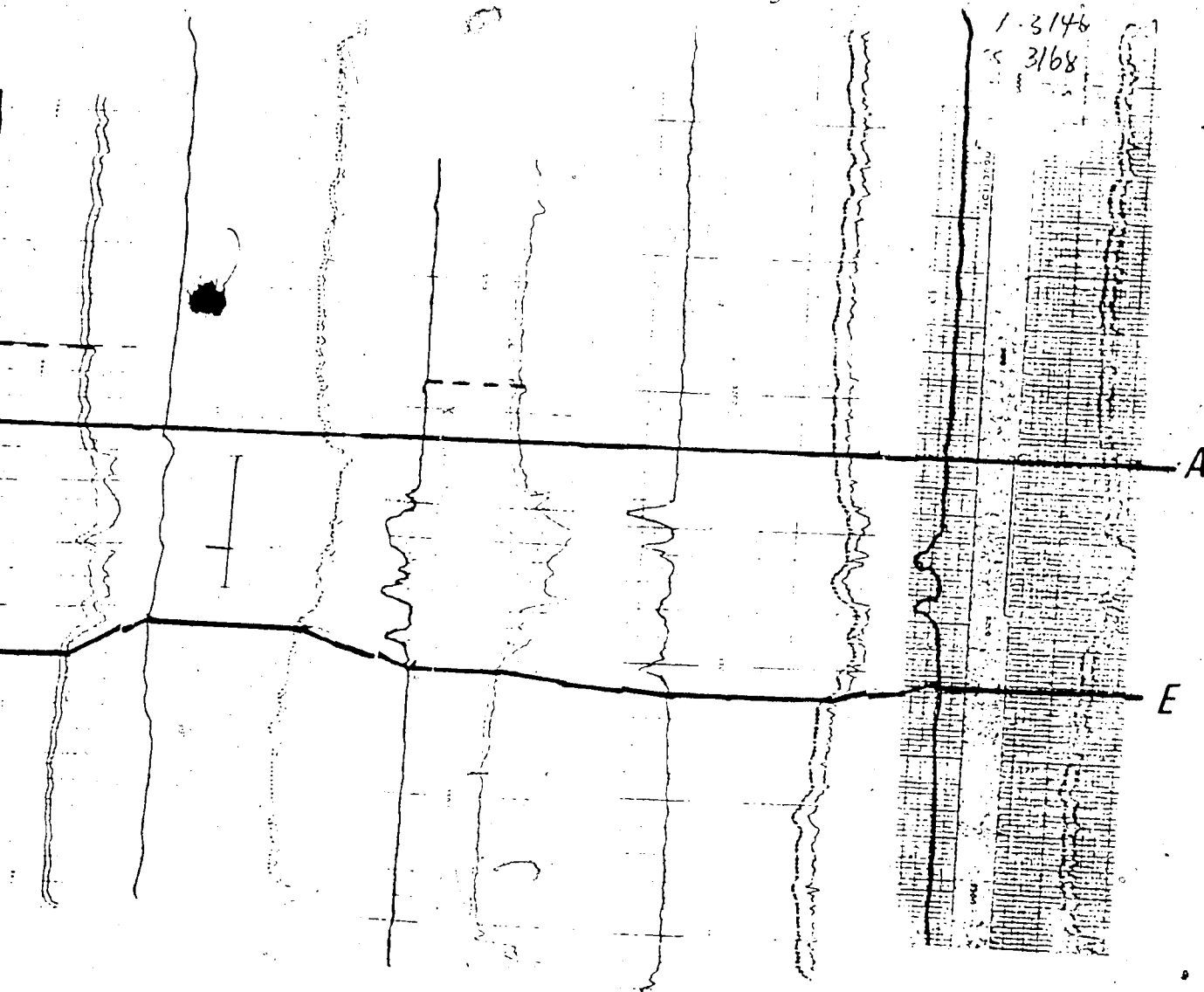
6-17-36-16W4

10-34-36-16W4

7-35-36-15W4

11-28-35-14W4

6-25-36-13W4



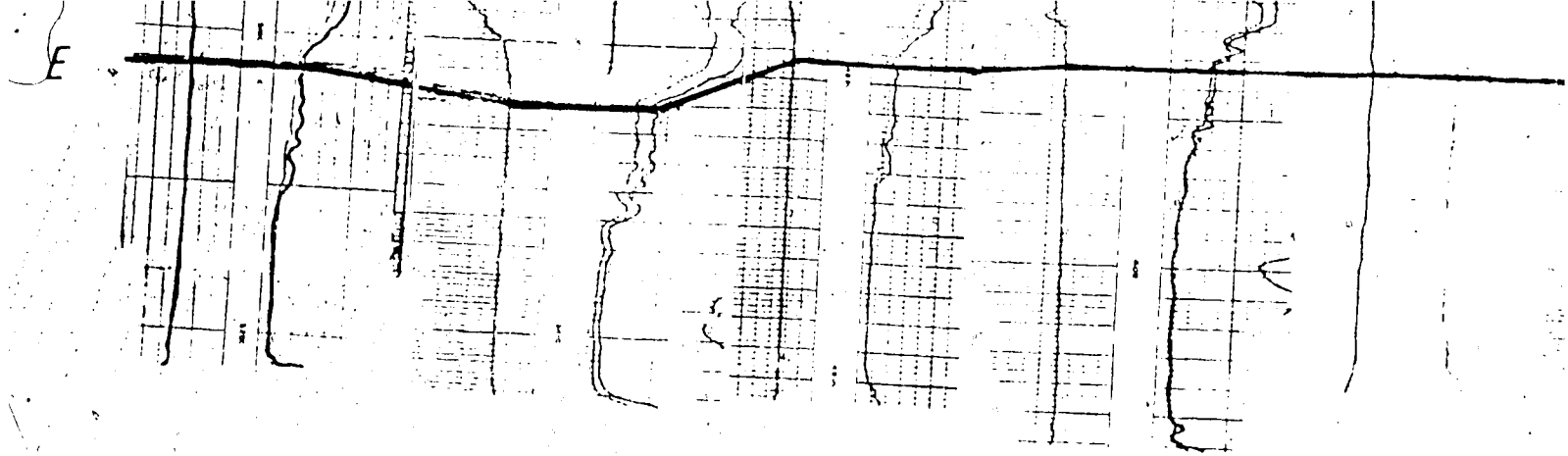


Figure 23

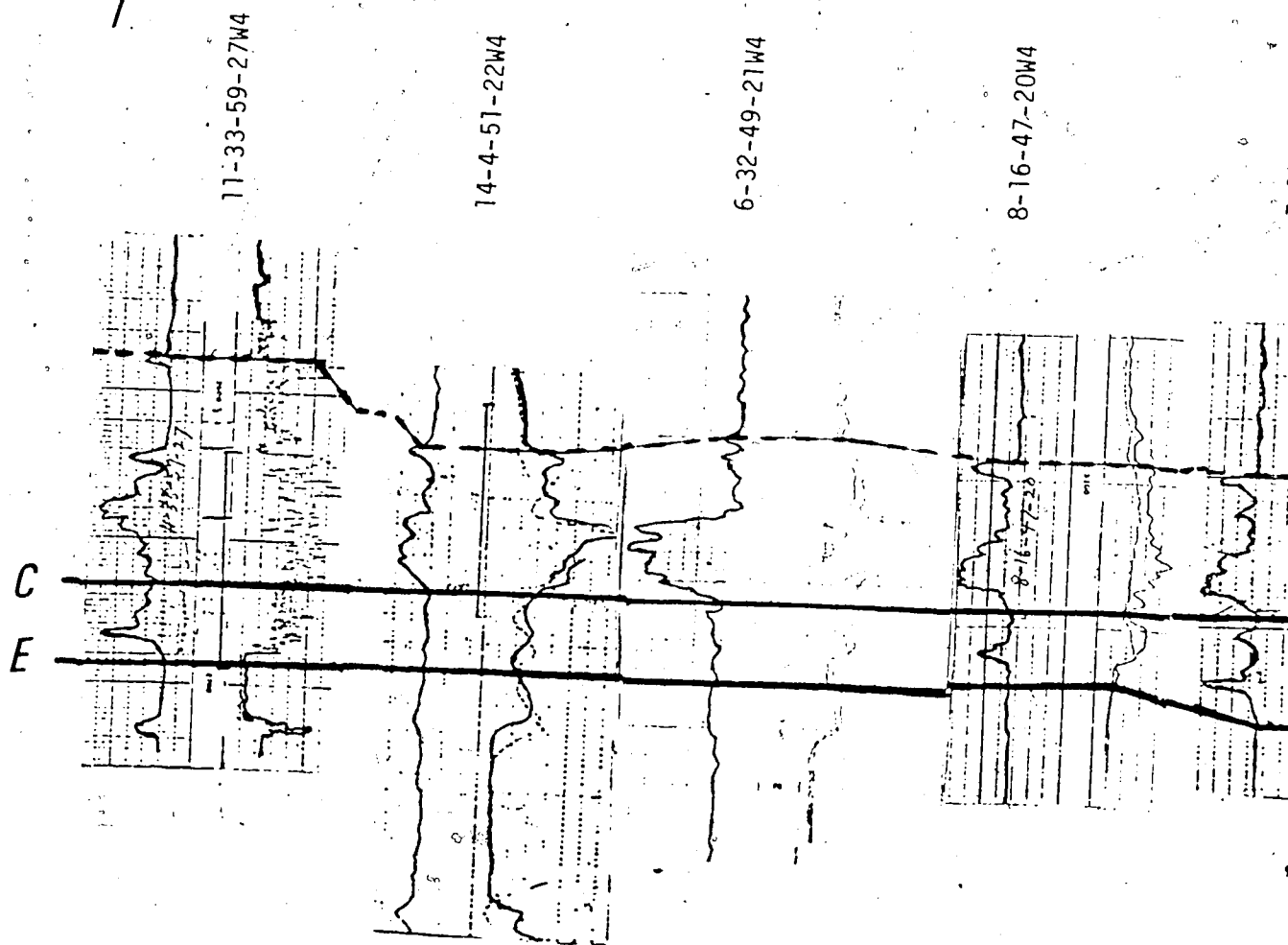


Figure 24. Cross Section I-I'.
(—— Bentonite Marker, ---- Top

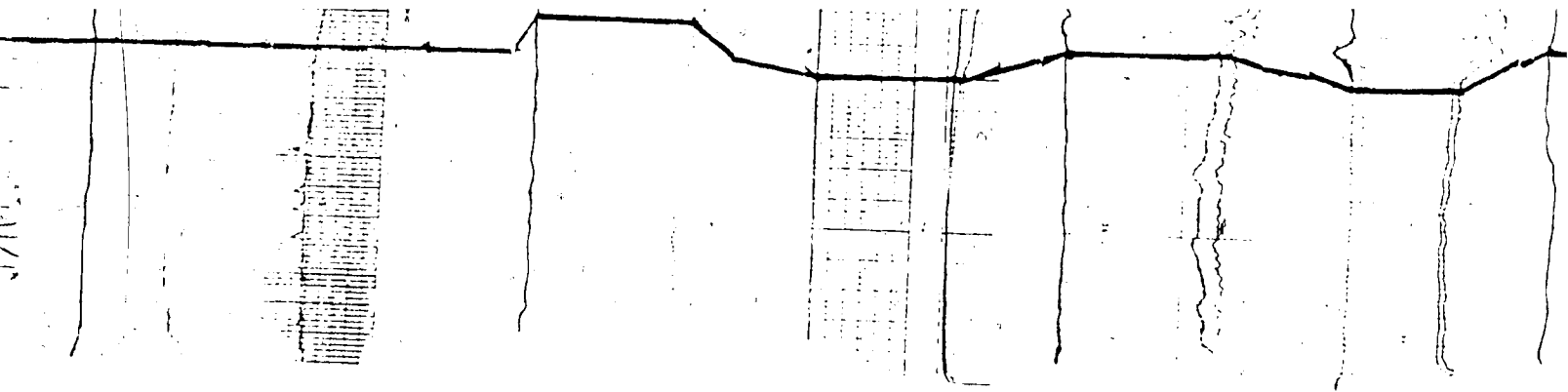


Figure 23. Cross Section H-H'.

54

8-16-47-20W4

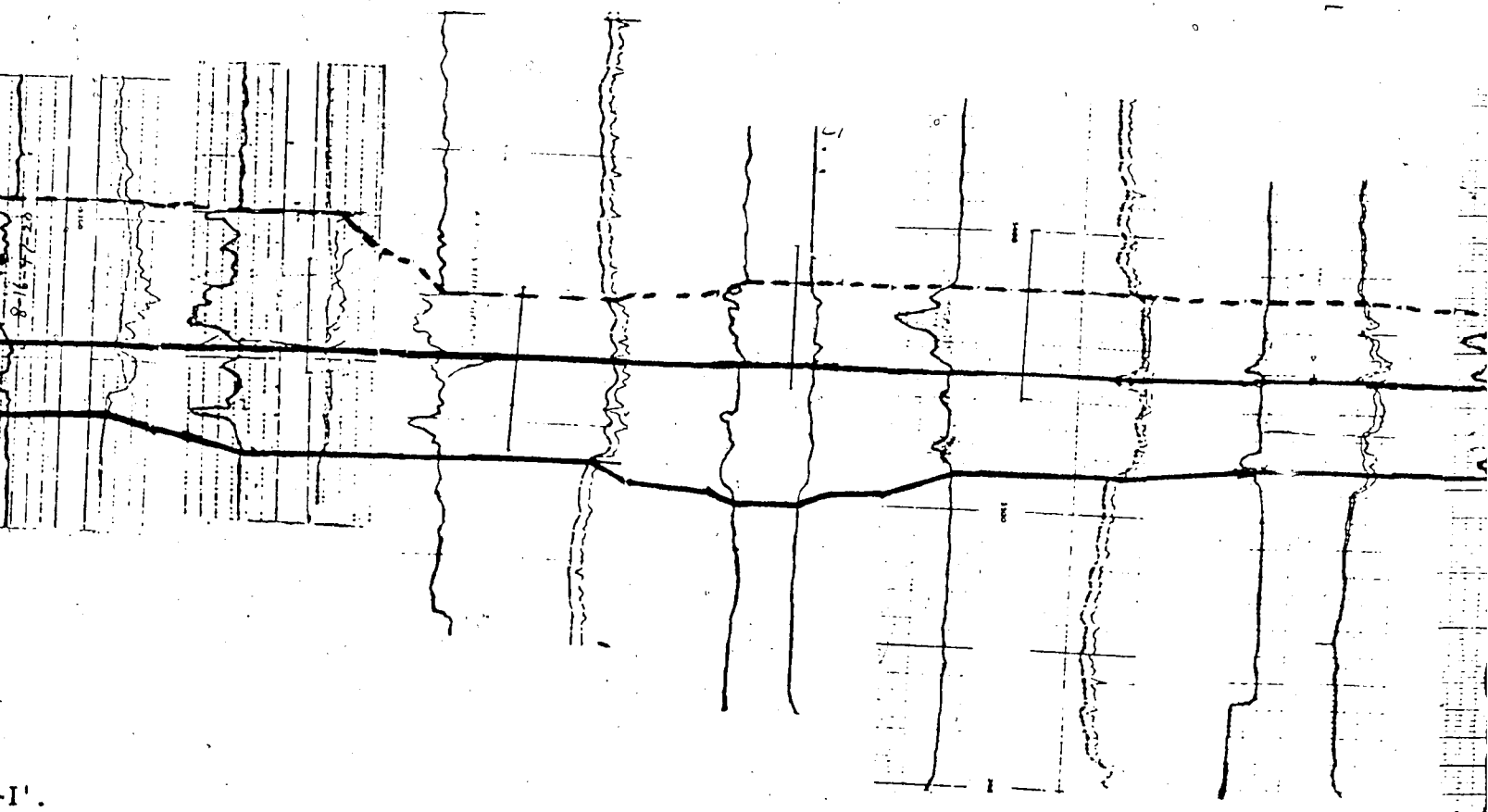
7-11-46-20W4

11-16-44-18W4

9-9-44-17W4

6-21-36-17W4

10-24-33-12W4



Ice Marker, ----- Top Viking Formation)

6-21-36-17W4

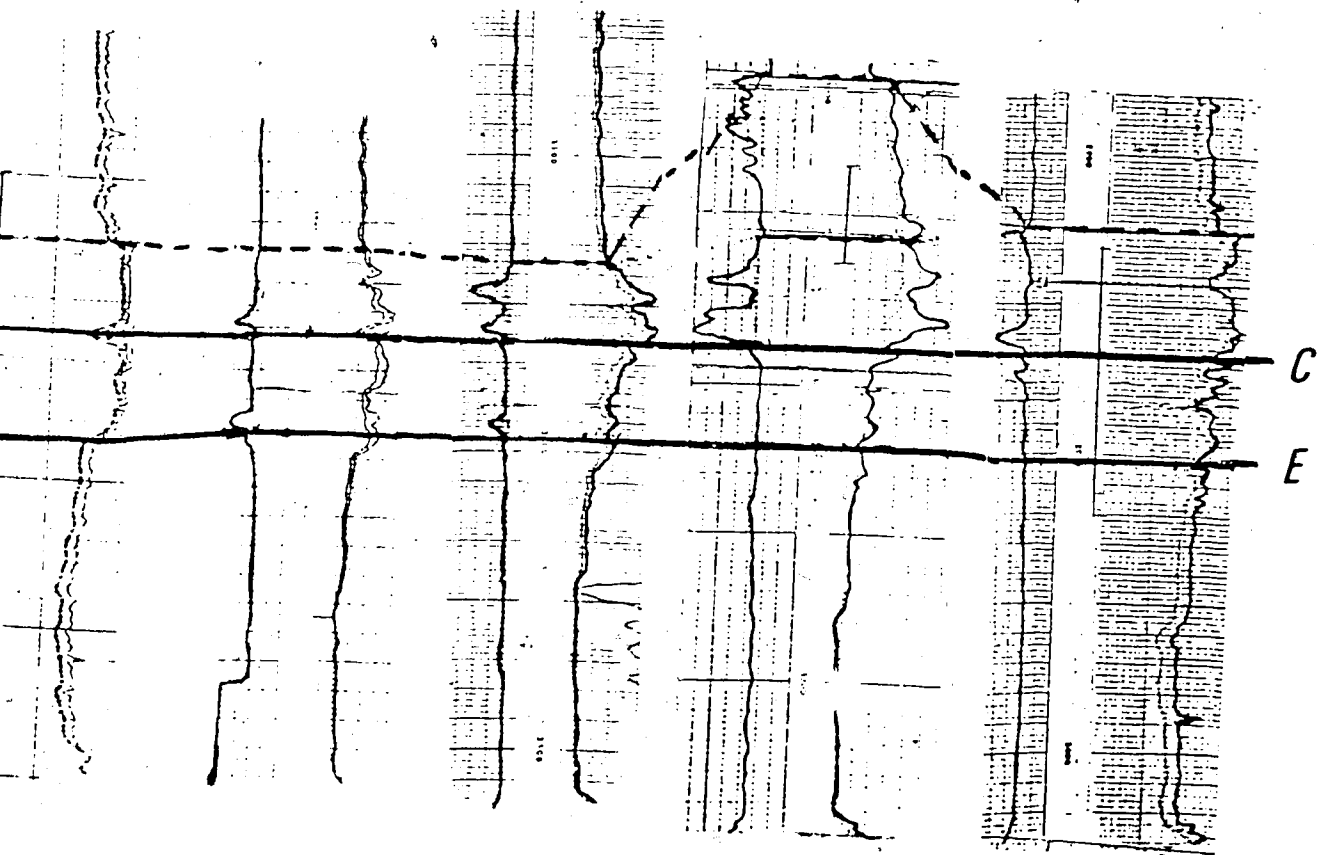
10-24-33-12W4

6-31-32-12W4

7-10-30-12W4

10-13-30-11W4

1'



J

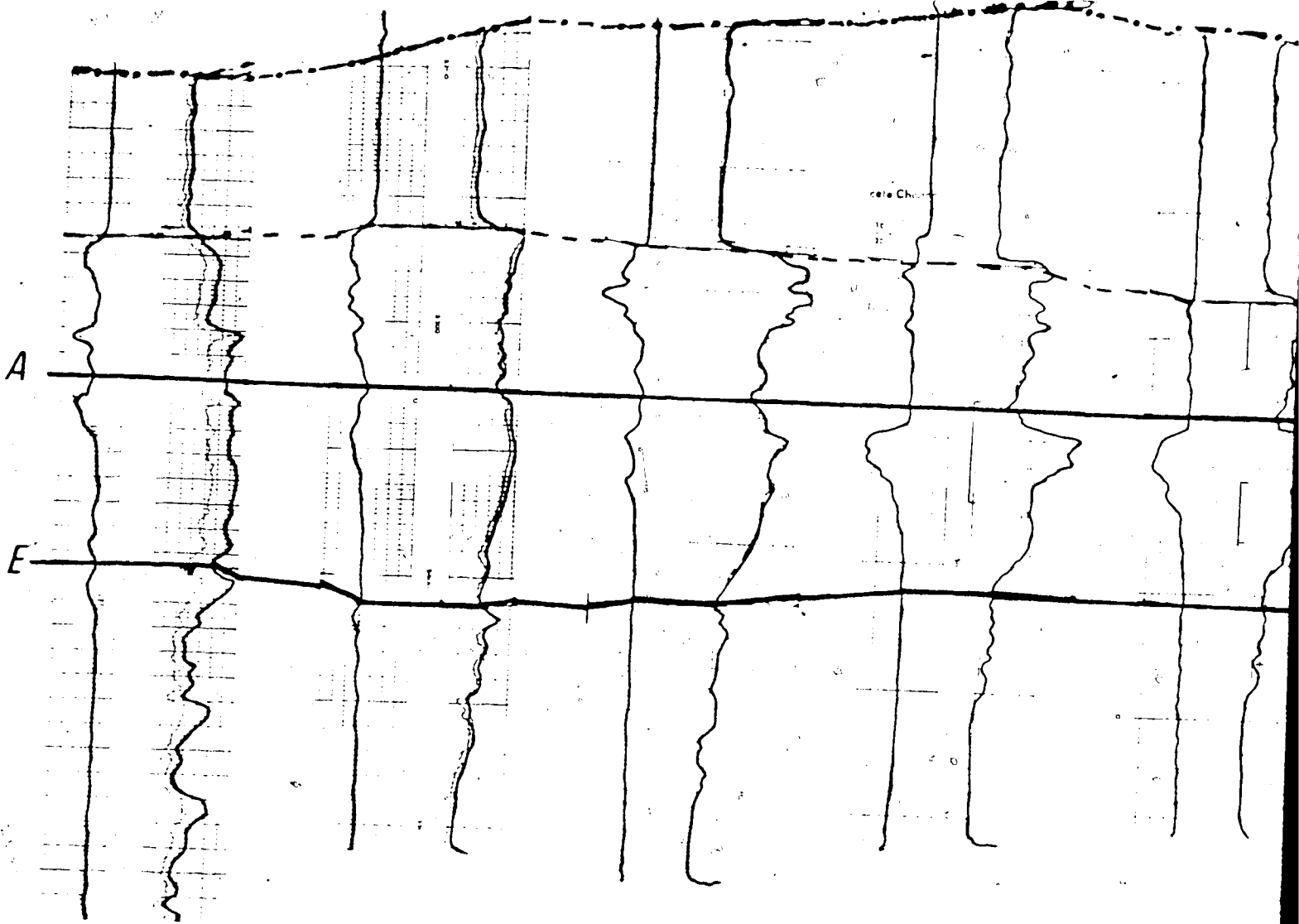
10-14-27-28W4

11-17-28-26W4

8-11-29-26W4

6-36-34-26W4

10-13-35-26W4



K

2-8-44-27W4

13-2-44-22W4

1-12-44-21W4

11-30-44-20W4

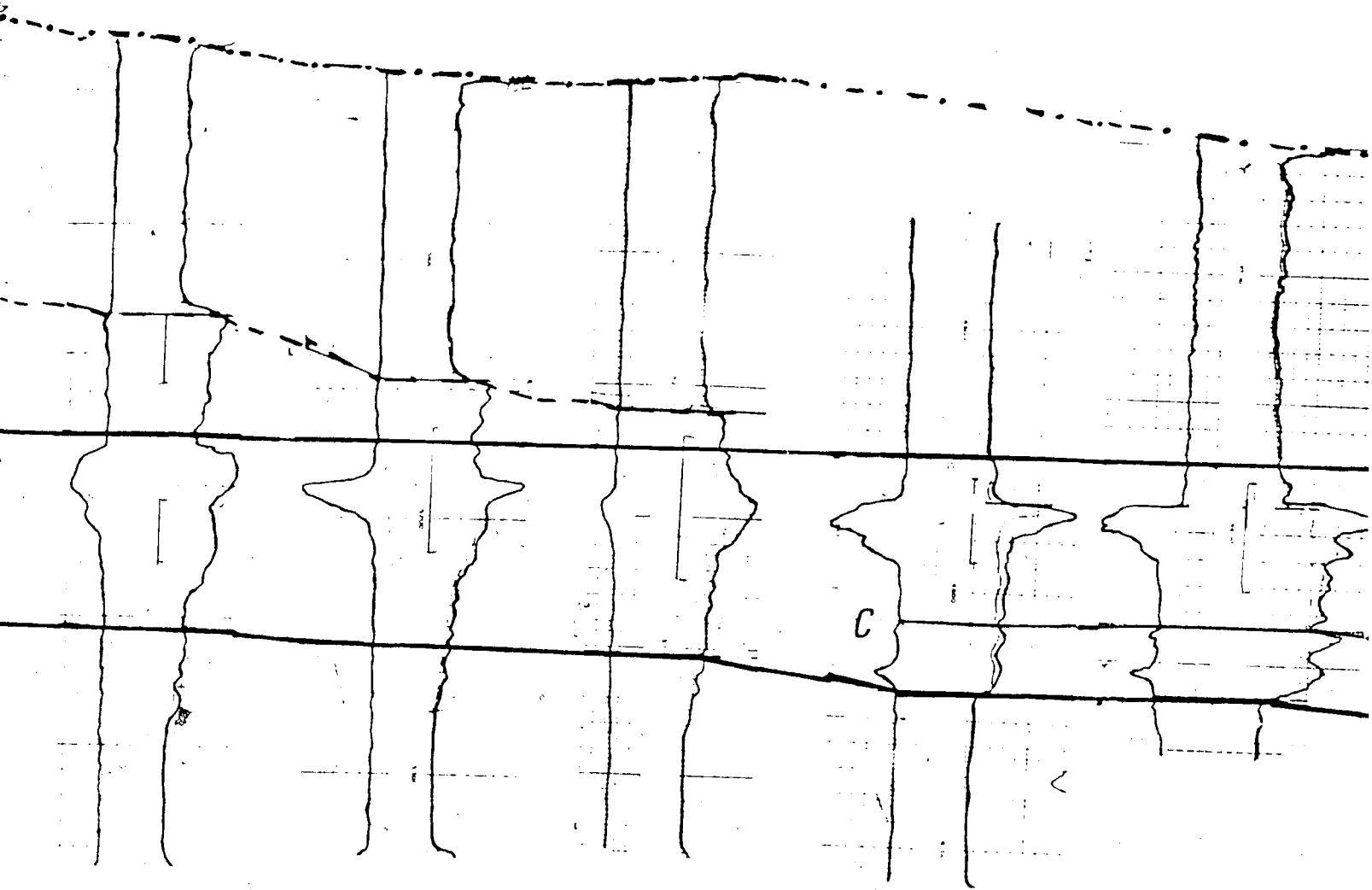


Figure 26. Cross Section J-J'

11-30-44-20W4

1-20-44-18W4

6-32-44-17W4

10-4-44-16W4

6-20-44-15W4

12-24-44-14W4

4-14-44-22W4

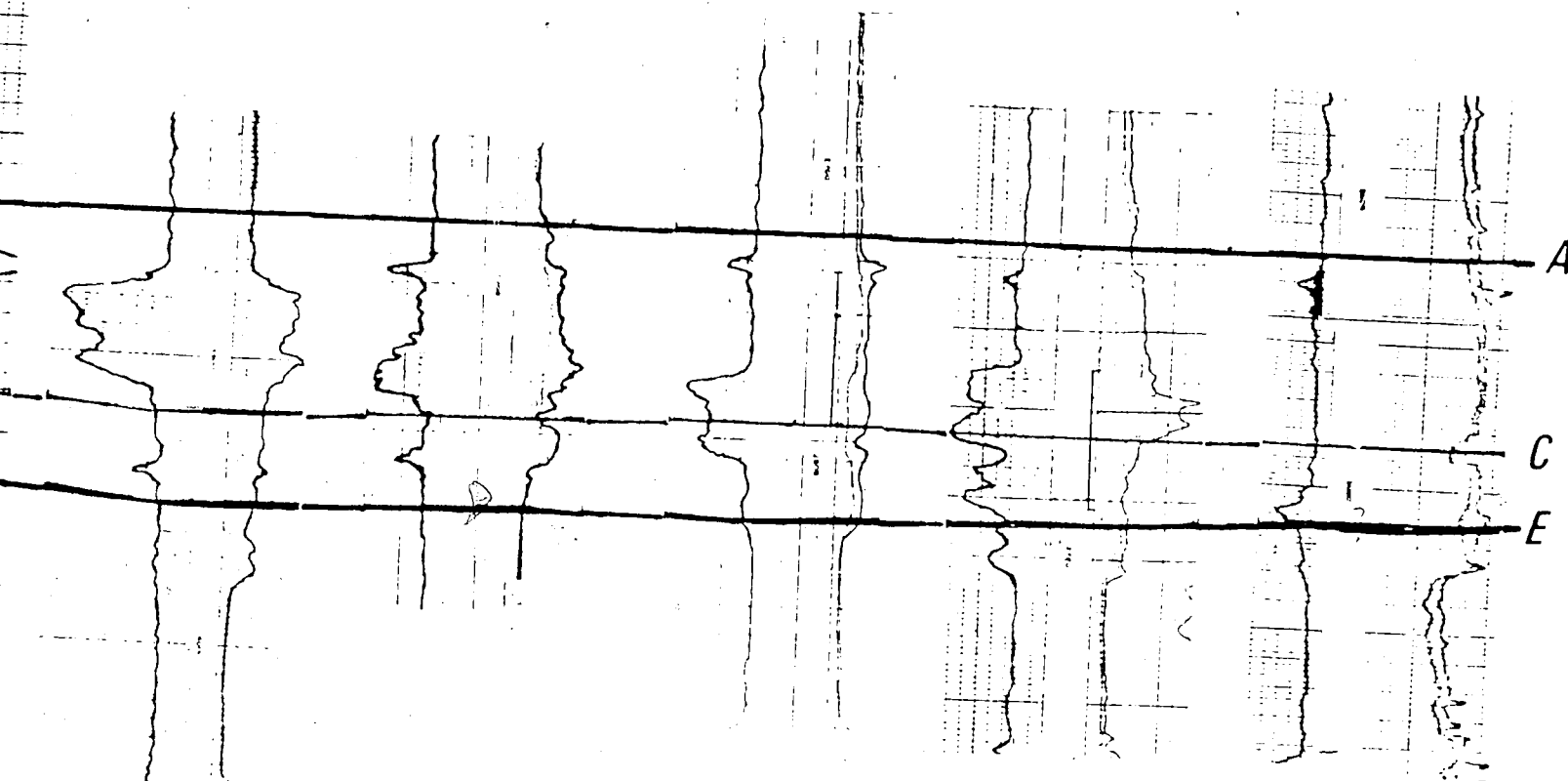
8-16-47-20W4

16-30-50-19W4

10-33-51-19W4

6-19-52-21W4

J'



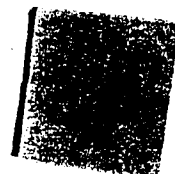
7-12-44-13W4

10-30-44-12W4

11-10-45-10W4

7-8-45-8W4

K'



K

2-8-44-27W4

13-2-44-22W4

1-12-44-21W4

11-30-44-20W4

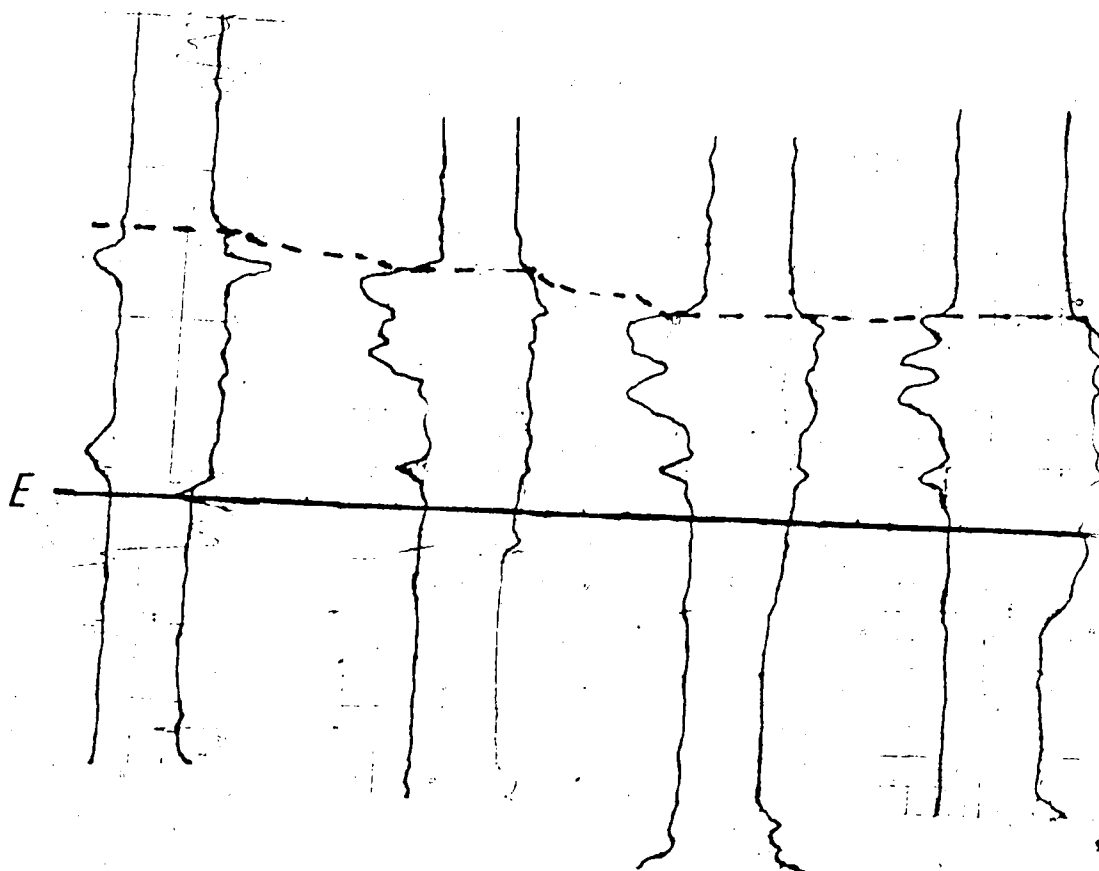


Figure 27. Cro

Figure 26. Cross Section J-J'.



11-30-44-20W4

1-20-44-18W4

6-33-44-17W4

10-4-44-16W4

6-20-44-15W4

12-24-44-14W4

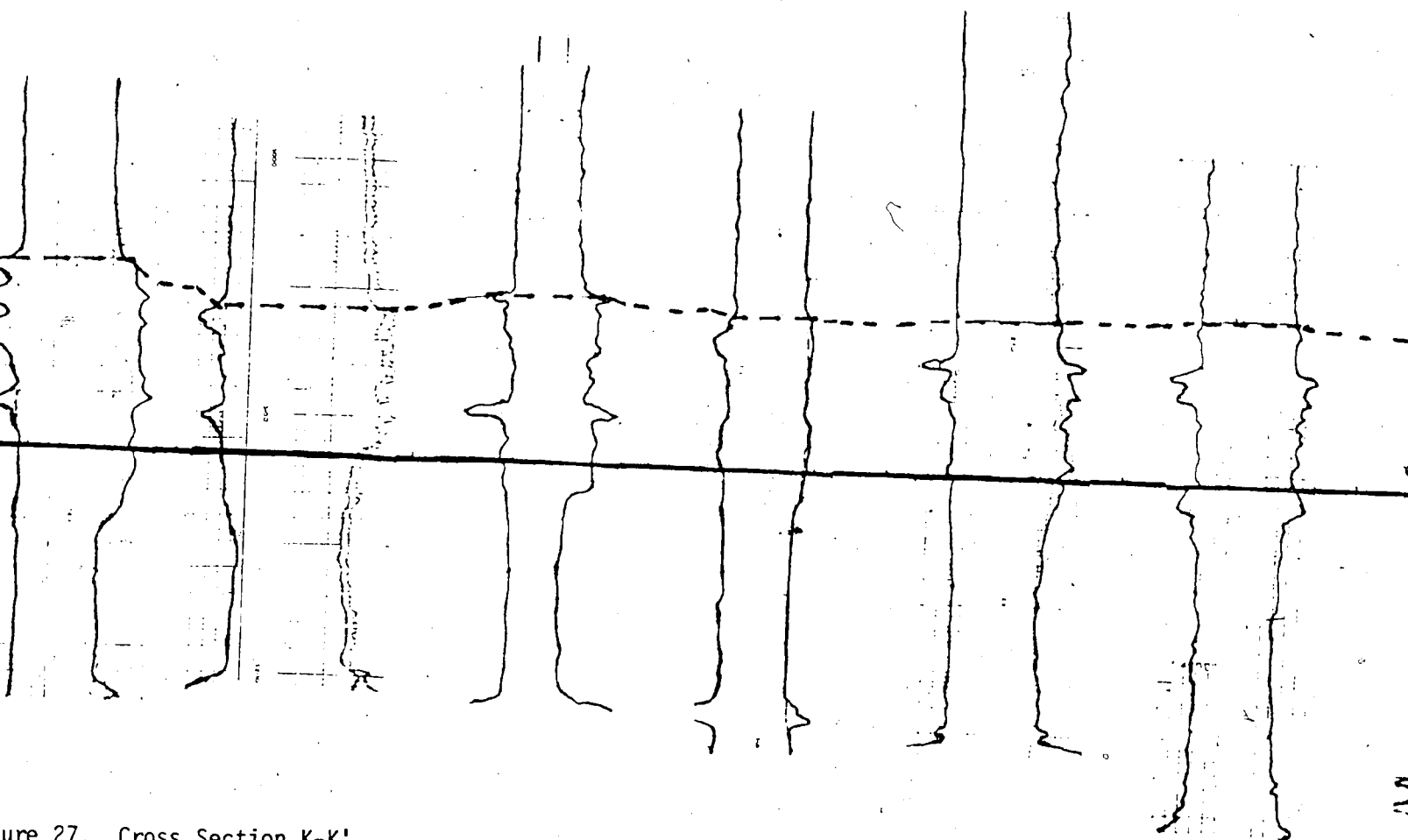


Figure 27. Cross Section K-K'.
(—— Bentonite Marker, ---- Top Viking Formation,
..... Base of Fish Scale Marker.)

12-24-44-14W4

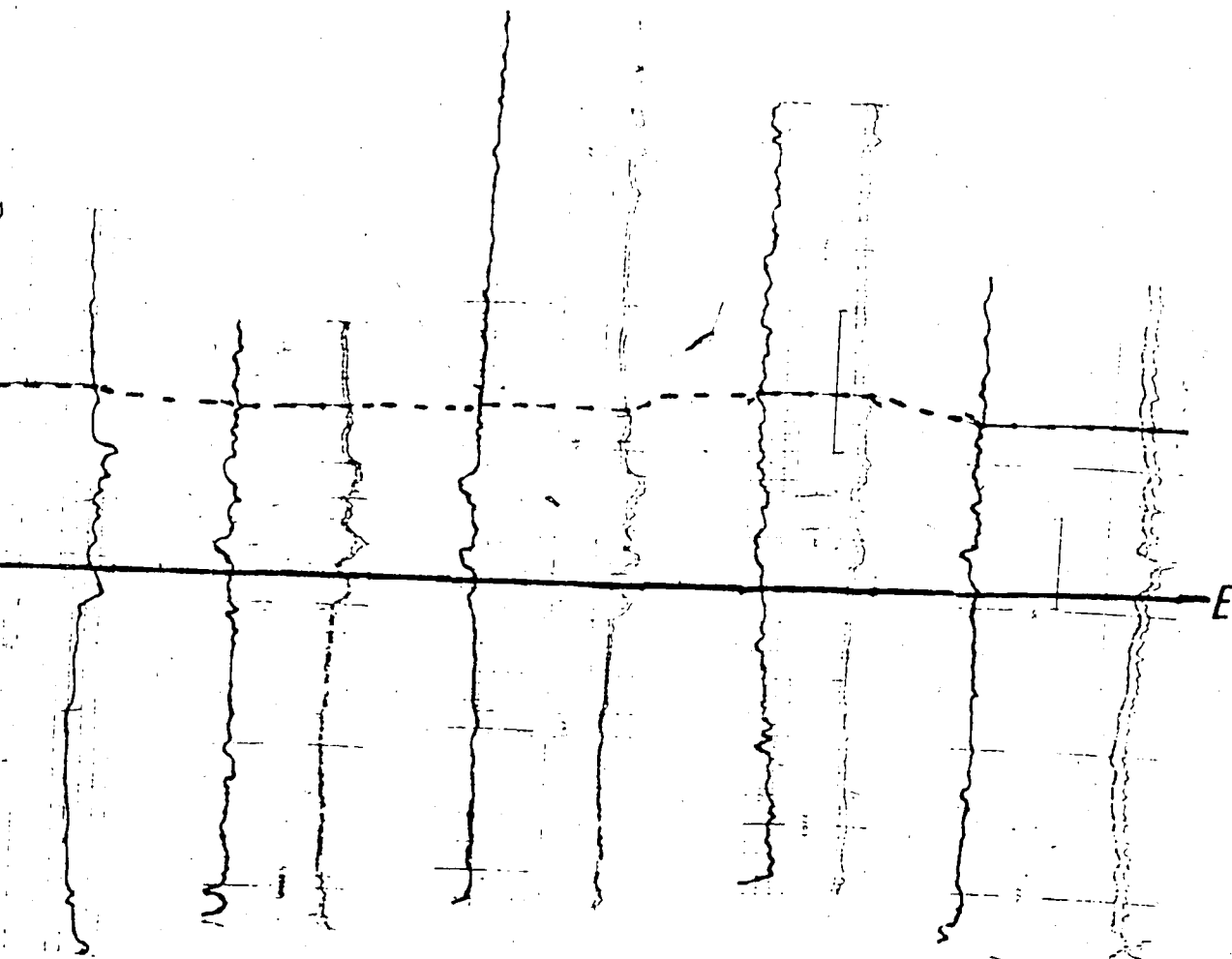
7-12-44-13W4

10-30-44-12W4

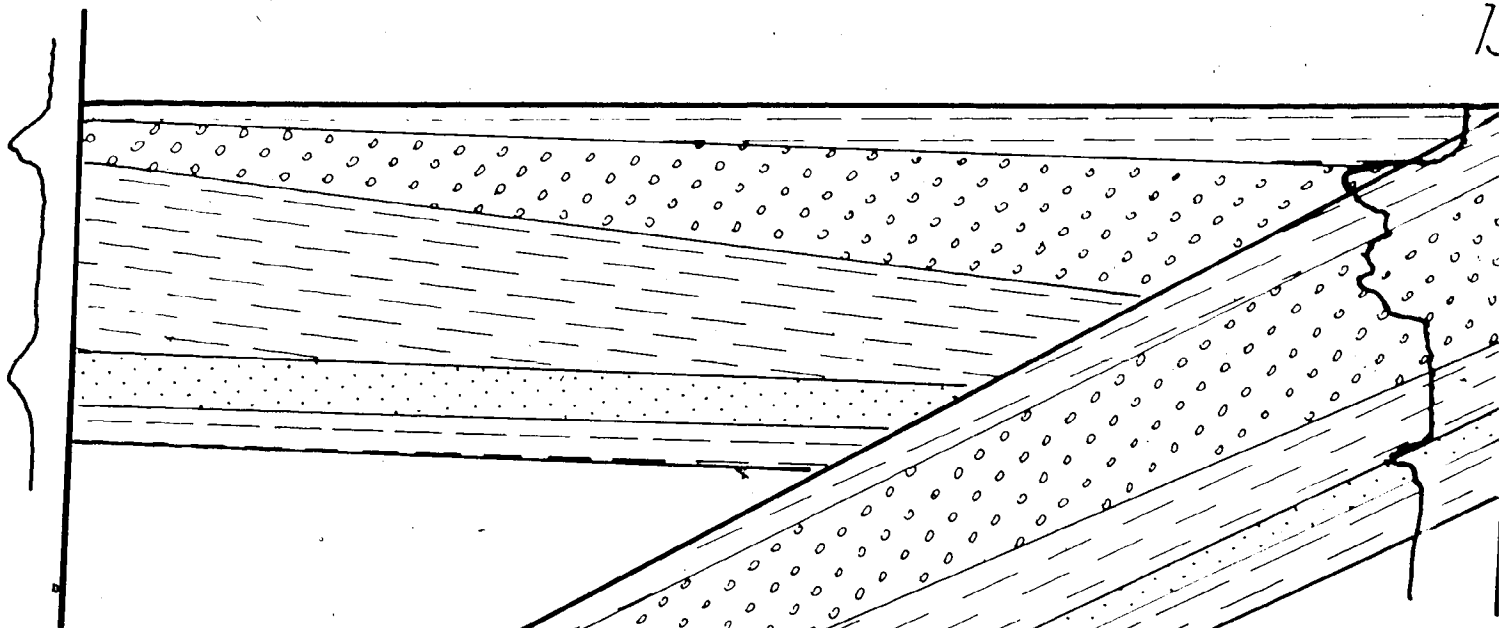
11-10-45-10W4

7-8-45-8W4

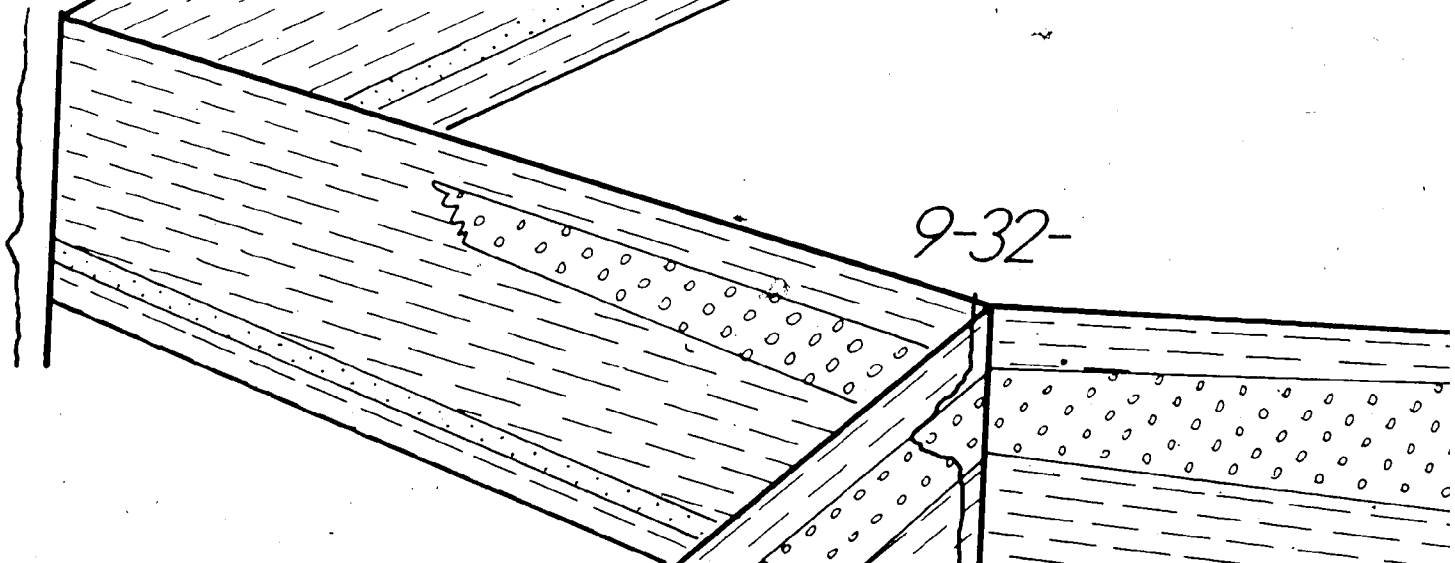
K'



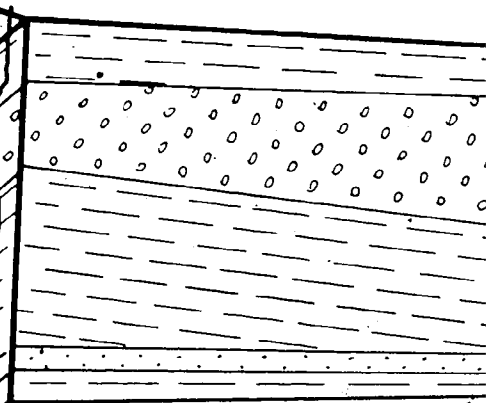
2-8



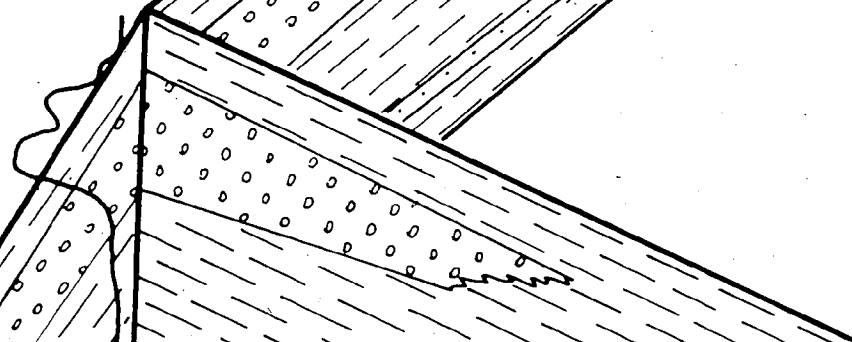
14-20-



9-32-



13-33-



10-19-



13-2-

15-1-

10-21-

10-6-



1-2-

15-1-

12-24-

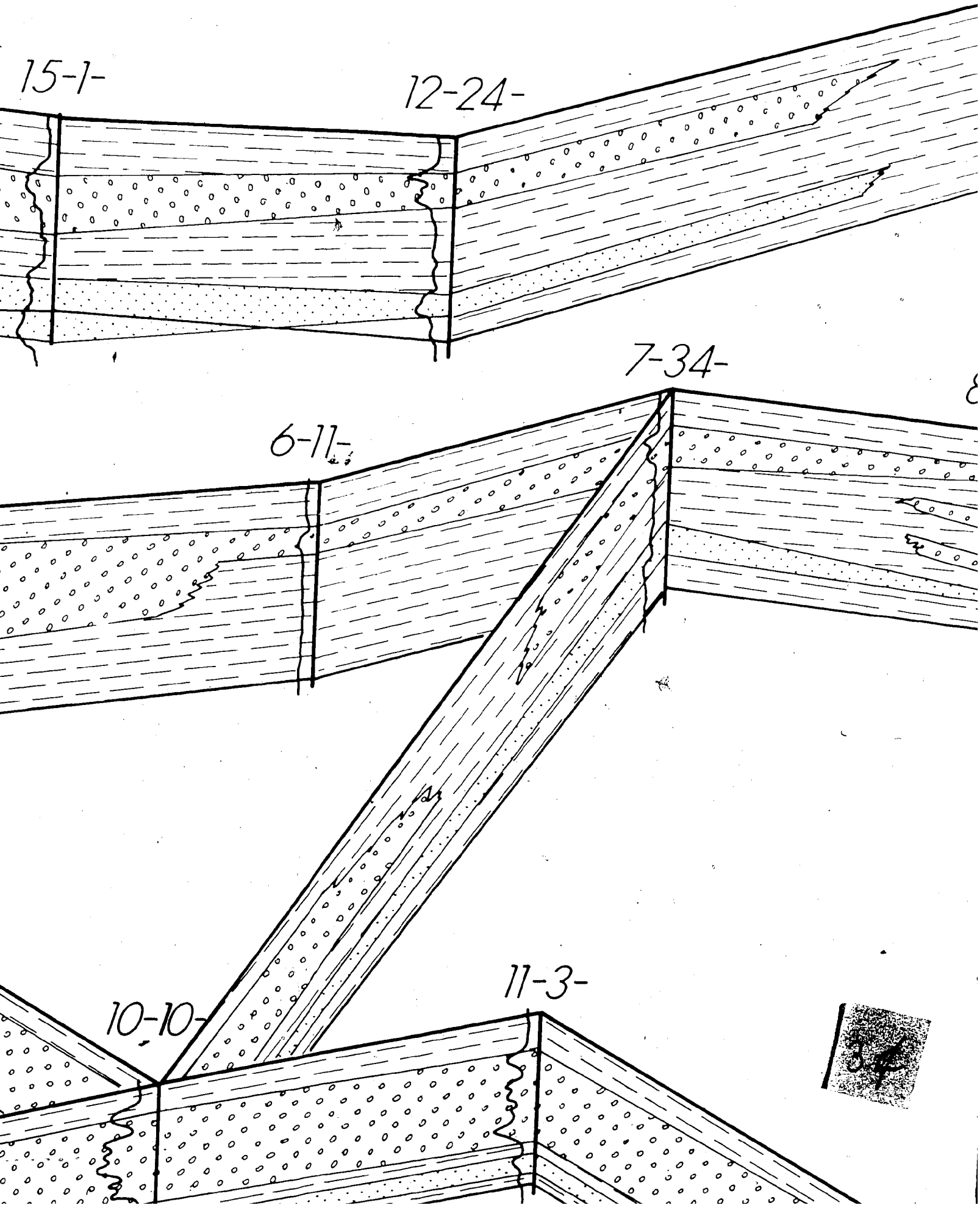
7-34-

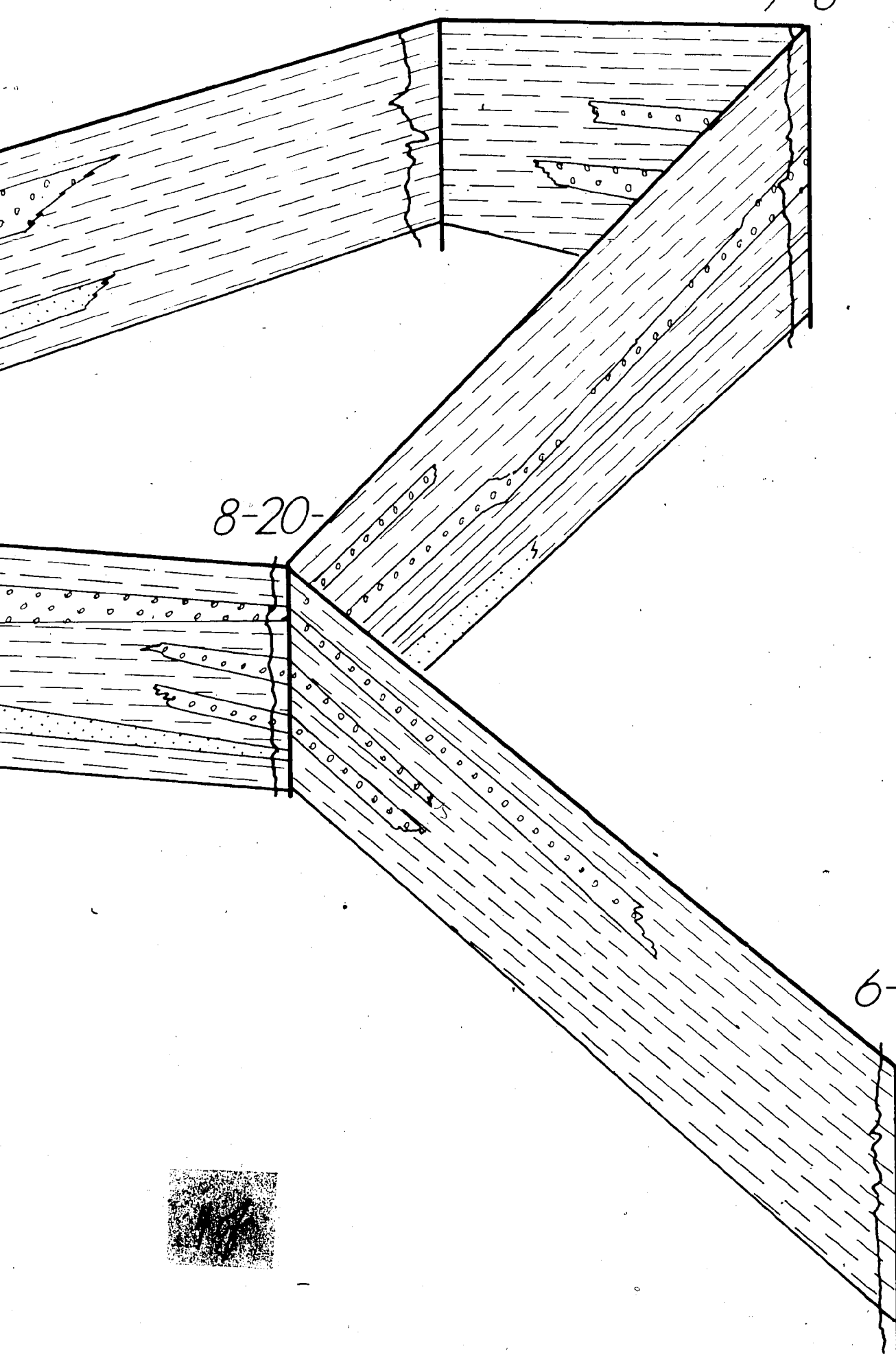
6-11-

10-10-

11-3-

34





8-20-

6-9-

12-11-

45

44

43

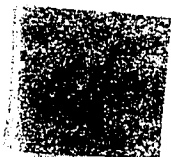
42

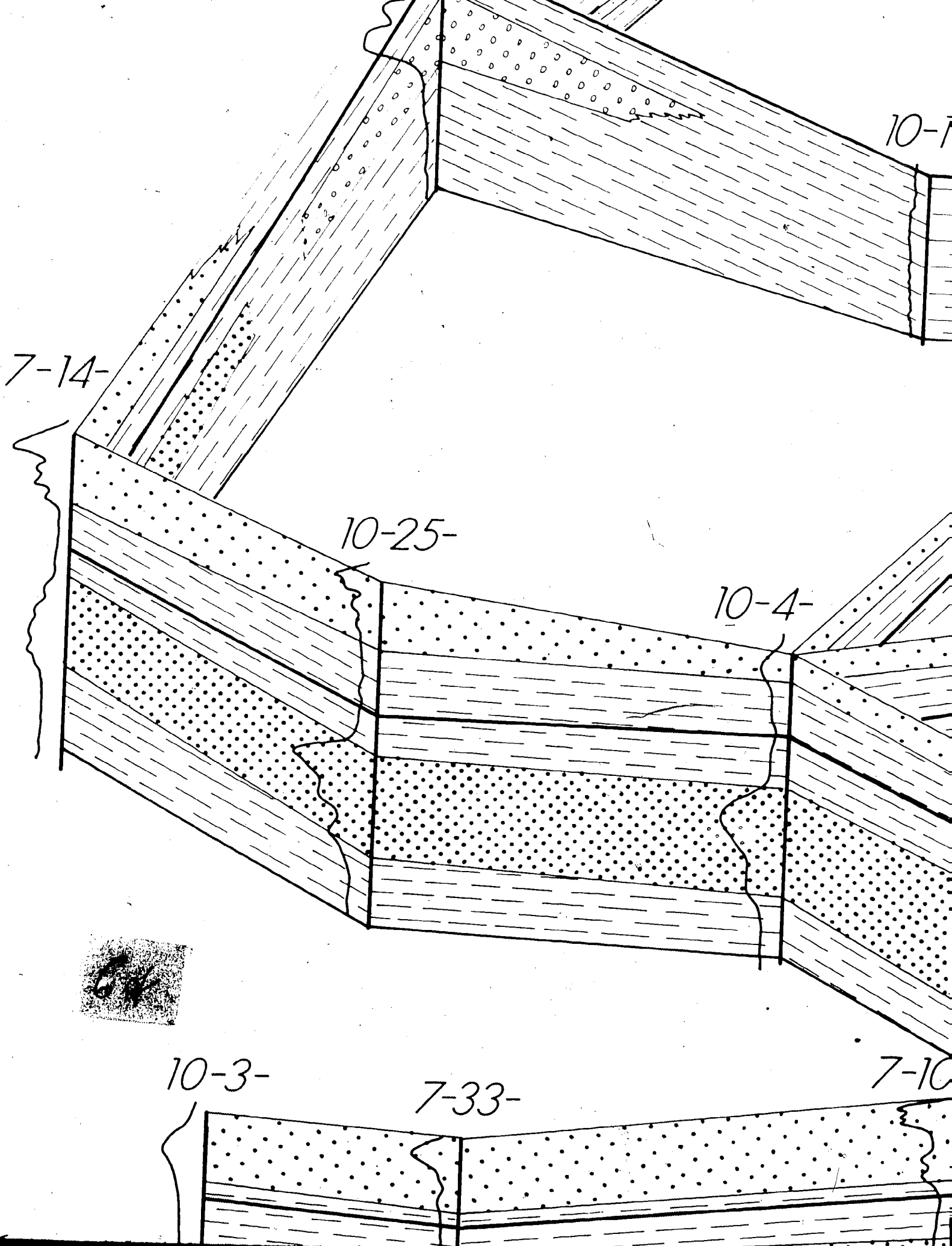
41

40

39

38





4-3-

7-2

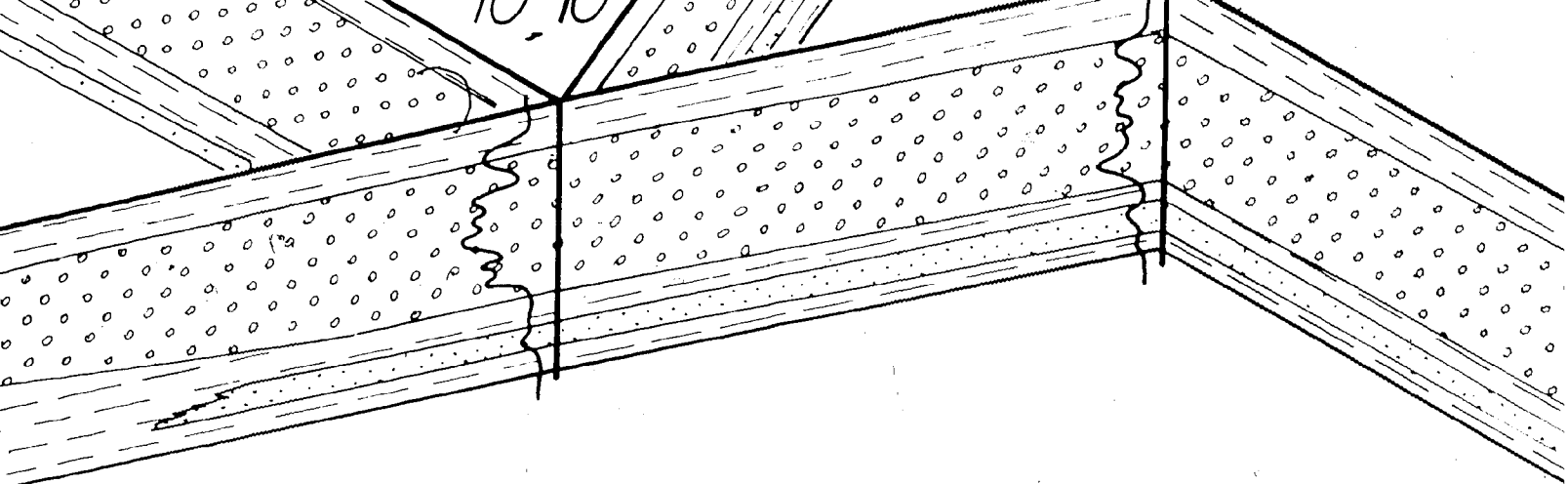
15-17-

12-16

7-24-

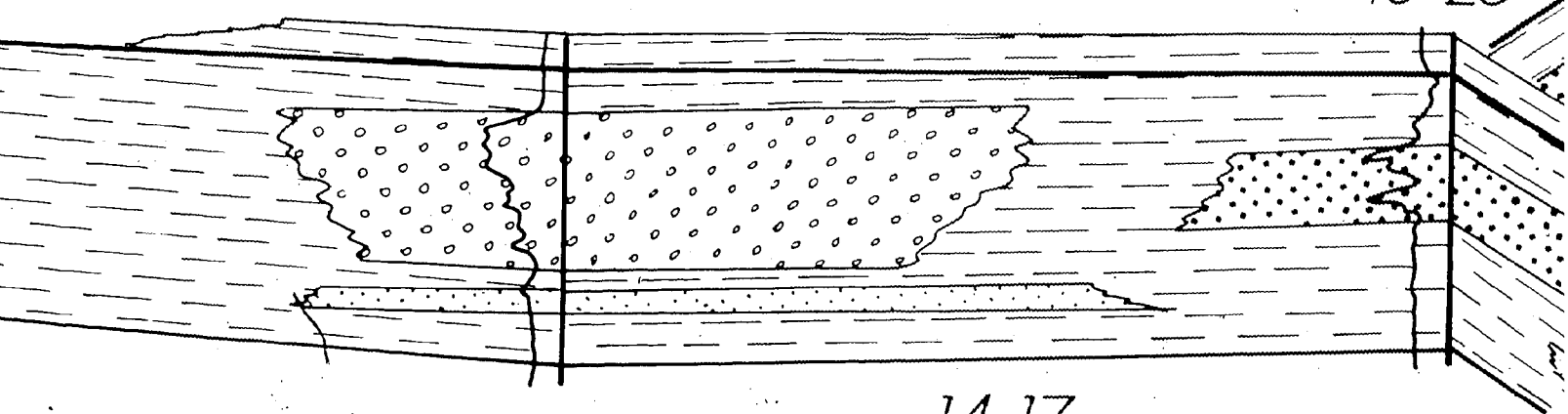
4-29-





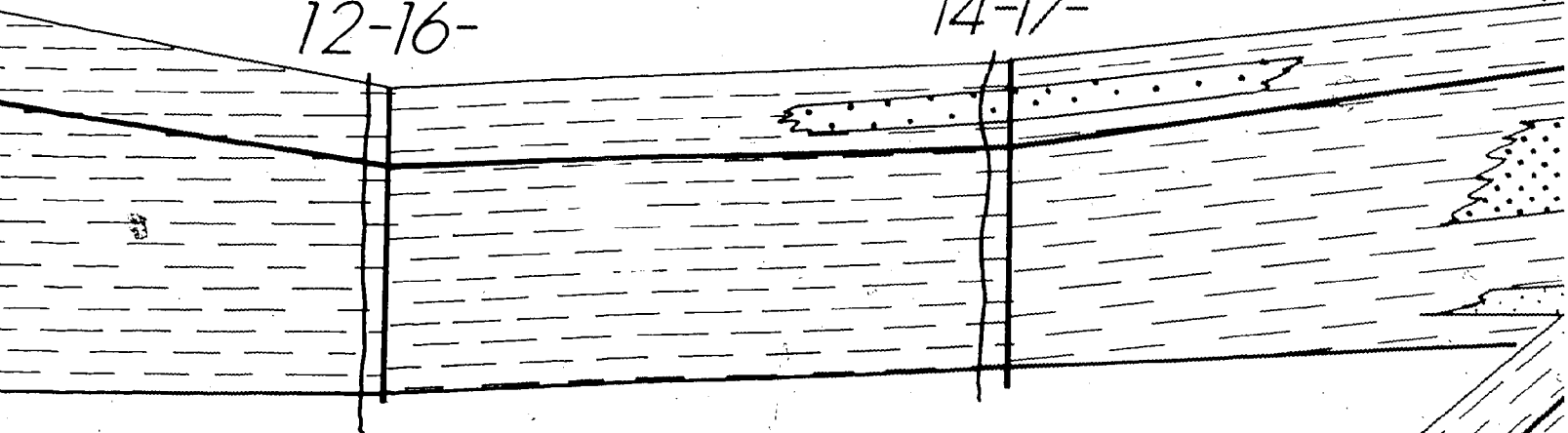
6-31-

10-25-



12-16-

14-17-

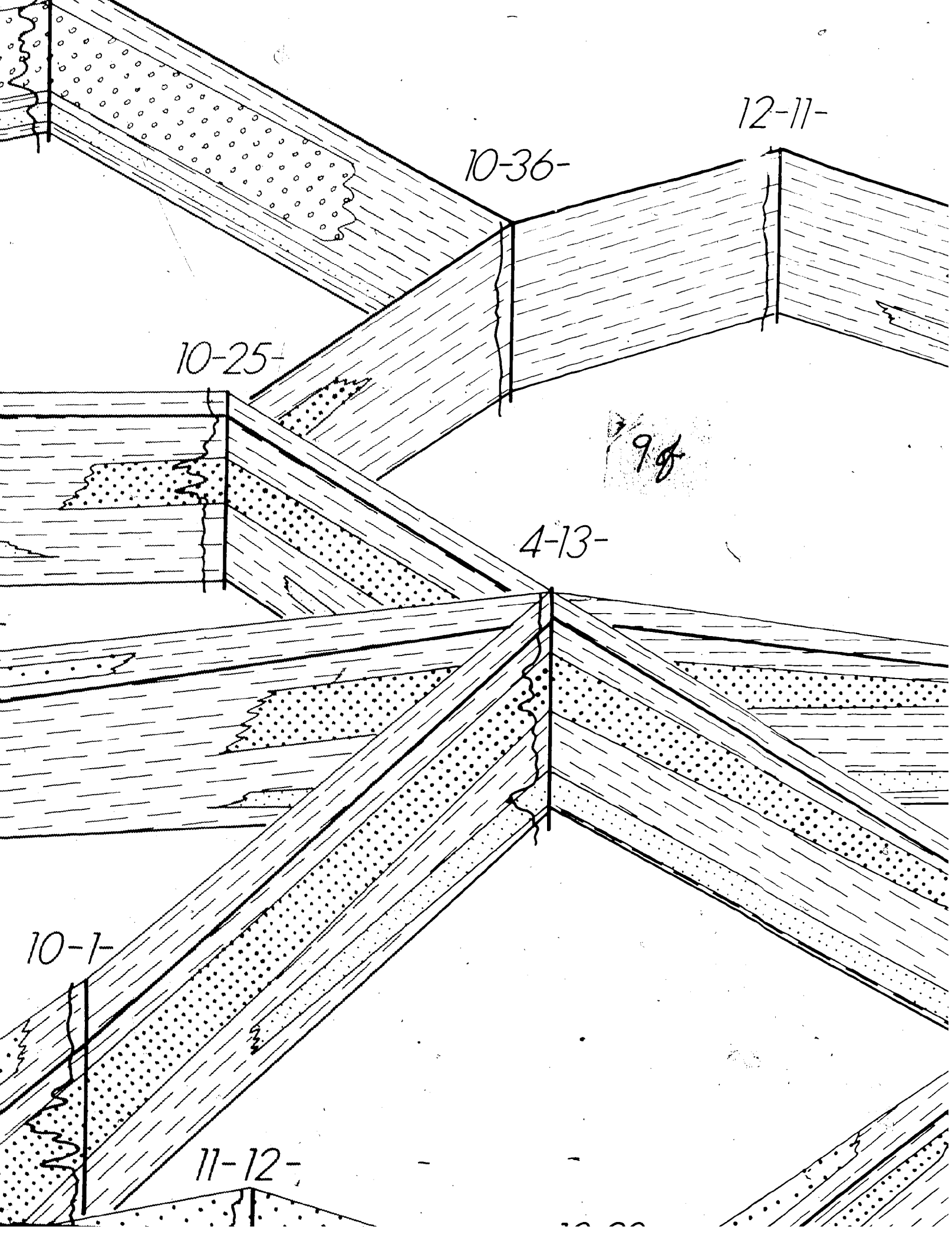


10-1-

4-29-

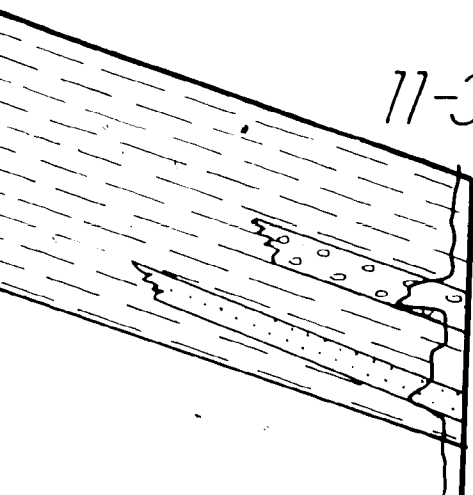


11-12-



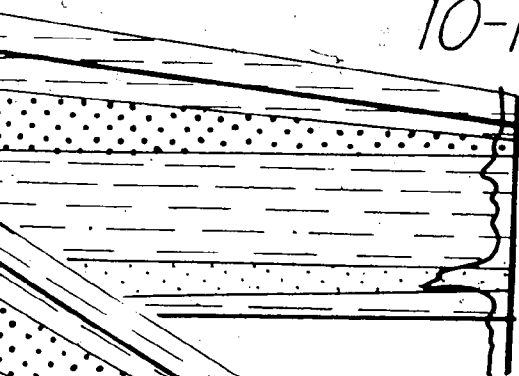
11-

11-35-

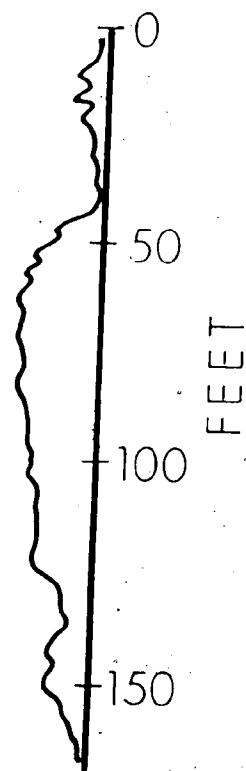
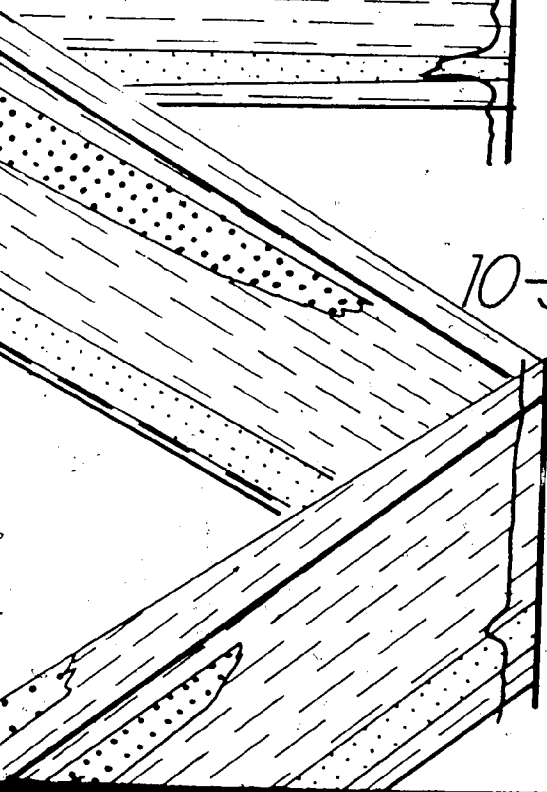


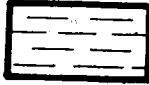


10-18-

108



10-33-



- Bentonite markers
-  Shale, mudstone - silt
-  Basal sand
-  Lower sand (South)

39

—

38

—

37

—

36

—

52°—35

—

34

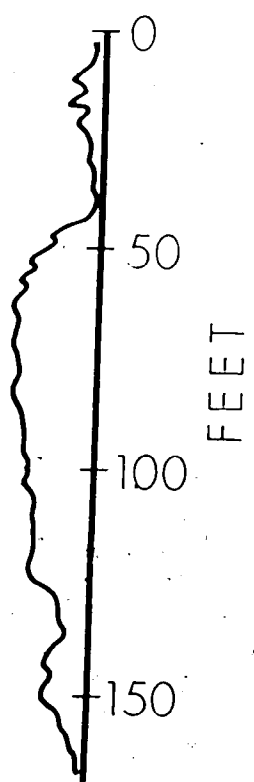
—

33

—

32

—



118.

entonite markers

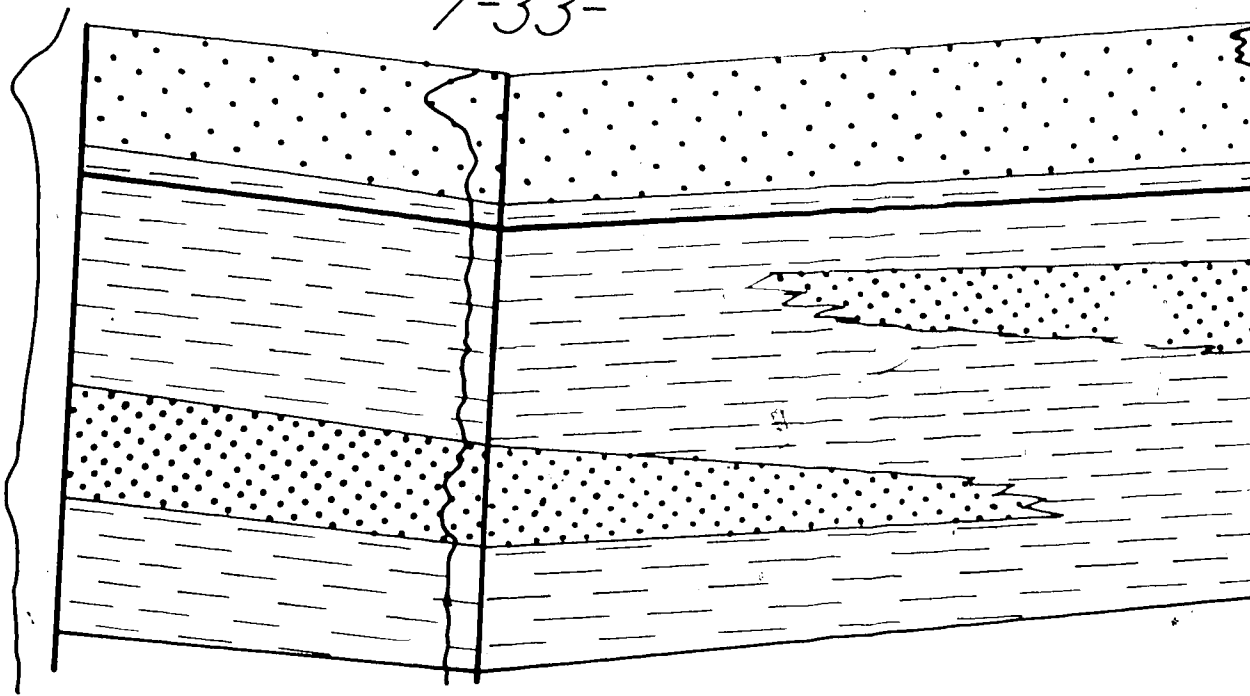
hale, mudstone - siltstone

asol sand -

10-3-

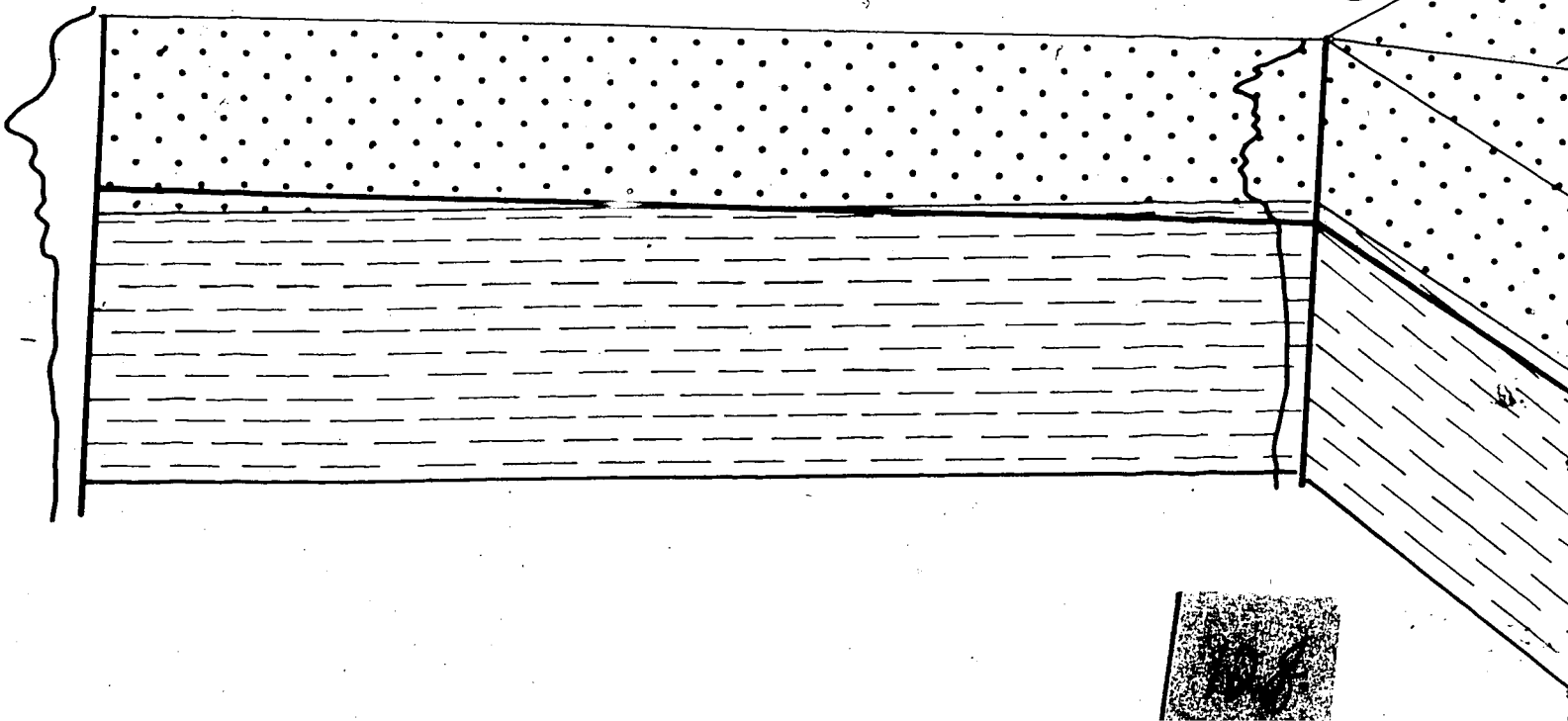
7-33-

7-

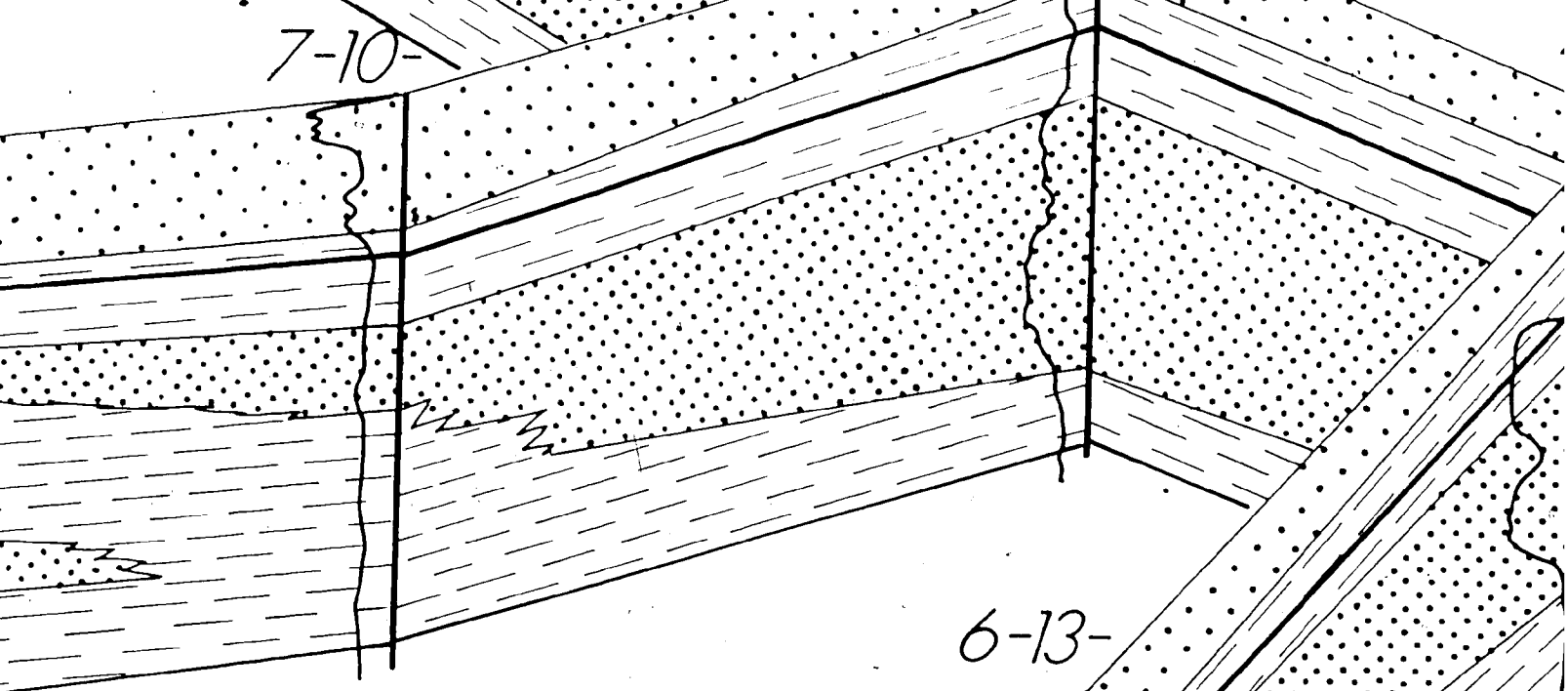


11-2-

6-26-



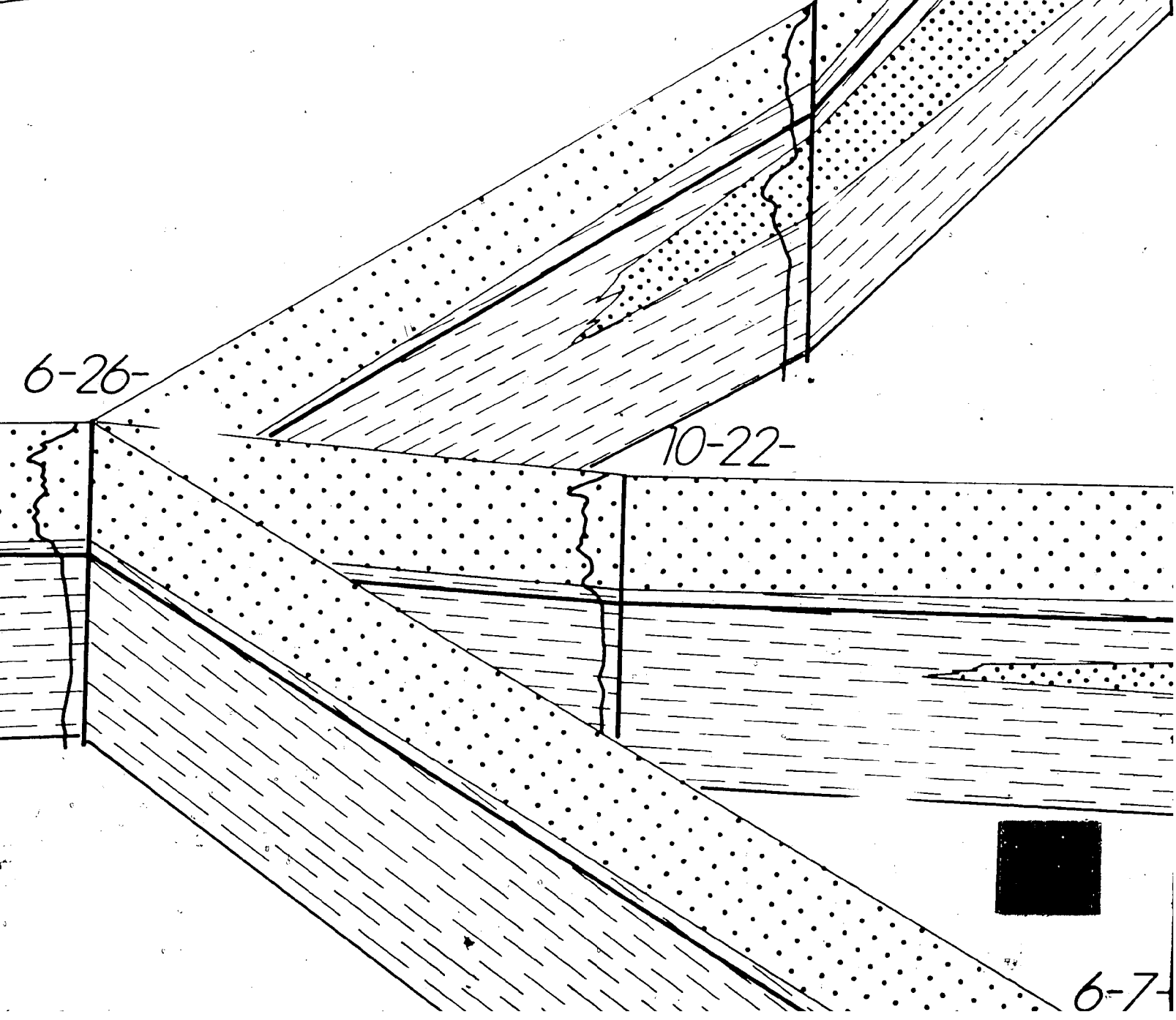
7-10-



6-13-

6-26-

10-22-



6-7-

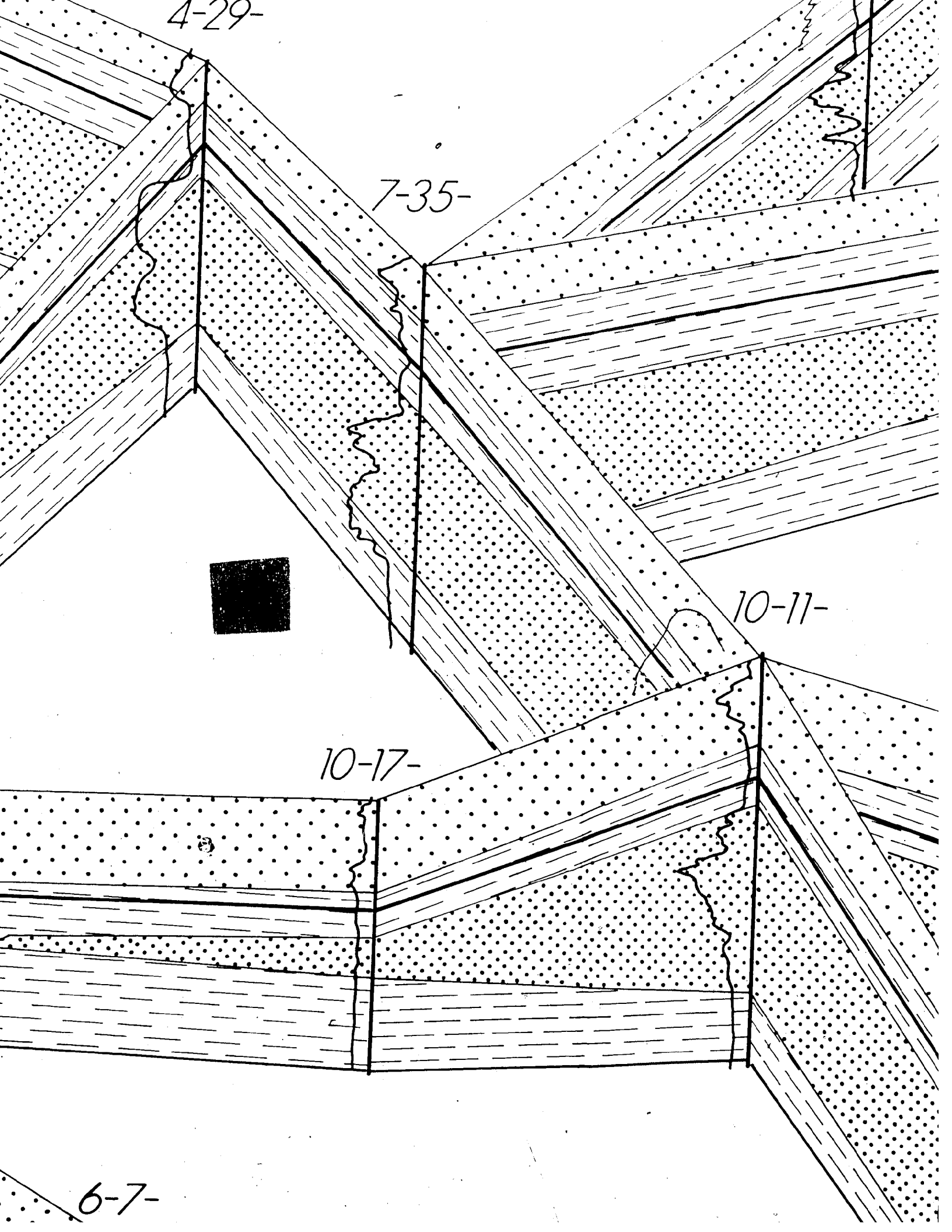
4-29-

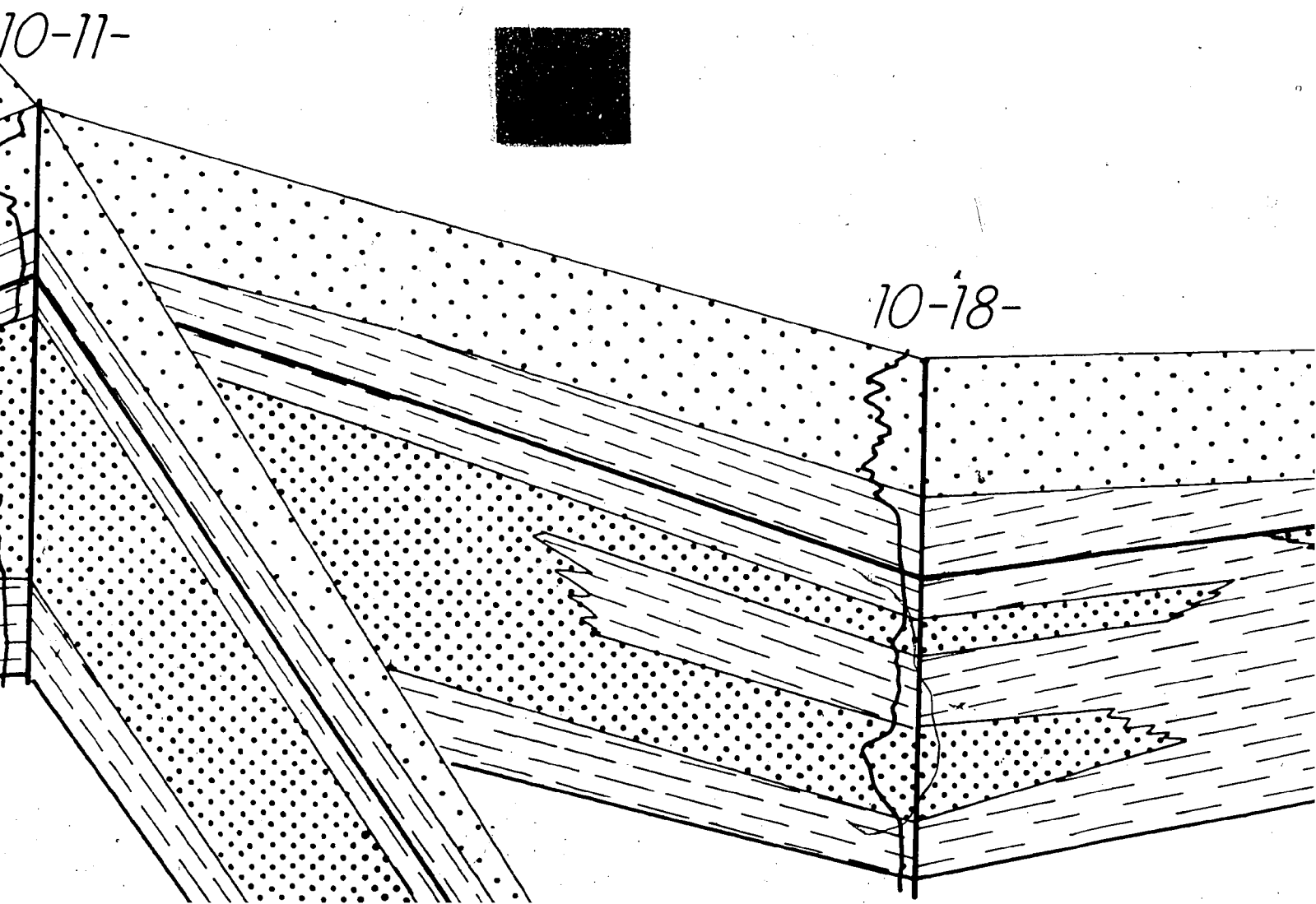
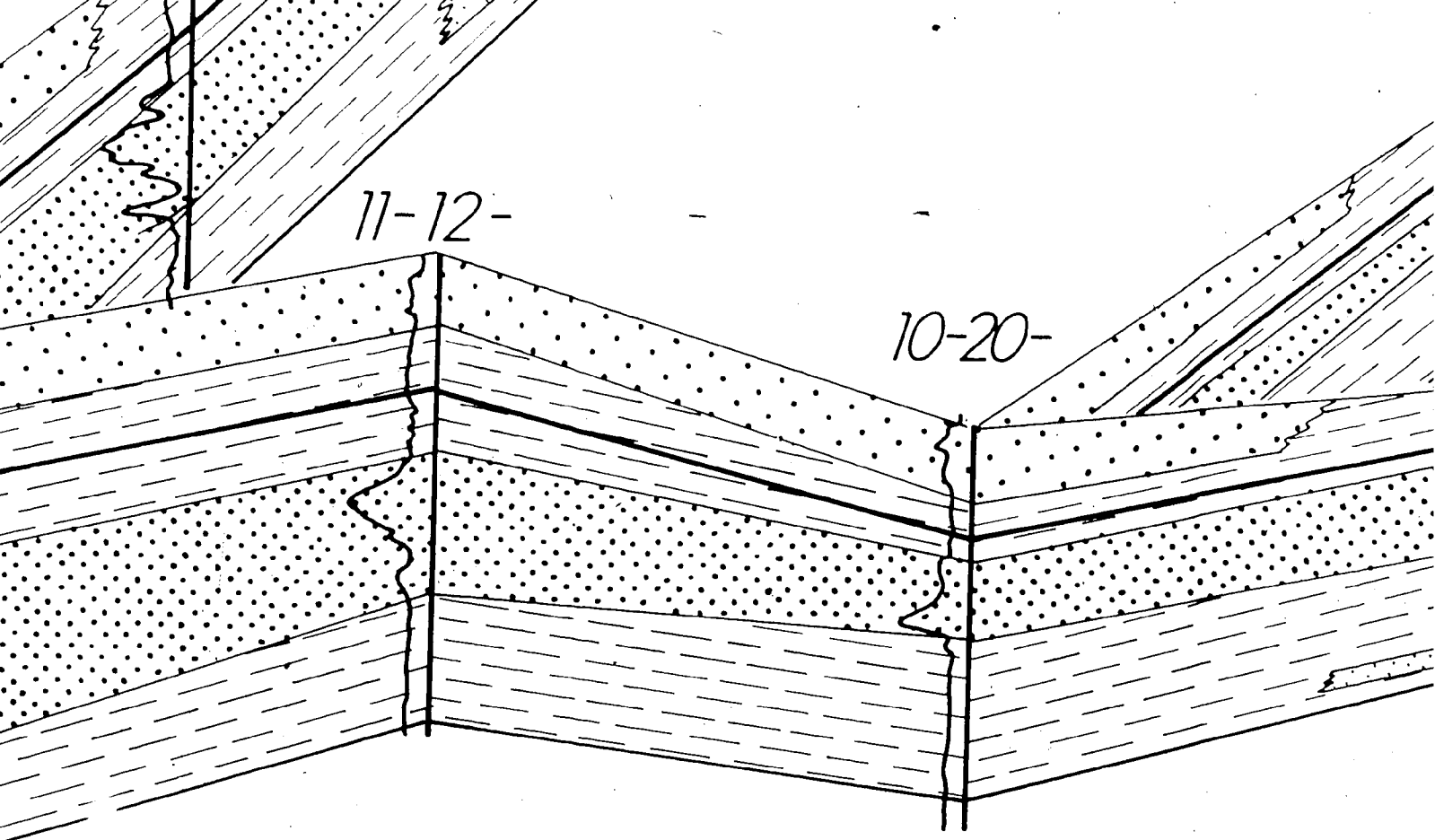
7-35-

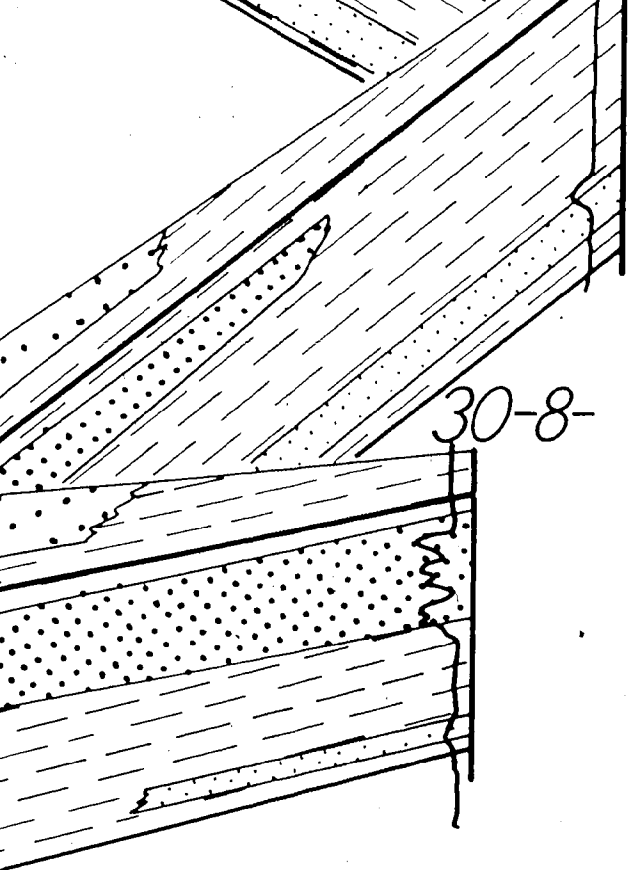
10-11-




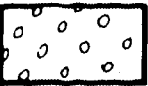

10-17-

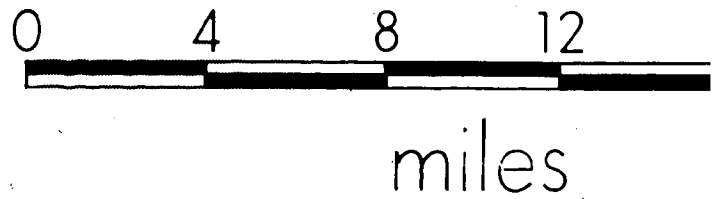
6-7-



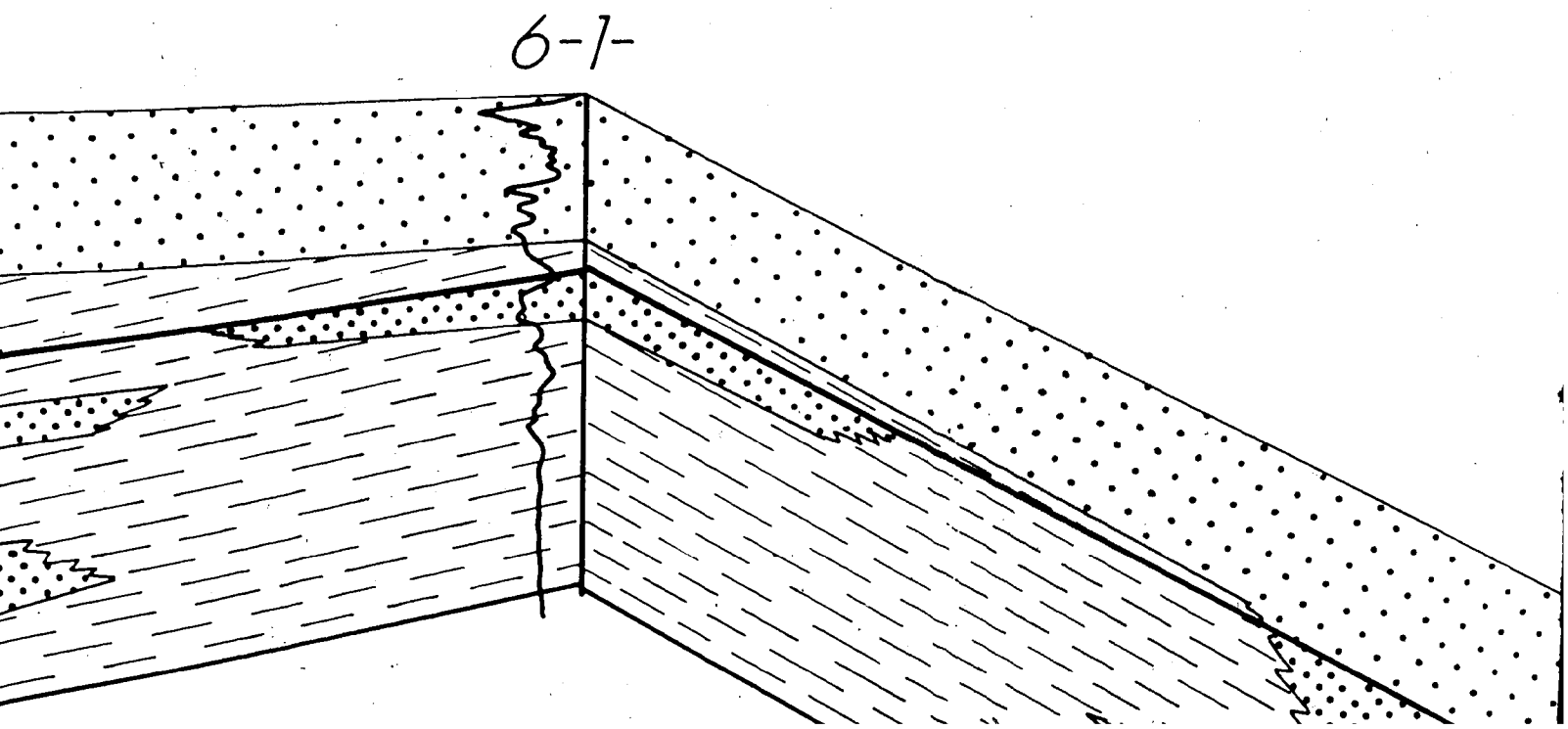




-  Shale, mudstone -
-  Basal sand -
-  Lower sand (South)
-  Lower sand (North)
-  Upper sand



166



chronologic markers

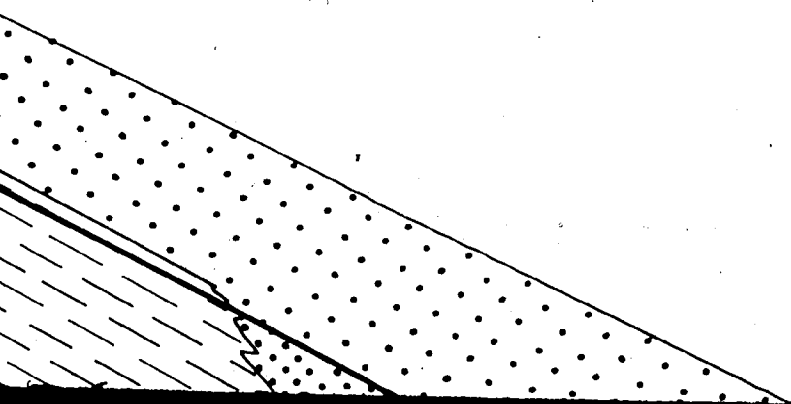
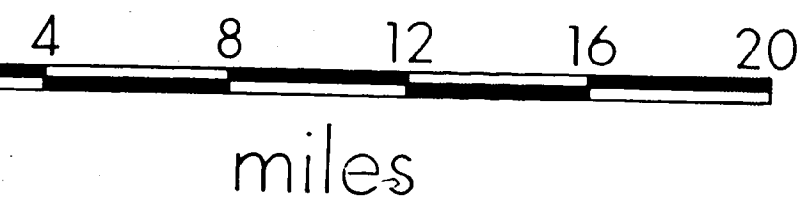
Shale, mudstone - siltstone

Basal sand

Lower sand (South)

Lower sand (North)

Upper sand



32

31

30

29

28

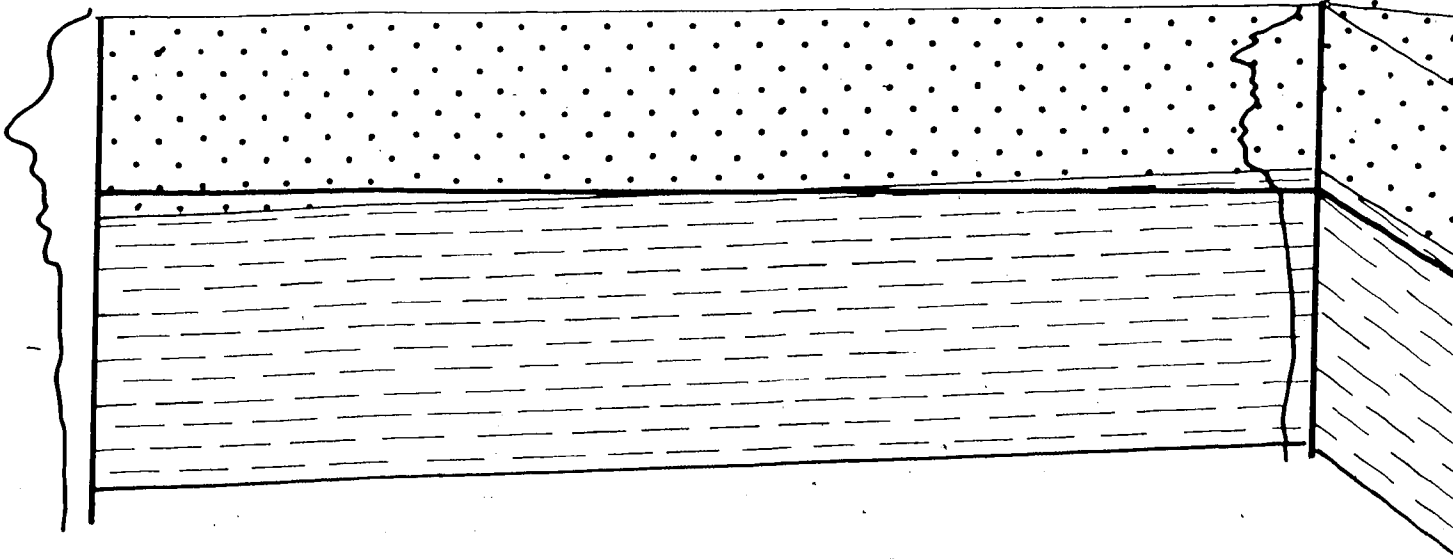
27

26

25

11-2-

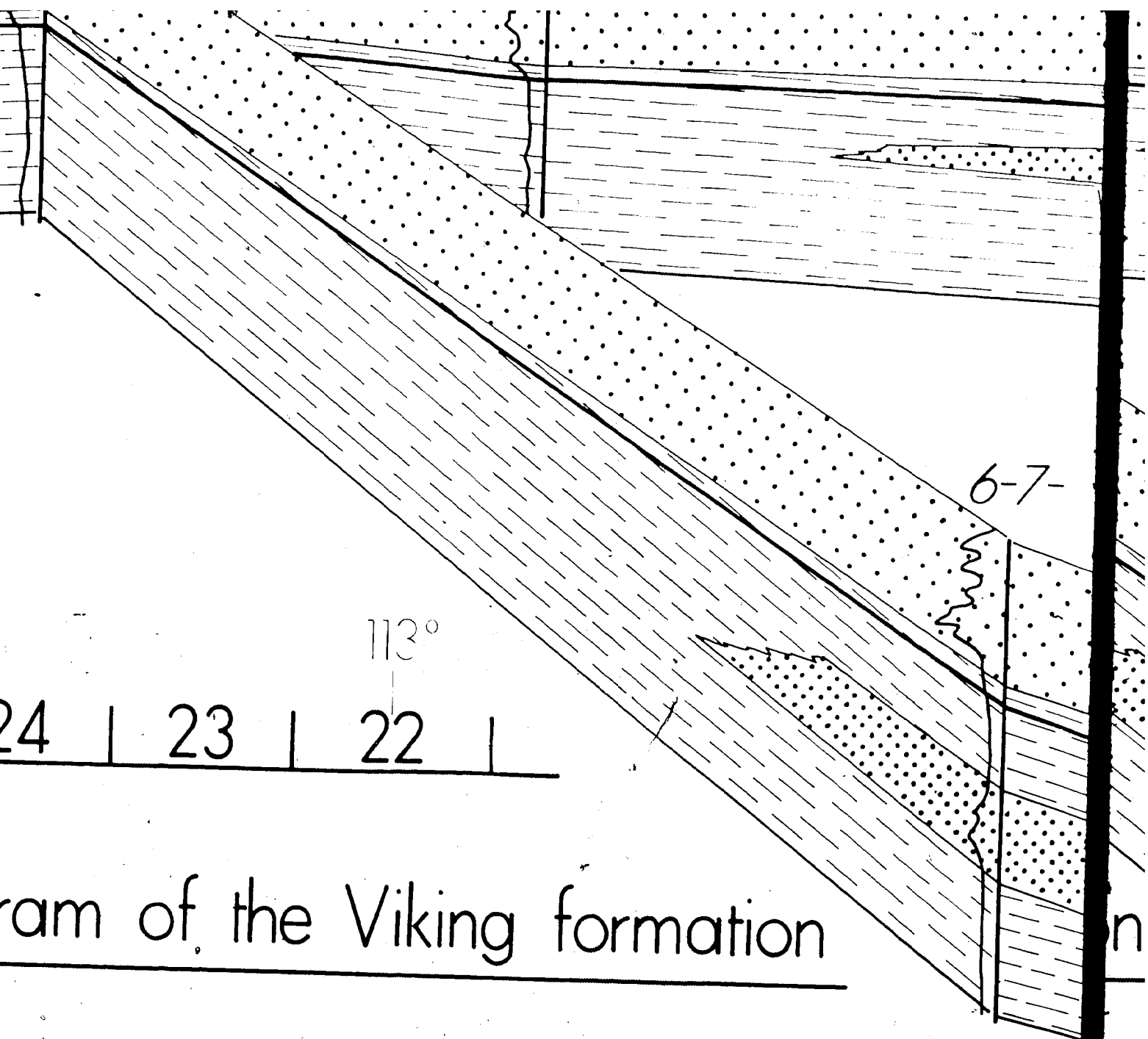
6-26-



28 | 27 | 26 | 25 | 24 |

Fig.29. Detailed fence diagram

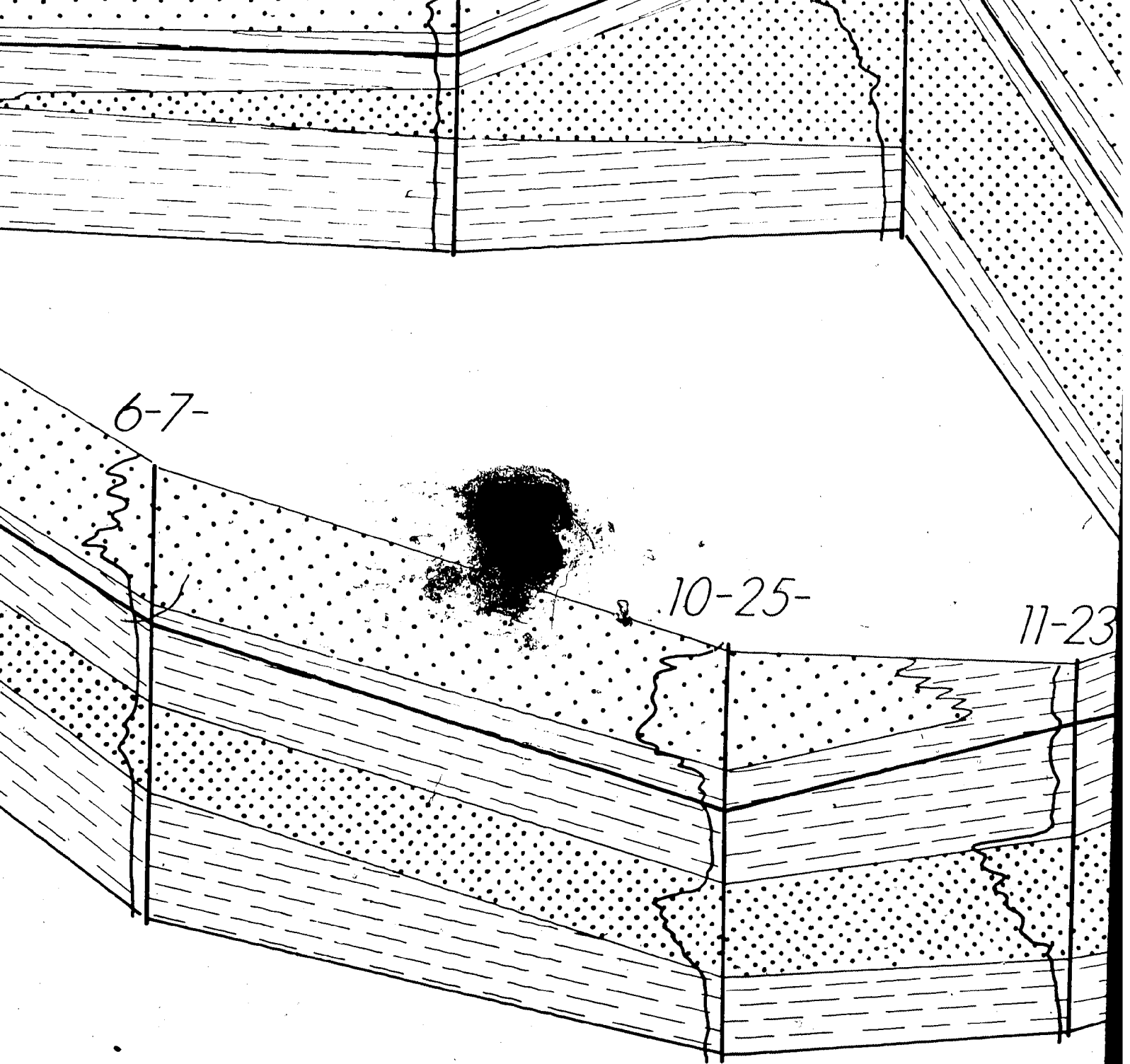
(Twps: 21 - 44, Range



ram of the Viking formation

anges: 3 - 28 W4M)

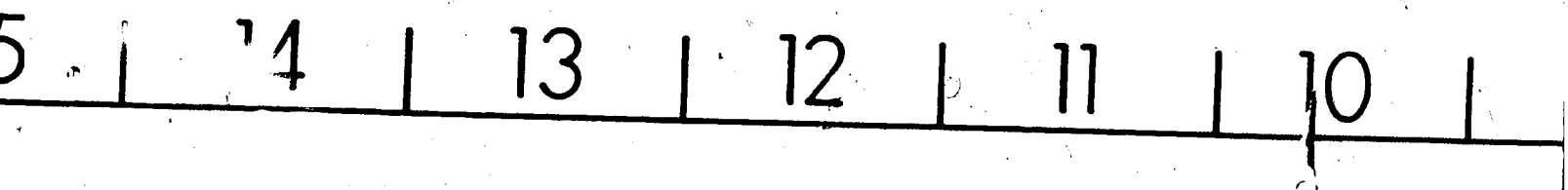
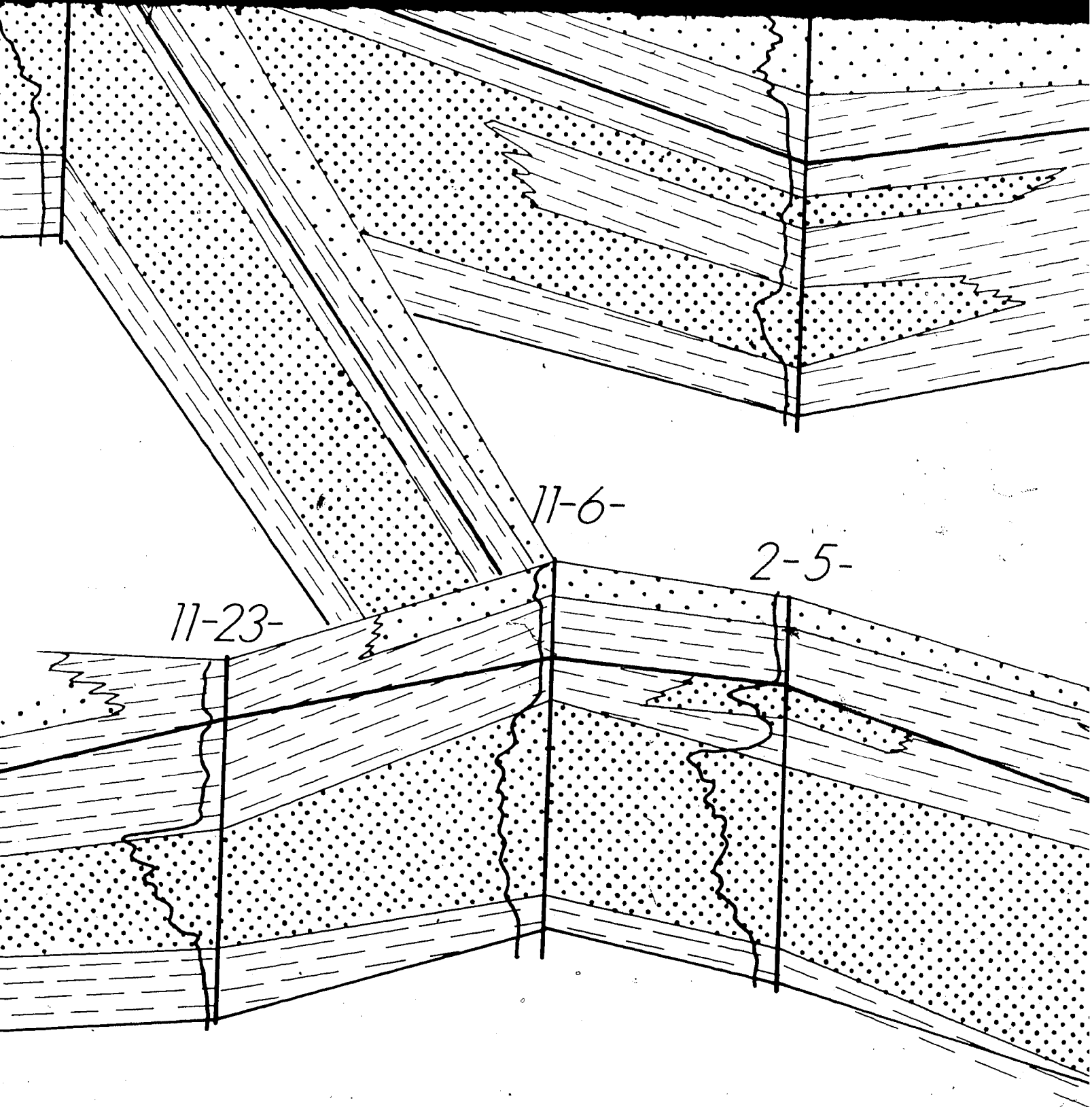
21 | 20 | 19 | 20

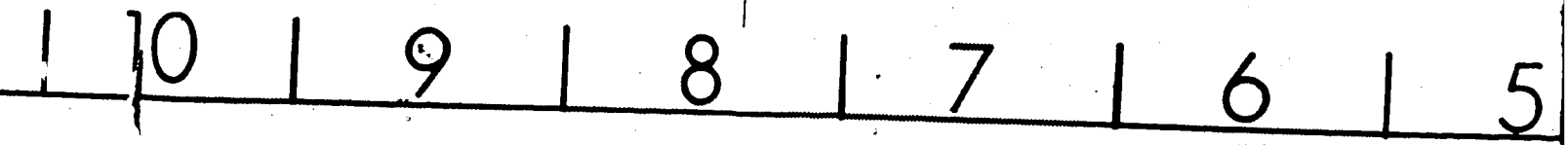
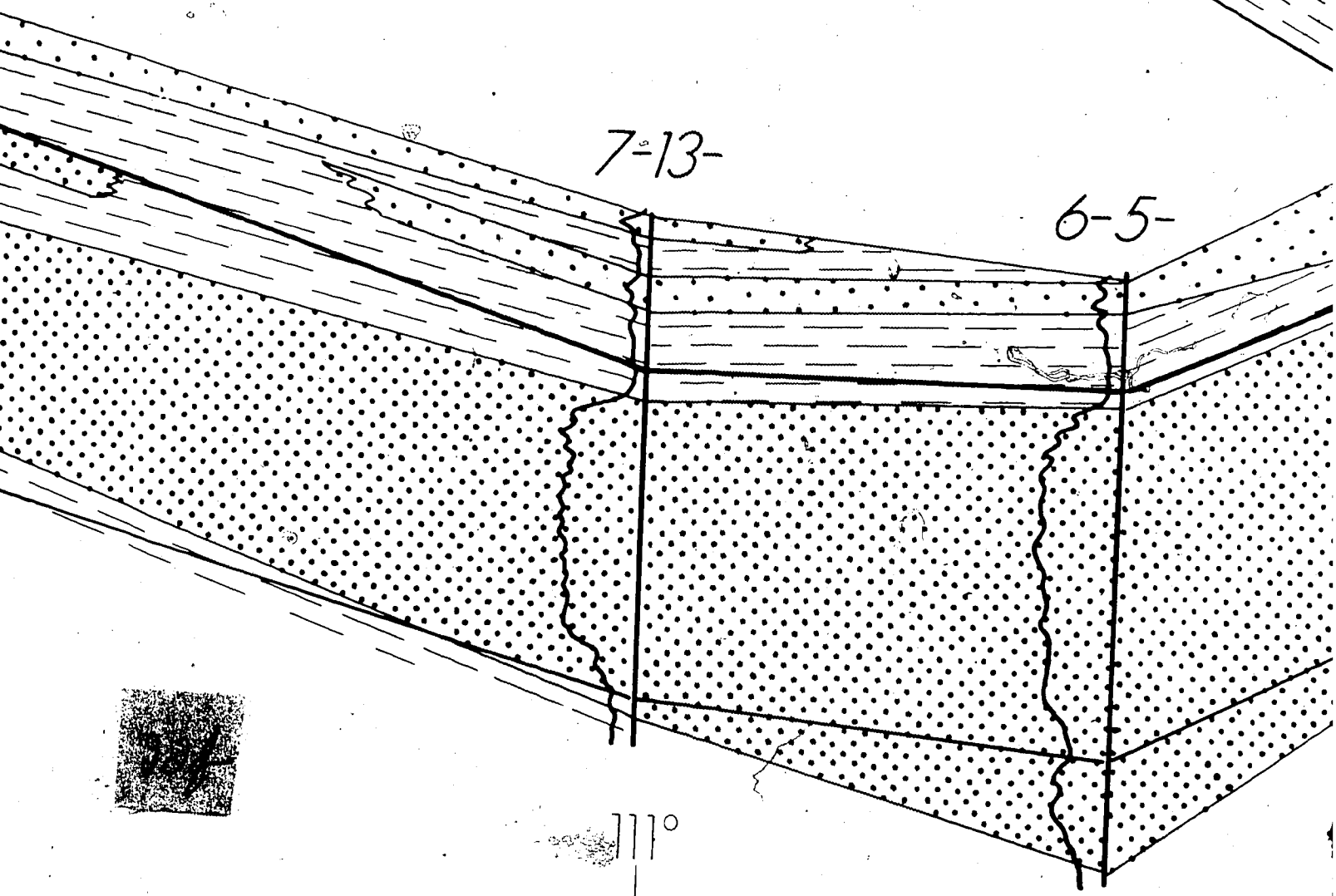
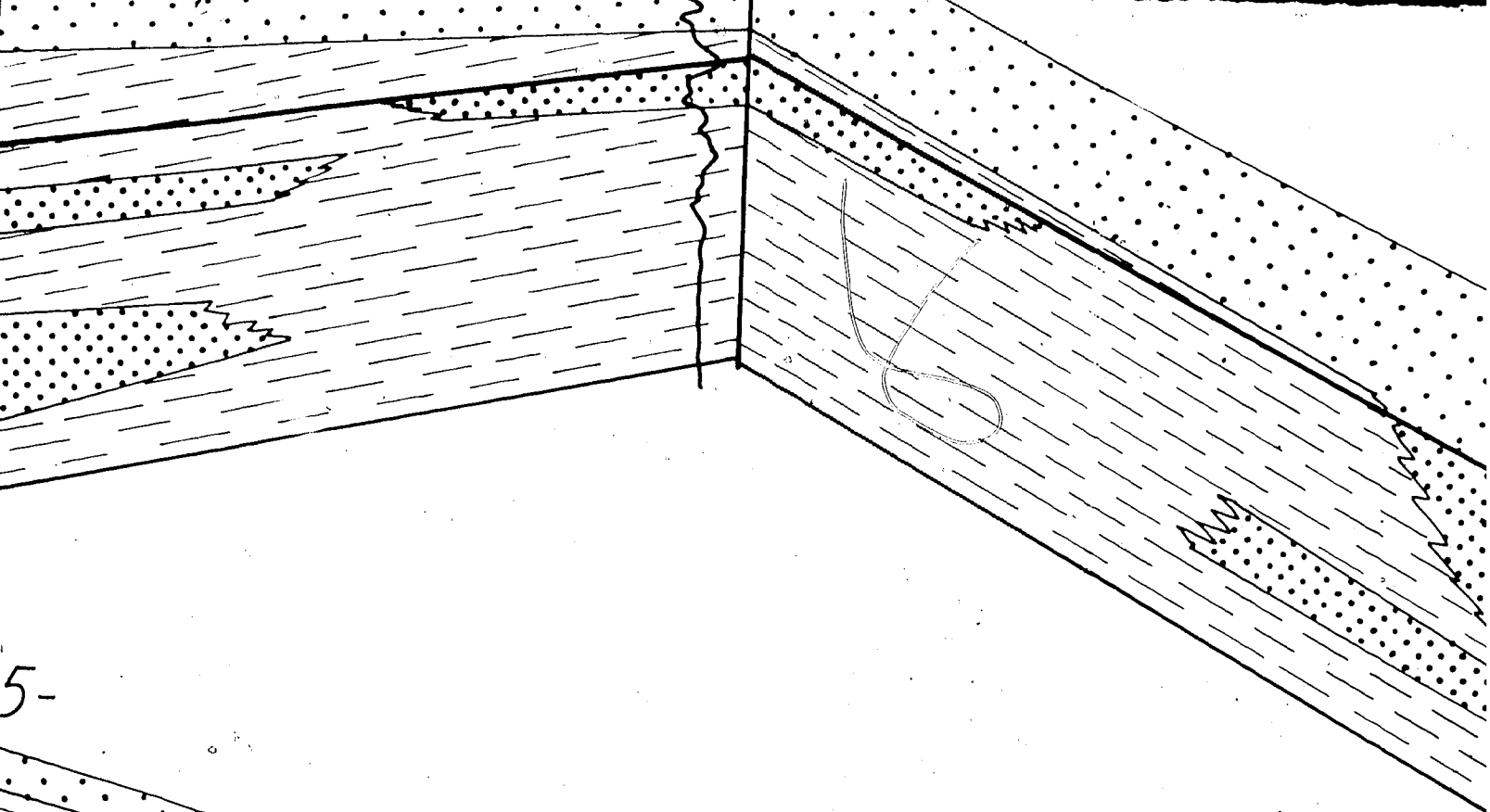


19 | 18 | 17 | 16 |

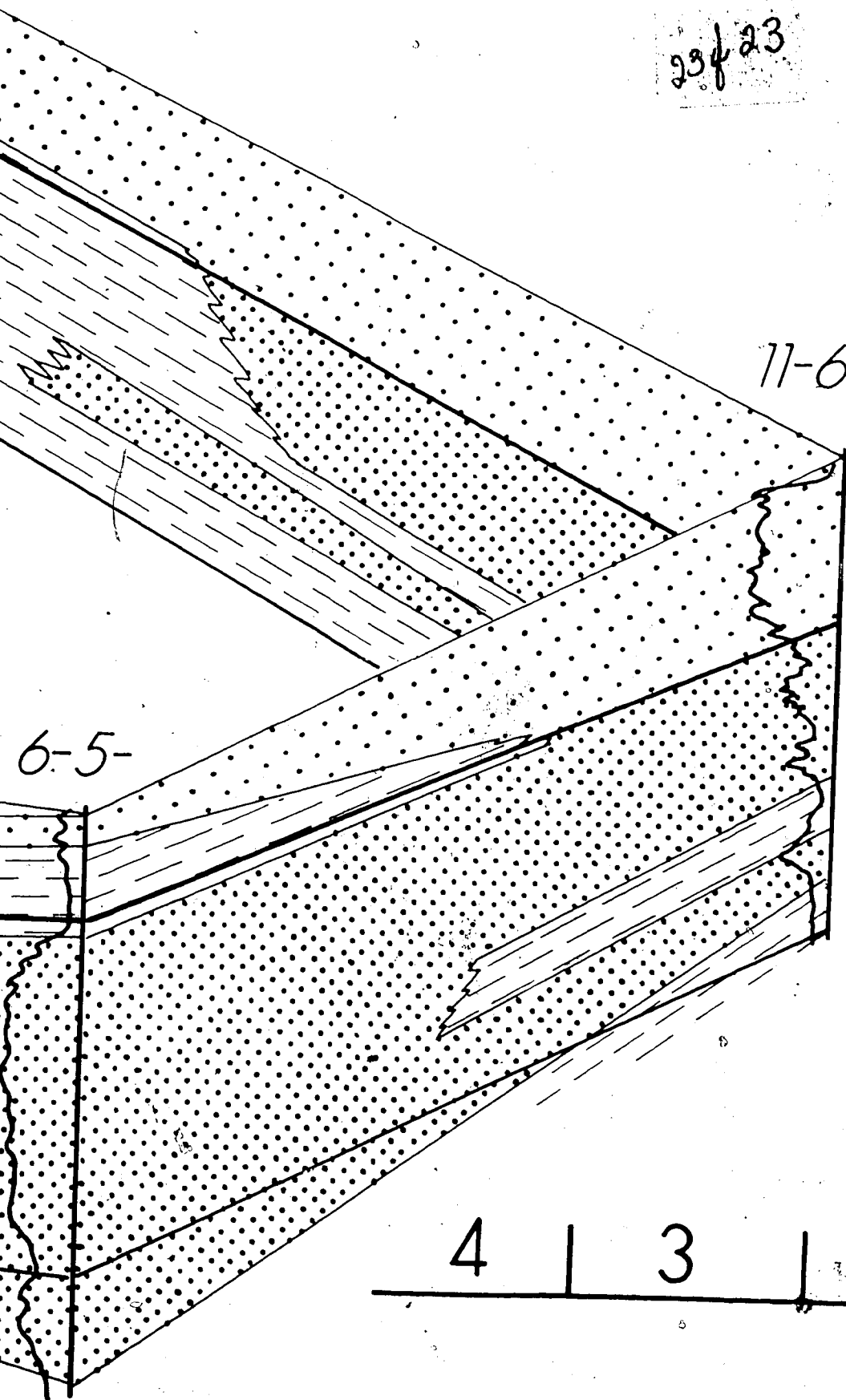
112°

15 | 14 |





23423



26

25

24

51°

23

22

21

4

3

2

1

110°

6

5